PLASMA INVERSE SCATTERING THEORY

Thesis by

George N. Balanis

In Partial Fulfillment of the Requirements

For the Degree of

Doctor of Philosophy

California Institute of Technology

Pasadena, California

1972

ACKNOWLEDGMENT

I wish to express my sincere gratitude to my research advisor Professor Charles Herach Papas, for his continued guidance and support during the course of this work, as well as for the unceasing encouragement and deep inspiration I received from him throughout my studies at the California Institute of Technology. His precious comments and suggestions shaped the form of this thesis. In addition, I gratefully acknowledge helpful discussions with Professor George R. Gavalas.

Special thanks are due to Mr. Panos Z. Marmarelis for assistance in the programming of the numerical computations and to Mrs. Ruth Stratton and Mrs. Karen Current for their excellent typing of the final manuscript.

ABSTRACT

The object of this report is to calculate the electron density profile of plane stratified inhomogeneous plasmas. The electron density profile is obtained through a numerical solution of the inverse scattering algorithm.

The inverse scattering algorithm connects the time dependent reflected field resulting from a δ-function field incident normally on the plasma to the inhomogeneous plasma density.

Examples show that the method produces uniquely the electron density on or behind maxima of the plasma frequency.

It is shown that the δ-function incident field used in the inverse scattering algorithm can be replaced by a thin square pulse.

TABLE OF CONTENTS

I. INTRODUCTION

A. Why Inverse Scattering

There exist situations in physics where we want to determine the properties of a medium without measuring them directly. Examples of such media are the ionosphere and dielectrics. Even though rockets can be equipped with devices that measure the dielectric constant of the ionosphere, we prefer other methods because of the huge costs involved in the construction and shooting of the rockets.

The case of the ionosphere is a particularly illuminating example. The ionosphere is a region surrounding the earth where there are appreciable concentrations of electrons and ions. To measure its dielectric constant we shoot vertically up an electromagnetic wave. When the reflected wave comes back we analyze it to infer properties of the ionosphere.

For dielectrics we have a variety of methods. Again we can study the reflected wave of an incident electromagnetic wave. However it is also possible to place the dielectric in a cavity resonator and observe the cavity resonant frequencies.

Methods which analyze the scattered wave from a medium and infer properties of the medium are called inverse scattering methods. The name inverse is attached to differentiate from situations where we know the properties of the medium and we are interested in the scattered wave properties.

B. Inverse Scattering Problems

As early as 1894 Lord Rayleigh[1] considers the problem of determining the tones of a slightly inhomogeneous vibrating string. For small displacements $y(z,t)$ and a time dependence $e^{-i\omega t}$ the string equation becomes

$$\frac{d^2}{dz^2} y(z,\omega) + \omega^2 \frac{\rho(z)}{T(z)} y(z,\omega) = 0$$

Lord Rayleigh finds that for a string clamped at both ends ($y(o,\omega)=y(L,\omega)=0$) and for an almost constant mass density

$$\rho(z) = \rho_o + \Delta\rho(z) \quad ,$$

the tones are given by

$$\tau_n^2 \sim \frac{4L^2\rho_o}{T_o n^2} (1 + \alpha_n)$$

where τ_n is the period of the n^{th} vibrational mode, L the string's length, T_o its tension (assumed constant) and α_n

$$\alpha_n = \frac{2}{L} \int_o^{L/2} \frac{\Delta\rho(z')}{\rho_o} (1 - \cos \frac{2\pi n z'}{L}) \, dz'$$

Assuming that $\Delta\rho(z)$ is symmetric about the midpoint of the string and expanding in a Fourier Series

$$\frac{\Delta\rho(z)}{\rho_o} = A_o + A_1 \cos \frac{2\pi z}{L} + \ldots + A_n \cos \frac{2\pi n z}{L} + \ldots$$

---

[1] See Reference 10.

Lord Rayleigh shows that

$$\alpha_n = A_o - \frac{1}{2} A_n$$

Lord Rayleigh realizes the importance of his results and remarks that it is possible to describe the inhomogeneity $\Delta\rho(z)$ from a knowledge of ρ_o and τ_n.

In 1929 V.A. Ambartsumyan[2] considers the eigenvalue problem

$$\frac{d^2\psi}{dz^2} + [k^2 - V(z)]\,\psi(z,k) = 0$$

$$\frac{d\psi}{dz}(o,k) = \frac{d}{dz}\psi(\pi,k) = 0$$

He shows that if the eigenvalues are $k_n^2 = n^2$, then $V(z)$ must be identically zero. His conclusions reveal the exciting possibility that the spectrum of the eigenvalue problem determines the function $V(z)$. In essence this marks the beginning of the inverse scattering theory.

Motivated by Ambartsumyan's results G. Borg[3] in 1946 and later B.M. Levitan and M.G. Gasymov[4] consider the eigenvalue problem

$$\frac{d^2\phi}{dz^2} + [\lambda - V(z)]\,\phi(z,\lambda) = 0$$

under two sets of boundary conditions

---

[2] See Reference 11.

[3] See Reference 12.

[4] See Reference 14.

$$\phi'(o,\lambda) - h_1 \phi(o,\lambda) = 0$$

$$\phi'(\pi,\lambda) + H \phi(\pi,\lambda) = 0$$

and

$$\phi'(o,\mu) - h_2 \phi(o,\mu) = 0$$

$$\phi'(\pi,\mu) + H \phi(\pi,\mu) = 0$$

They prove that both sets of eigenvalues $\lambda_1, \lambda_2,\ldots,\lambda_n,\ldots$ and $\mu_1, \mu_2,\ldots,\mu_n,\ldots$ are needed to determine uniquely $V(z)$, h_1, h_2, and H. Ambartsumyan's example is an exceptional case.

In 1933 R.E. Langer[5] considers the possibility of determining the conductivity of the earth as a function of depth. He supposes that a small electrode supplies a direct electric current to the earth's surface and the resulting surface potential $\phi(\rho,o)$ is measured as a function of the radius ρ from the electrode. He questions whether the surface potential determines uniquely the conductivity as a function of depth.

Using Maxwell's equations

$$\nabla \cdot \sigma \underline{E} = 0$$

and

$$\underline{E} = - \nabla\phi$$

the potential $\phi(\rho,z)$ solves the differential equation

$$\frac{\partial^2\phi}{\partial\rho^2} + \frac{1}{\rho}\frac{\partial\phi}{\partial\rho} + \frac{\sigma'(z)}{\sigma(z)}\frac{\partial\phi}{\partial z} = 0$$

---

[5] See Reference 15.

where z is the depth and ρ the horizontal radius from the electrode.

Separating the variables Langer obtains two differential equations

$$\frac{d^2V}{d\rho^2} + \frac{1}{\rho}\frac{dV}{d\rho} + \lambda^2 V(\rho,\lambda) = 0$$

$$\text{(i)} \qquad \frac{d^2u}{dz^2} + \frac{\sigma'(z)}{\sigma(z)}\frac{du}{dz} - \lambda^2 u(z,\lambda) = 0$$

Since $\phi(\rho,\lambda)$ is finite for small ρ

$$V(\rho,\lambda) = J_o(\lambda\rho)$$

Then

$$\phi(\rho,z) = \int_o^\infty A(\lambda)U(z,\lambda)J_o(\lambda\rho)\, d\lambda$$

where $U(z,\lambda)$ is the solution of (i) that decreases exponentially with z. Incorporating the boundary conditions at z = 0, namely

$$\frac{\partial\phi}{\partial z}(\rho,o) = -\frac{I}{2\pi a\sigma(o)}\frac{1}{\sqrt{a^2 - \rho^2}} \qquad \rho < a$$

$$\frac{\partial\phi}{\partial z}(\rho,o) = 0 \qquad \rho \geq a$$

where a is the electrode radius, I the current injected on the surface, $\sigma(o)$ the conductivity at the surface,

Langer shows that the potential is given by

$$\phi(\rho,z) = -\frac{I}{2\pi a\sigma(o)}\int_o^\infty \frac{U(z,\lambda)}{U'(o,\lambda)} J_o(\lambda\rho)\sin\lambda a\, d\lambda$$

Defining $\underline{o}(\lambda)$

$$\underline{o}(\lambda) = -\lambda \frac{U(o,\lambda)}{U'(o,\lambda)}$$

Fourier-Bessel Transform techniques yield

$$\underline{o}(\lambda) \frac{I \sin\lambda a}{2\pi a\lambda^2 \sigma(o)} = \int^{\infty} \phi(\rho,o)\ J_o(\lambda\rho)\ d\rho$$

Langer observes that $\phi(\rho,o)$ and $\sigma(o)$ determine in principle $\underline{o}(\lambda)$. Relating the conductivity $\sigma(z)$ to $\underline{o}(\lambda)$ is no simple matter. However, Langer is able to show that $\underline{o}(\lambda)$ determines the ratio $\frac{\sigma'(z)}{\sigma(z)}$. He deduces that the potential at the surface of the earth and the value of the conductivity at the surface determine uniquely the conductivity $\sigma(z)$ as a function of depth z.

In the 1950's inverse scattering theory experiences a tremendous growth. Leading quantum physicists and mathematicians strongly hint that the interaction between two particles can uniquely determine the Hamiltonian of the system.

Under certain approximations the interaction between two particles is governed by the radial Schrödingers equation

(ii) $$\frac{d^2\psi}{dr^2} + [k^2 - \frac{\ell(\ell+1)}{r^2} - V(r)]\psi(r,k) = 0, \quad r > 0$$

$$\psi(o,k) = 0\ \frac{\partial}{\partial r}\psi(o,k) = 1$$

For V(r) decreasing sufficiently fast as $r \to \infty$, $\psi(r,k)$ takes the form

$$\psi(r,k) \sim \frac{A(k)}{k} \sin[kr - \frac{\pi \ell}{2} - n(k)] \quad \text{as } r \to \infty$$

The question concerning quantum physicists is: Does $\psi(r,k)$ for large r determine uniquely V(r)? Assuming that n(k) determines uniquely V(r), Heisenberg[6] suggests that perhaps the scattering operator S(k)

$$S(k) = e^{-2in(k)}$$

is a more fundamental quantity than the Hamiltonian.

In 1951 a basic paper by I.M. Gelfand and Levitan[7] describes a procedure that produces the potential V(r) from a knowledge of the spectral function associated with $\psi(r,k)$. In 1952[8] Marchenko shows that when there are bound states one needs to know the bound states as well as appropriate normalizing constants in order to determine uniquely V(r).

Gelfand's formulation where applied to (ii) for $\ell = 0$ and no bound states shows that if one knows W(k)

$$W(k) = \frac{1}{A^2(k)}$$

for all k then

$$V(r) = 2 \frac{d}{dr} K(r,r)$$

---

[6] See Reference 21.

[7] See References 16, 21.

[8] See References 17, 21.

where K(r,y) is the solution of the integral equation

$$K(r,y) + \underline{o}(r,y) + \int_o^r K(r,r')\ \underline{o}(r',y)dr' = 0, \quad y < r$$

with

$$\underline{o}(r,y) = \frac{2}{\pi} \int_o^\infty \sin kr \sin ky\ [W(k) - 1]\ dk$$

Marchenko's formulation for $\ell = 0$ and no bound states shows that if one knows S(k)

$$S(k) = e^{-2in(k)}$$

for all k then

$$V(r) = -2 \frac{d}{dr} A(r,r)$$

where A(r,y) is the solution of the integral equation

$$A(r,y) = F(r,y) + \int_r^\infty A(r,r')F(r'+y)\ dr' \ , \ r < y$$

with

$$F(r) = \frac{1}{2\pi} \int_{-\infty}^{+\infty} [S(k)-1]e^{ikr}\ dk$$

Agranovitch and Marchenko[9] at a later time expand the previous formulations to include the case $\ell \neq 0$.

In 1955 I. Kay[10] examines the one dimensional inverse scattering

---

[9] See Reference 18.

[10] See References 1,2,3.

problem

$$\frac{d^2\psi}{dz^2} + [k^2 - V(z)]\psi(z,k) = 0 \qquad z \geq 0$$

$$\frac{d^2\psi}{dz^2} + k^2\,\psi(z,k) = 0 \qquad z < 0$$

Assuming that for $z < 0$ $\psi(z,k)$ is a combination of an incident wave e^{ikz} and a reflected wave $r(k)e^{-ikz}$, Kay shows that $r(k)$ determines uniquely $V(z)$. Then he proceeds to deduce $V(z)$ when $r(k)$ is a rational function of k.

In 1963 C.B. Sharpe[11] transforms the basic equations for lossless nonuniform transmission lines to the one dimensional Schrödinger's equation. He shows that when the input admittance to the line is a known rational function of the frequency, the characteristic resistance of the line can be found.

Using similar ideas with Sharpe, in 1963 Moses and deRidder[12] reduce the equations governing the propagation of a plane wave inside a plane stratified dielectric to the one dimensional Schrödinger's equation and then proceed to solve examples when the reflected wave in the frequency domain is a known rational function of k.

---

[11] See Reference 7.

[12] See Reference 9.

C. Statement of the Problem

Up to today very little research has been devoted to solving inverse scattering problems. Mostly the theory has concentrated on developing algorithms relating scattering parameters to the potential of Schrödinger's equation. Few researchers have solved the algorithms where the scattering parameters are rational functions of frequency.

In reality the scattering parameters are complex irrational functions of the frequency. Then how does one solve an inverse scattering problem?

Statement of the Problem

A cold, collisionless and unbiased plasma exists in the region $z > 0$. The plasma is plane stratified in the z-direction. The plasma density $N(z)$ (Electrons/m^3) is an arbitrary function of z. Air of a constant index of refraction $\eta=1$ fills the whole space.

A plane electromagnetic wave is incident normally on the plasma from the region $z < 0$. The incident electric field is an "ideal" pulse, a δ-function $\delta(z-ct)$, where c = speed of light in free space, t = time. A reflected wave results and propagates in the -z direction.

An observer in the region $z < 0$ measures the reflected wave as it evolves with time. From the time record of the reflected wave the observer deduces the plasma density as a function of z.

The thesis chapter material is divided as follows:

In Chapter 2 we present the inverse scattering theory. We show that a relation exists between the time dependent reflected wave and N(z).

In Chapter 3 we solve the relation between the reflected wave and N(z) by numerical means. A computer program is formulated that has as input uniformly sampled values of the reflected wave. The output is the electron density N(z). If the incident probing wave is not a δ-function but a thin square pulse we show that we can still use the program.

In Chapter 4 we sketch an alternative method for finding N(Z). We compare the inverse scattering method with the other method.

II. PLASMA INVERSE SCATTERING THEORY

This chapter presents the inverse scattering theory from first principles. First, the direct scattering problem is developed in the time domain. The causality condition is introduced. Next the inverse scattering problem is solved and an integral equation relating the reflected wave with the electron density is obtained. Certain interesting details are followed through.

A. Direct Scattering Theory

In this section we develop the need to introduce causality into the direct scattering problem in the time domain.

We consider that a plasma is located in region $z > 0$. The plasma has a density $N(z)$ (electrons/m^3) that depends on z and falls to zero for large z. Air of constant index of refraction $\eta = 1$ fills the whole space. A plane electromagnetic wave $\underline{E}_{inc} = \delta(z-ct)\underline{e}_x$ is indicent on the plasma and a reflected field $\underline{E}_{refl} = R(z+ct)\underline{e}_x$ results. The equations governing the propagation of the plasma fields are to be derived.

In the M.K.S. system of units Maxwell's equations give

$$\frac{\partial E}{\partial z} = -\mu_o \frac{\partial H}{\partial t} \tag{1}$$

$$\frac{\partial H}{\partial z} = -J - \varepsilon_o \frac{\partial E}{\partial t} \tag{2}$$

where

μ_o = magnetic permittivity of free space

ε_o = electric permeability of free space

J = induced current density produced by the motion of the changed particles because of the presence of an electric field

$c = \frac{1}{\sqrt{\varepsilon_o \mu_o}}$ = speed of light in free space

The incident electromagnetic field produces a plasma field polarized in the x direction which drags along the charged particles to create the current density $\underline{J} = J\underline{e}_x$. The ions, which are much heavier than the electrons, move very little. The ion produced current density is negligible where compared to the electron current density.

Balancing the forces on an electron and neglecting the small magnetic force gives

$$m \frac{d^2x}{dt^2} = q\ E \tag{3}$$

where m,q are the mass and change of an electron. The time derivative of a current density is given by

$$\frac{\partial J}{\partial t} = q\ N(z) \frac{d^2x}{dt^2}$$

Simple substitution shows that

$$\frac{\partial J}{\partial t} = \frac{q^2 N(z)}{m} E \tag{4}$$

Using (1), (2), (3), (4) we obtain the equation for the electric field inside the plasma

$$\frac{\partial^2 E}{\partial z^2} - \frac{1}{c^2}\frac{\partial^2 E}{\partial t^2} - k_p^2(z)E = 0, \quad z > 0$$

where

$$k_p^2(z) = \frac{\mu_o q^2}{m} N(z)$$

The constant $\frac{\mu_o q^2}{m}$ has a value of 3.54×10^{-14}, the variable $k_p(z)$ is the plasma wave number.

The time variable, for reasons of convenience, is replaced by the distance variable ct in all of the work to follow.

Boundary conditions at the interface between air and plasma show that the electric and magnetic fields must be continuous. So,

$$E(z,ct), \frac{\partial E}{\partial t}(z,ct) \quad \text{continuous across } z = 0$$

The plasma electric field created by the incident δ-function solves the problem

$$\frac{\partial^2 E}{\partial z^2} - \frac{1}{c^2}\frac{\partial^2 E}{\partial t^2} - k_p^2 E(z,ct) = 0, \quad z > 0 \tag{5}$$

$$E(z,ct), \frac{\partial E}{\partial z}(z,ct) \quad \text{continuous across } z = 0 \tag{6}$$

$$E(z,ct) = \delta(z-ct) + R(z+ct), \quad z < 0 \tag{7}$$

$$k_p^2(z) = 3.54 \times 10^{-14} N(z) \tag{8}$$

For the direct scattering problem one knows $k_p^2(z)$ and finds R(z+ct). It is interesting to see whether the above equations yield a unique reflected wave.

Introducing Fourier transforms for the time dependent fields

$$E(z,ct) = \frac{1}{2\pi} \int_{-\infty}^{+\infty} \hat{E}(z,k) e^{-ikct}\, dk$$

$$\delta(z-ct) = \frac{1}{2\pi} \int_{-\infty}^{+\infty} e^{ik(z-ct)}\, dk$$

$$R(z+ct) = \frac{1}{2\pi} \int_{-\infty}^{\infty} r(k) e^{-ik(z+ct)}\, dk$$

with r(k) the familiar reflection coefficient equations (5) - (8) become

$$\frac{\partial^2}{\partial z^2} E(z,k) + [k^2 - k_p^2(z)]\hat{E}(z,k) = 0, \quad z > 0 \tag{9}$$

$$\hat{E}(z,k), \frac{\partial \hat{E}}{\partial z}(z,k) \quad \text{continuous across } z = 0 \tag{10}$$

$$\hat{E}(z,k) = e^{ikz} + r(k)e^{-ikz}, \quad z < 0 \tag{11}$$

$$k_p^2(z) = 3.54 \times 10^{-14} N(z) \tag{12}$$

It is well known that the direct problem as posed in equations (9), (10), (11) does not give a unique reflection coefficient. To get unique conditions one uses the Sommerfeld radiation condition

$$\frac{\partial \hat{E}}{\partial z}(z,k) - ik\,\hat{E}(z,k) \sim 0 \quad \text{as } z \to \infty \quad \text{provided } N(z) \to 0$$

as $z \to \infty$.

The form of $E(z,k)$ satisfying the Sommerfeld condition is

$$\hat{E}(z,k) \sim t(k)e^{ikz} \quad \text{as } z \to \infty \tag{13}$$

Equations (9), (10), (11), (12), (13) yield a unique reflection coefficient and field $\hat{E}(z,k)$.

The time domain description of a radiation condition is not included in the time domain equations (5), (6), (7), (8) for the plasma field $E(z,ct)$.

The time domain radiation condition must convey the idea that the time dependent field evolves as a wave propagating in the z-direction. At a point inside the plasma there are no fields until the plasma fields generated by the incoming δ-function reach the point.

The appropriate condition is the causality condition. With the causality condition the equations describing the electric field inside the plasma become

$$\frac{\partial^2 E}{\partial z^2} - \frac{1}{c^2}\frac{\partial^2 E}{\partial t^2} - k_p^2(z)\,E(z,ct) = 0, \quad z > 0 \tag{14}$$

$$E(z,ct),\ \frac{\partial E}{\partial z}(z,ct) \quad \text{continuous across } z = 0 \tag{15}$$

$$E(z,ct) = \delta(z-ct) + R(z+ct), \quad z < 0 \tag{16}$$

$$E(z,ct) = 0 \quad \text{for } t < \frac{z}{c} \quad \text{(causality condition)} \tag{17}$$

$$k_p^2(z) = 3.54 \times 10^{-14} N(z) \tag{18}$$

Knowing N(z) we can, in principle, find E(z,ct) and R(z+ct).

B. Plasma Inverse Problem[1]

In this section we use the equations describing the time dependent fields inside the plasma to derive an integral equation relating the reflected wave to the plasma density.

The previous section has shown that the electric field inside the plasma obeys the equations

$$\frac{\partial^2 E}{\partial z^2} - \frac{1}{c^2}\frac{\partial^2 E}{\partial t^2} - k_p^2(z)E(z,ct) = 0 , \quad z > 0 \tag{1}$$

$$E(z,ct) = \delta(z-ct) + R(z+ct) , \quad z < 0 \tag{2}$$

$$E(z,ct),\ \frac{\partial E}{\partial z}(z,ct) \quad \text{continuous across } z = 0 \tag{3}$$

$$E(z,ct) = 0 \quad \text{for } t < \frac{z}{c} \quad \text{(causality condition)} \tag{4}$$

$$k_p^2(z) = 3.54 \times 10^{-14} N(z) \tag{5}$$

A relation is to be found between the time record of the reflected wave and the electron density. Expressing the fields in their Fourier Transforms

---

[1] This section is an outgrowth of a careful study of the works of I. Kay. See References 1,2,3.

$$E(z,ct) = \frac{1}{2\pi} \int_{-\infty}^{+\infty} \hat{E}(z,k) e^{-ikct}\, dk \tag{6}$$

$$\delta(z-ct) = \frac{1}{2\pi} \int_{-\infty}^{+\infty} e^{ik(z-ct)}\, dk$$

$$R(z+ct) = \frac{1}{2\pi} \int_{-\infty}^{+\infty} r(k) e^{-ik(z+ct)}\, dk \tag{8}$$

equations (1), (2), (3), (4), (5) become

$$\frac{\partial^2 \hat{E}}{\partial z^2} + [k^2 - k_p^2(z)]\hat{E}(z,k) = 0 \ , \quad z > 0 \tag{9}$$

$$\hat{E}(z,k) = e^{ikz} + r(k)e^{-ikz} \ , \quad z < 0 \tag{10}$$

$$\hat{E}(z,k), \ \frac{\partial E}{\partial z}(z,k) \ \text{ continuous across } z = 0 \tag{11}$$

$$E(z,ct) = 0 \qquad t < \frac{z}{c} \tag{12}$$

$$k_p^2(z) = 3.54 \times 10^{-14} N(z) \tag{13}$$

We need certain concepts.

Characteristic Fields

Definition: Let the total field in region $z < 0$ be e^{ikz}. By characteristic field at a point $z = z_1$ inside the plasma we mean the difference between the actual field at $z = z_1$ and the field resulting at z_1 if the outside field (field in region $z < 0$) was left free to propagate in space. We write this characteristic field $\hat{C}_1(z,k)$. If the total outside field is e^{-ikz} then a similar procedure

defines $\hat{C}_2(z,k)$.

From its definition

$$\hat{C}_1(z,k) = \begin{cases} 0, & z \leq 0 \\ \hat{F}_1(z,k) - e^{ikz}, & z \geq 0 \end{cases} \tag{14}$$

where $\hat{F}_1(z,k)$ is the plasma field due to an outside field e^{ikz}.

From its definition

$$\hat{C}_2(z,k) = \begin{cases} 0, & z \leq 0 \\ \hat{F}_2(z,k) - e^{-ikz}, & z \geq 0 \end{cases} \tag{15}$$

where $F_2(z,k)$ is the field inside the plasma due to an outside field e^{-ikz}.

Equations (14), (15) show that the time dependent characteristic fields obey the equations

$$C_1(z,ct) = \begin{cases} 0, & z \leq 0 \\ F_1(z,ct) - \delta(z-ct), & z \geq 0 \end{cases} \tag{16}$$

$$C_2(z,ct) = \begin{cases} 0, & z \leq 0 \\ F_2(z,ct) - \delta(z+ct), & z \geq 0 \end{cases} \tag{17}$$

where

$$C_1(z,ct) = \frac{1}{2\pi} \int_{-\infty}^{+\infty} \hat{C}_1(z,k) e^{-ikct}\, dk \tag{18}$$

$$C_2(z,ct) = \frac{1}{2\pi} \int_{-\infty}^{+\infty} \hat{C}_2(z,k) e^{-ikct}\, dk \tag{19}$$

Properties of Characteristic Fields

1. The characteristic fields are unique. The field $\hat{F}_1(z,k)$ was defined to be the plasma field for an outside field e^{ikz}. $\hat{F}_1(z,k)$ is the solution of (9), (10), (11) where $r(k) = 0$.

$$\frac{\partial^2 \hat{F}_1}{\partial z^2} + [k^2 - k_p^2(z)]\hat{F}_1 = 0, \quad z > 0$$

$$\hat{F}_1 = e^{ikz}, \quad z < 0$$

$$\hat{F}_1, \frac{\partial \hat{F}_1}{\partial z} \quad \text{continuous across} \quad z = 0$$

Setting $\hat{F}_1 = e^{ikz} + \hat{C}_1$ we get

$$\frac{\partial^2 \hat{C}_1}{\partial z^2} + [k^2 - k_p^2(z)]\hat{C}_1(z,k) = k_p^2(z) e^{ikz}, \quad z > 0 \tag{20}$$

$$\hat{C}_1(o,k) = \frac{\partial \hat{C}_1}{\partial z}(o,k) = 0 \tag{21}$$

$$\hat{C}_1(z,k) = 0, \quad z < 0 \tag{22}$$

Equation (20) is an ordinary differential equation. When $k_p^2(z)$ is known, boundary conditions (21) uniquely determine the solution of (20). We conclude that $\hat{C}_1(z,k)$ is unique.

A similar procedure for $\hat{C}_2(z,k)$ shows that $\hat{C}_2(z,k)$ is unique.

Equations (18), (19) show that $C_1(z,ct)$ and $C_2(z,ct)$ are unique.

2. The characteristic fields are zero outside the plasma.

This property is a direct consequence of the definitions of the characteristic fields for $z < 0$.

3. The characteristic fields are related.

It is easy to show that $C_2(z,k)$ obeys the differential equation

$$\frac{d^2\hat{C}_2}{dz^2} + (k^2 - k_p^2)\hat{C}_2 = k_p^2 e^{-ikz}, \quad z > 0 \tag{23}$$

$$\hat{C}_2(o,k) = \frac{\partial \hat{C}_2}{\partial z}(o,k) = 0 \tag{24}$$

Comparison with (20), (21) shows that

$$\hat{C}_2(z,k) = \hat{C}_1(z,-k) \tag{25}$$

Equations (25) and (19) show

$$C_2(z,ct) = C_1(z,-ct) \tag{26}$$

4. A characteristic field uniquely determines the plasma.

If one knows $\hat{C}_1(z,k)$ in a neighborhood of z_1 and at a wave number k_1, he solves for $k_p^2(z_1)$ in equation (20). Equation (23) shows that the same procedure can be followed for $\hat{C}_2(z,k)$.

In the time domain the characteristic fields uniquely determine $k_p^2(z)$. Fourier Transforming equations (20), (21), (22) according to (18) we obtain

$$\frac{\partial^2 C_1}{\partial z^2}(z,ct) - \frac{1}{c^2}\frac{\partial^2 C_1}{\partial t^2}(z,ct) - k_p^2(z)C_1(z,ct) = k_p^2(z)\delta(z-ct), \quad z > 0 \tag{27}$$

$$C_1(o,ct) = \frac{\partial C_1}{\partial z}(o,ct) = 0 \tag{28}$$

Appendix A shows that equations (27), (28) are equivalent to[2]

$$\frac{\partial^2 C_1}{\partial z^2}(z,ct) - \frac{1}{c^2}\frac{\partial^2 C_1}{\partial t^2}(z,ct) - k_p^2(z)C_1(z,ct) = 0, \quad -z < ct < z \tag{29}$$

$$\frac{d}{dz}C_1(z,z) = \frac{1}{2}k_p^2(z) \tag{30}$$

Signature equation ($\frac{d}{dz}$ = total derivative with respect to z)

$$C_1(z,-z) = 0 \tag{31}$$

$$C_1(z,ct) = 0 , \quad ct > z \tag{32}$$

$$C_1(z,ct) = 0 , \quad ct < -z \tag{33}$$

The time domain characteristic fields uniquely describe the plasma. If one knows $C_1(z,ct)$ around $z = z_1$, $ct = ct_1$, he can determine $k_p^2(z_1)$ from equation (29). However, if he knows $C_1(z,ct)$

---

[2]Equations (29), (30), (31) form the Goursat problem of partial differential equations. See Reference 24, p. 27.

near $z = z_1$ and $ct = z_1$ he can also determine $k_p^2(z_1)$ from the signature equation.

Equation (30) provides the simplest way by which one can find $k_p^2(z)$ from the characteristic fields. Using equation (13) relating the plasma wave number to the electron density, he finds $N(z)$.

Similar procedures show that one can find $N(z)$ from $C_2(z,ct)$.

Plasma Inverse Problem (continued)

We return to the inverse problem in the frequency domain. Let e^{ikz} be an incident wave to a plasma with an electron density $N(z)$ and $k_p^2(z) = 3.54 \times 10^{-14} \times N(z)$. The plasma density is assumed to be zero for $z < 0$. Due to the presence of the plasma a reflected field will appear. Using the principle of superposition and the definition of characteristic fields we write the solution of (9), (10), (11) as

$$\hat{E}(z,k) = e^{ikz} + r(k)e^{-ikz} + \hat{C}_1(z,k) + r(k)\hat{C}_1(z,-k), \quad z \geq 0 \qquad (35)$$

where $C_1(z,k)$ is the characteristic field determined by $k_p^2(z)$.

Equation (35) does not correspond to the physical situation of incident e^{ikz} and reflected $r(k)e^{-ikz}$ waves. We haven't imposed the requirement of no sources at $z = \infty$. To insure $\hat{E}(z,k)$ is the actual plasma field we need to satisfy the causality condition (12).

Taking Fourier transforms according to (6), (7), (8), (18) we obtain

$$E(z,ct) = \delta(z-ct) + R(z+ct) + C_1(z,ct) + \frac{1}{2\pi}\int_{-\infty}^{+\infty} r(k)\hat{C}_1(z,-k)\bar{d}^{ikct}\,dk$$

The last integral is a convolution integral. Doing the algebra we find

$$E(z,ct) = \delta(z-ct) + R(z+ct) + C_1(z,ct) + \int_{-\infty}^{+\infty} C_1(z,z')R(z'+ct)dz', \qquad z \geq 0$$

$C_1(z,ct)$ is the plasma characteristic field. Equation (32) shows that we can replace the upper limit of the integral. We obtain

$$E(z,ct) = \delta(z-ct) + R(z+ct) + \int_{-\infty}^{z} C_1(z,z')R(z'+ct)dz' + C_1(z,ct), \qquad z \geq 0$$

Imposing the causality condition on $E(z,ct)$ we find

$$R(z+ct) + C_1(z,ct) + \int_{-\infty}^{z} C_1(z,z')R(z'+ct)dz' = 0 \qquad z \geq 0,\ ct < z$$

The above equation was first obtained by I. Kay in 1955.[3] In Appendix B we show that the equation is satisfied even for $ct = z$. Thus,

$$R(z+ct) + C_1(z,ct) + \int_{-\infty}^{z} C_1(z,z')R(z'+ct)dz' = 0,\ z \geq 0,\ ct \leq z \qquad (36)$$

In Appendix C we show that if the integral equation

---

[3] See Reference 1, p. 13. Note that here we have no poles of $\hat{E}(z,k)$ in the upper half-k plane since $k_p^2(z) \geq 0$.

$$R(z,ct) + f(z,ct) + \int_{-\infty}^{z} f(z,z')R(z'+ct)dz' = 0, \quad z \geq 0, \quad ct \leq z$$

has a solution f(z,ct) for $ct \leq z$, then the solution is unique. Since equation (36) shows that the characteristic field is one solution of (37), then the solution of (37) coincides with the characteristic field in the region $ct \leq z$. Therefore f(z,ct) satisfies equations (29), (31), (34). In particular the signature equation is satisfied

$$\frac{d}{dz}f(z,z) = \frac{1}{2}k_p^2(z)$$

We have shown that equation (36) uniquely determines $C_1(z,ct)$ in the region $ct \leq z$.

The function R (z+ct) has a meaning explained by the characteristic field definition. R(z+ct) is a free space field in the region $z > 0$ propagating towards the -z direction. When this field reaches the region $z \leq 0$ it becomes indistinguishable from the observed reflected wave. In short, R(z+ct) is the reflected wave travelling freely in all space.

In the Appendix D we show that

$$R(z+ct) = 0, \quad z + ct \leq 0 \tag{38}$$

Using equations (31), (34), (36) we find this equation (38) satisfied

With the help of equations (31), (34) equation (36) takes its final form.[4]

---

[4]Equation (39) is a Fredholm integral equation. See Reference 25 for more details.

$$R(z+ct) + C_1(z,ct) + \int_{-ct}^{z} C_1(z,z')R(z'+ct)dz' = 0$$

$$z \geq 0, \quad -z \leq ct \leq z \tag{39}$$

Main Integral Equation

Equation (39) along with the signature equation and the equation relating $k_p^2(z)$ to $N(z)$

$$\frac{d}{dz}C_1(z,z) = \frac{1}{2} k_p^2(z) \qquad \text{Signature Equation} \tag{40}$$

$$k_p^2(z) = 3.54 \times 10^{-14} N(z) \qquad k_p^2 - N \text{ Relation} \tag{41}$$

completely describe the electron density $N(z)$ when the reflected wave time record (reflected wave as recorded by an observer situated at the origin $z = 0$) $R(ct)$ is given.

Summary

We have seen that if a δ-function field, $\delta(z-ct)$ is incident on a plane stratified plasma located in the region $z > 0$, a reflected wave results. We assume that the reflected wave is recorded by an observer situated at $z = 0$.

We have shown that the reflected wave determines the plasma density $N(z)$ as a function of z. One solves the main integral equation for the characteristic field $C_1(z,ct)$. Using the signature equation and the k_p^2 - N relation he obtains $N(z)$.

$$R(z+ct) + C_1(z,ct) + \int_{-ct}^{z} C_1(z,z')R(z'+ct)dz' = 0$$

$$z \geq 0, \quad -z \leq ct \leq z \qquad (42)$$

Main Integral Equation

$$\frac{d}{dz} C_1(z,z) = \frac{1}{2} k_p^2(z) \quad \text{Signature Equation} \qquad (43)$$

$$k_p^2(z) = 3.54 \times 10^{-14} N(z) \quad k_p^2 - N \text{ Relation} \qquad (44)$$

Equations (42), (43), (44) describe the inverse scattering algorithm for the plane stratified plasma.

C. Inverse Scattering Algorithm

In this section we explain the inverse scattering algorithm obtained in the last section. We provide a simple conceptual model of the procedure one follows to solve the algorithm. Useful properties of the reflected wave are given.

We have shown an algorithm, equations (1), (2), (3), which provides the electron density N(z) from the reflected wave

$$R(z+ct) + C_1(z,ct) + \int_{-ct}^{z} C_1(z,z')R(z'+ct)dz' = 0, \quad z \geq 0$$

$$-z \leq ct \leq z \qquad (1)$$

Main Integral Equation

$$\frac{d}{dz} C_1(z,z) = \frac{1}{2} k_p^2(z) \qquad \text{Signature Equation} \qquad (2)$$

$$k_p^2(z) = 3.54 \times 10^{-14} N(z) \qquad k_p^2 - N \text{ Relation} \qquad (3)$$

Our problem considers a δ-function field $\delta(z-ct)$ normally incident on the plasma from the region $z < 0$. The δ-function arrives at $z = 0$ at time $t = 0$. $R(ct)$ is the reflected wave which an observer at $z = 0$ observes passing by.

We can show that $R(ct)$ is a continuous function of ct.

$R(ct)$ is a continuous function of ct[1] (4)

$R(ct)$ is equal to zero for $z \leq 0$.

---

[1] See Appendix D.

$$R(ct) = 0, \quad ct \leq 0 \tag{5}$$

We define as "distance" record of the reflected wave the graph as a function of ct, time x speed of light, produced by a monitor stationed at z = 0.

The distance record of the reflected wave is an easily measured quantity. Any observer in the region $z < 0$ obtains the "distance" record by proper time shifting.

We formulate a simple conceptual model for solving the inverse scattering algorithm (equations (1), (2), (3)). An observer in the region $z < 0$ finds the electron density N(z) as follows:

Step 1 He decides at which distance inside the plasma he wants the electron density. Say, he wants to find the electron density at $z = z_1$.

Step 2 Using the distance record of R(ct) from ct = 0 to $ct = 2z_1$, he solves the main integral equation (1) for $C_1(z_1,ct)$. He obtains $C_1(z_1,z_1)$.

Step 3 He repeats the steps 2,3 for $z = z_1 - \ell$, ℓ small. He finds $C_1(z_1-\ell, z_1-\ell)$.

Step 4 He uses the signature equation (2) to find $k_p^2(z)$

$$k_p^2(z_1) \sim \frac{C_1(z_1,z_1) - C_1(z_1-\ell,z_1-\ell)}{\ell}$$

Step 5 He uses the k_p^2 - N relation (3) to find $N(z_1)$ from $k_p^2(z_1)$.

The above mentioned procedure is a simple structural model of the way one goes about solving the inverse scattering algorithm. The next chapter shows how one carries out steps 2,3,4.

Until this point in the thesis we haven't pointed out any requirements on the nature of $k_p^2(z)$ for $z \geq 0$. We have assumed that $k_p^2(z)$ is a non-negative[2], continuous, bounded function of z which drops to zero "fast enough" when z is large. Under these assumptions $C_1(z,ct)$ is a continuous function in $z \geq 0$, $-z \leq ct \leq z$. Also R(ct) is a continuous function of ct.

However, it seems that the requirements are too strict. We have shown that to find $k_p^2(z_1)$ at $z = z_1$, one needs the distance record of the reflected wave from ct = 0 to $ct = 2z_1$. This means that one needs to know the time record of the reflected wave from the moment the δ-function hits the beginning of the plasma to the time it takes for the δ-function generated plasma fields to travel with the speed of light to the point $z = z_1$ and come back. It is clear that the time record of the reflected wave for time $0 \leq t \leq \frac{2z_1}{c}$ cannot depend on the values of $k_p^2(z_1)$ for $z > z_1$.

Appendix D shows that the reflected wave R(ct) is a continuous function of ct for piecewise continuous, bounded, positive $k_p^2(z)$ which drop to zero when z is large. Assuming that the main

---

[2] The requirement that $k_p^2(z)$ be a non-negative function of z expresses the physical constraint that the number of electrons/m^3 N(z) is always a number greater than or equal to zero.

integral equation (1) holds for piecewise continuous $k_p^2(z)$, then $C_1(z,ct)$ must be a continuous function for $z \geq 0$, $-z \leq ct \leq z$.

It seems possible that one can extend formally the inverse scattering algorithm to include a wide class of allowable electron densities N(z). In particular it seems permissible to use the inverse scattering algorithm equations (1), (2), (3) to obtain N(z) in a region $0 \leq z < L$ when N(z) is positive, piecewise continuous, bounded function of z in the region $0 \leq z \leq L$. The functions R(ct), $C_1(z,ct)$ will be continuous,

$R(ct)$ continuous for $0 \leq ct \leq 2L$

$C_1(z,ct)$ continuous for $0 \leq z \leq L$, $-z \leq ct \leq z$.

III. NUMERICAL METHOD

This chapter describes a numerical method solving the plasma inverse scattering algorithm. Examples are provided to test the accuracy of the solution. We show that a thin square pulse can be used instead of a δ-function incident wave.

A. Numerical Solution

This section describes a numerical solution of the inverse scattering algorithm.

$$R(z+ct) + C_1(z,ct) + \int_{-ct}^{z} C_1(z,z')R(z'+ct)dz' = 0 \qquad z \geq 0, \quad -z \leq ct \leq z \qquad (1)$$

Main Integral Equation

$$\frac{d}{dz} C_1(z,z) = \frac{1}{2} k_p^2(z) \qquad \text{Signature Equation} \qquad (2)$$

$$k_p^2(z) = 3.54 \times 10^{-14} N(z) \qquad k_p^2 - N \text{ Relation} \qquad (3)$$

a. Characteristic Field

This subsection describes a numerical solution of the main integral equation for the characteristic field $C_1(z,ct)$ at any point inside the plasma.

The characteristic field $C_1(z,ct)$ and the reflected wave $R(ct)$ are related by the main integral equation

$$R(z+ct) + C_1(z,ct) + \int_{-ct}^{z} C_1(z,z')R(z'+ct)dz' = 0 \ , \quad z \geq 0,$$
$$-z \leq ct \leq z \qquad (4)$$

We solve (4) by matrix inversion. That is, we fix z to a certain value and then we divide the ct-interval from -z to +z into 2M equal intervals of width h. Then we write a system of integral equations. In each equation ct takes a different value.

$$R(z+ct_i) + C_1(z,ct_i) + \int_{-ct_i}^{z} C_1(z_1z')R(z'+ct_i)dz' = 0, \quad i = 1,2...2M+1 \qquad (5)$$

where

$$ct_i = -z + (i-1)h$$

$$h = \frac{z}{M}$$

In each of equations (5) we expand the integrals using some integration rule which involves $C_1(z,ct_i)$, $R(z+ct_i)$.

We obtain 2M+1 linear equations for 2M+1 unknowns $C_1(z,ct_i)$. Solving the system by matrix inversion, we obtain $C_1(z,ct_i)$ and $C_1(z,z)$

$$C_1(z,z) = C_1(z,ct_{2M+1})$$

The details for the linearization of (4) are rather cumbersome to write down because of the inconvenience which arises from the fact that the lower limit of integration in the integrals

of equation (5) is a function of ct. This property of the lower limit forces us to choose a combination of Simson and trapezoidal rules for finding out the approximate value of the integrals. Simson's rule alone does not work because it requires that the number of division sub-intervals in the interval $-ct_i \leq ct \leq z$ is an even number[1] and in our integrations this is not always the case. For example the integral

$$\int_{-ct_i}^{z} C_1(z,z')R(z'+ct)dz'$$

contains an odd number od division sub-intervals for $ct_i = 2M, 2M-2,\ldots 2$. For these cases we take care of the extra interval by writing

$$\int_{-ct_i}^{z} C_1(z,z')R(z'+ct_i)dz' = \int_{z-h}^{z} C_1(z,z')R(z'+ct_i)dz' + \int_{-ct_i}^{z-h} C_1(z,z')R(z'+ct_i)dz' \qquad (6)$$

The first integral on the right hand side of (6) is found by the trapezoidal rule. The second integral on the right hand side has an even number of division sub-intervals. We use Simson's rule for its evaluation.

---

[1] See Reference 26.

The numerical procedure yields a matrix equation of the form

$$\mathcal{A}X + \mathcal{R} = 0 \tag{7}$$

where

$$X = (x_i), \quad X \text{ is a } 2M+1 \text{ vector}$$

$$x_i = C_1[z,(M+1-i)h] \quad \text{for } i = 1,2,\ldots,2M+1$$

$$\mathcal{R} = (r_i), \quad \mathcal{R} \text{ is a } 2M+1 \text{ vector}$$

$$r_i = R[(i-1)h] \quad \text{for } i = 1,2,\ldots,2M+1$$

$$h = \frac{z}{M}$$

$$\mathcal{A} = (a_{ij}), \quad \mathcal{A} \text{ is a } (2M+1) \times (2M+1) \text{ matrix}$$

$$a_{ij} = a'_{ij} + \delta_{i,2M+1-j}, \quad \text{for } i,j = 1,2\ldots,2M+1$$

The elements $a'_{i,j}$ are

$$a'_{i+k,i} = \begin{cases} \frac{h}{2} r_{k+1} & \text{for } i = 1 \text{ and } k = 1,3,5\ldots,2M-1 \\ \frac{4}{3}h\, r_{k+1} & \text{for } i = 2,3\ldots,2M+1-k \text{ and } k = 1,3,5\ldots,2M-1 \end{cases}$$

$$a'_{i+k,i} = \begin{cases} \frac{h}{3} r_{k+1} & \text{for } i = 1 \text{ and } k = 2,4,6,\ldots,2M-2 \\ \frac{5h}{6} r_{k+1} & \text{for } i = 2 \text{ and } k = 2,4,6,\ldots,2M-2 \\ \frac{2h}{3} r_{k+1} & \text{for } i = 3,5,7,\ldots 2M+1-k \text{ and } k = 2,4,6,\ldots,2M-2 \end{cases}$$

$$a'_{i,i} = \begin{cases} 0 & \text{for } i = 1 \\ \frac{h}{2} r_1 & \text{for } i = 2 \\ \frac{h}{3} r_1 & \text{for } i = 3,4\ldots,2M+1 \end{cases}$$

$$a'_{i,j} = 0 \quad \text{for } i < j$$

The Kronecker δ-function is defined to be

$$\delta_{i,j} = \begin{cases} 0 & \text{for } i \neq j \\ 1 & \text{for } i = j \end{cases}$$

We invert matrix equation (7). We obtain X

$$X = \mathcal{A}^{-1}(-R) \tag{8}$$

The value of the characteristic field at ct = z is found from x_1

$$C_1(z,z) = x_1 \tag{9}$$

The numerical method described in this section has been incorporated into a main computer program in the form of a sub-routine named INVER.[2] Vector R is the input to INVER. The output is $C_1(z,z)$.

We show some examples of the numerical procedure.

For M = 1, the matrices in equation (7) have the form

$$\mathcal{A} = \begin{bmatrix} 0 & 0 & 1 \\ \frac{h}{2} r_2 & 1+\frac{h}{2} r_1 & 0 \\ 1+\frac{h}{3} r_3 & \frac{4h}{3} r_2 & \frac{h}{3} r_1 \end{bmatrix} \quad X = \begin{bmatrix} C_1(z,z) \\ C_1(z,0) \\ C_1(z,-z) \end{bmatrix} \quad R = \begin{bmatrix} R(o) \\ R(h) \\ R(2h) \end{bmatrix}$$

[2] See Appendix E for computer flow chart.

with

$$h = z$$

For M = 3, we find

$$a = \begin{bmatrix} 0 & 0 & 0 & 0 & 0 & 0 & 1 \\ \frac{h}{2}r_2 & \frac{hr_1}{2} & 0 & 0 & 0 & 1 & 0 \\ \frac{h}{3}r_3 & \frac{4h}{3}r_2 & \frac{h}{3}r_1 & 0 & 1 & 0 & 0 \\ \frac{h}{2}r_4 & \frac{5h}{6}r_3 & \frac{4h}{3}r_2 & 1+\frac{h}{3}r_1 & 0 & 0 & 0 \\ \frac{h}{3}r_5 & \frac{4h}{3}r_4 & 1+\frac{2h}{3}r_3 & \frac{4h}{3}r_2 & \frac{h}{3}r_1 & 0 & 0 \\ \frac{h}{2}r_6 & 1+\frac{5h}{6}r_5 & \frac{4h}{3}r_4 & \frac{2h}{3}r_3 & \frac{4h}{3}r_2 & \frac{h}{3}r_1 & 0 \\ 1+\frac{h}{3}r_7 & \frac{4h}{3}r_6 & \frac{2h}{3}r_5 & \frac{4h}{2}r_4 & \frac{2h}{3}r_3 & \frac{4h}{3}r_2 & 1+\frac{h}{3}r_1 \end{bmatrix}$$

$$X = (x_i) \; ; \quad x_i = C_1[z,(4-i)h] \quad \text{for } i = 1,\ldots,7$$

$$R = (r_i) \; ; \quad r_i = R[(i-1)h] \quad \text{for } i = 1,\ldots,7$$

$$h = \frac{z}{3}$$

b. Electron Density

This subsection describes a method with which we obtain the electron density N(z) from the characteristic field $C_1(z,z)$.

The last subsection describes a method with which we obtain the characteristic field $C_1(z,z)$ from the distance record of the reflected wave R(ct). We show how to find N(z) from $C_1(z,z)$.

Taylor series expansion shows

$$C_1(z+\ell) - C_1(z,z) = \ell \frac{d}{dz} C_1(z,z) + \text{higher order terms} \tag{10}$$

$$C_1(z-\ell,z-\ell) - C_1(z,z) = -\ell \frac{d}{dz} C_1(z,z) + \text{h.o.t.} \tag{11}$$

Subtracting (11) from (10) we get

$$\frac{d}{dz} C_1(z,z) = \frac{C_1(z+\ell,z+\ell) - C_1(z-\ell,z-\ell)}{\ell} + \text{h.o.t.} \tag{12}$$

Using the signature equation and the k_p^2 - N relation we obtain

$$N(z) \sim \frac{2}{3.54 \times 10^{-14}} \frac{C_1(z+\ell,z+\ell) - C_1(z-\ell,z-\ell)}{\ell} \tag{13}$$

Equation (13) shows how we obtain N(z) from $C_1(z+\ell,z+\ell)$, $C_1(z-\ell,z-\ell)$, ℓ small and $\ell > 0$. The numerical method described in this section has been incorporated into a main computer program in the form of a subroutine named ELECTRON DENSITY.[3] $C_1(z+\ell,z+\ell)$, $C_1(z-\ell,z-\ell)$ are the inputs to ELECTRON DENSITY. The subroutine provides N(z) using equation (13).

c. Errors

In this sub-section we discuss the accuracy of the numerical solution of the inverse scattering algorithm.

We define the approximate quantities $\tilde{C}_1(z,z;M)$, $\tilde{N}(z;M)$ and percent errors $\varepsilon(z;M)$, $\mu(z;M)$.

---

[3] See Appendix E.

Definitions

$\tilde{C}_1(z,z;M)$ is an approximate value for the characteristic field at z,ct = z. We obtain $\tilde{C}_1(z,z;M)$ with the numerical method described in Section A.a. M is the number of intervals we divide the distance from 0 to z.

$\tilde{N}(z;M)$ is an approximate value for the electron density at z. We obtain $\tilde{N}(z;M)$ with the numerical method described in Section A.b. $\mu(z;M)$ is the percent error in the characteristic field

$$\mu(z;M) = \frac{C_1(z,z) - \tilde{C}_1(z,z;M)}{C_1(z,z)} \times 100 \qquad (14)$$

$\varepsilon(z;M)$ is the percent error in the electron density

$$\varepsilon(z;M) = \frac{N(z) - \tilde{N}(z;M)}{N(z)} \times 100 \qquad (15)$$

$C_1(z,z)$ is the exact value of the characteristic field. It is obtained when one solves exactly the inverse scattering algorithm.

N(z) is the exact value of the electron density. It is obtained when one solves exactly the inverse scattering algorithm.

The percent error $\varepsilon(z;M)$ is a useful quantity. It indicates how well the numerical method produces the electron density of the plasma. However, we cannot give an exact formula for $\varepsilon(z;M)$. We do not know N(z). We developed the inverse scattering algorithm to find N(z). The only thing we know about N(z) is the distance record of the reflected wave R(ct). We have reason to believe that the relation between R(ct) and N(z) is complicated. Only complex

mathematical abstractions, such as the inverse scattering algorithm, describe the relation. It is clear that we should not ask for an expression for the percent error $\varepsilon(z;M)$ that involves $N(z)$.

The numerical method described in Sections Aa, Ab, shows that we have at our disposal two parameters which we can change at will when we calculate the approximate electron density $\tilde{N}(z;M)$. The two parameters are ℓ, and M.

The parameter ℓ has dimensions of length. We introduced it in order to carry out numerically the differentiation described by the signature equation (2). The error introduced by the numerical differentiation of the signature equation is negligible if ℓ is small.

To find $\tilde{N}(z;M)$ we use equation (15)

$$\tilde{N}(z;M) = \frac{2}{3.54\text{x}10^{-14}} \text{ x } \frac{\tilde{C}_1(z+\ell,z+\ell) - \tilde{C}_1(z-\ell,z-\ell)}{\ell} \tag{16}$$

In theory, we can take ℓ as small as we want.[4] For ℓ sufficiently small[5] the right hand side of equation (16) becomes

$$\tilde{N}(z;M) \cong \frac{2}{3.54 \text{ x } 10^{-14}} \frac{d}{dz} \tilde{C}_1(z,z;M) \tag{17}$$

From the signature equation (2) and the k_p^2-N relation we get

---

[4] Care must be exercised so that we do not choose ℓ too small. Otherwise single precision programming gives 0 for the difference $\tilde{C}_1(z+\ell,z+\ell;M) - \tilde{C}_1(z-\ell,z-\ell;M)$.

[5] The magnitude of the parameter ℓ is connected with the local variation of the electron density at z. If λ is the wavelength of the variation of $N(z)$ at z, then for $\lambda >> \ell$ equation (17) is satisfied.

$$N(z) = \frac{2}{3.54 \times 10^{-14}} \frac{d}{dz} C_1(z,z) \tag{18}$$

Equations (17) and (18) show that $\tilde{N}(z;M)$ is close to $N(z)$ if $\tilde{C}_1(z,z;M)$ is close to $C_1(z,z)$.

From the definition of the percent error in the characteristic field we obtain

$$\frac{d}{dz}\mu(z,M) = \frac{[\frac{d}{dz} C_1(z,z) - \frac{d}{dz}\tilde{C}_1(z,z;M)]\, C_1(z,z)}{C_1^2(z,z)} \times 100$$

$$- \frac{[C_1(z,z) - C_1(z,z;M)]\frac{d}{dz} C_1(z,z)}{C_1^2(z,z)} \times 100$$

Multiplying both sides of the above equation by the ratio

$$\frac{C_1(z,z)}{\frac{d}{dz} C_1(z,z)}$$

and using (17), (18) we get

$$\frac{C_1(z,z)}{\frac{d}{dz} C_1(z,z)} \frac{d}{dz}\mu(z;M) = \frac{N(z) - \tilde{N}(z;M)}{N(z)} \times 100 - \frac{C_1(z,z) - \tilde{C}_1(z,z;M)}{C_1(z,z)} \times 100$$

Equations (14) and (15) used on the equation above show that

$$\varepsilon(z;M) = \mu(z;M) + \frac{C_1(z,z)}{\frac{d}{dz} C_1(z,z)} \frac{d}{dz}\mu(z;M) \tag{19}$$

From the signature equation

$$\frac{d}{dz} C_1(z,z) = \frac{1}{2} k_p^2(z)$$

we obtain

$$C_1(z,z) = \frac{1}{2} \int_o^z k_p^2(\xi)\, d\xi$$

Using the k_p^2 - N relation

$$k_p^2(z) = 3.54 \times 10^{-14} N(z)$$

we find that

$$\frac{C_1(z,z)}{\frac{d}{dz} C_1(z,z)} = \frac{\int_o^z N(\xi) d\xi}{N(z)}$$

Finally equation (19) becomes

$$\varepsilon(z;M) = \mu(z;M) + \frac{\int_o^z N(\xi) d\xi}{N(z)} \frac{d}{dz} \mu(z;M) \qquad (20)$$

Equation (20) relates the percent error $\varepsilon(z;M)$ in the electron density to the percent error in the characteristic field $\mu(z;M)$. We show that the percent error $\varepsilon(z;M)$ decreases with M.

The parameter M is a number. We introduced M in Section A.a as the number of equal subintervals we divide the interval from 0 to z. The parameter M serves an important function. It controls the percent error $\varepsilon(z;M)$. The bigger M is, the smaller the error $\varepsilon(z;M)$.

Error Statement

For small[6] percent errors $\varepsilon(z;M)$, $\varepsilon(z;M)$ is to a good approximation inversely proportional to the fourth power of M.

In Appendix F we prove the statement by showing that

$$\mu(z;M) \tilde{=} \frac{1}{0.9M^4} \frac{z^5}{C_1(z,z)} \frac{\partial^4}{\partial z'^4} R(z'+z)C_1(z,z') \quad , |z'| \leq z \qquad (21)$$

Equation (21) when substituted into (20) shows the statement.

The error statement shows that the numerical method converges. That is for small $\varepsilon(z,M)$ increasing the number of subintervals we divide the interval 0 to z, increases the accuracy of the method.

This property of the converging error shows that one can say a posteriori something about the accuracy of the approximate electron density. For example suppose we obtain a value $\tilde{N}_1(z;M_1)$ for the approximate electron density at z and $M = M_1$. Then we increase M to M_2, say $M_2 = 2M_1$, and we use the numerical method again to find another approximate value $\tilde{N}_2(z;M_2)$. If the percent error

$$\left| \frac{\tilde{N}_2 - \tilde{N}_1}{\tilde{N}_2} \right| \times 100$$

is small, we can say that $\tilde{N}_2(z;M_2)$ is close to the exact electron density.

---

[6] Our examples show that we can take as small percent errors $\varepsilon(z;M)$ all errors $\varepsilon(z;M)$ whose absolute value is less than 20%.

Additional comments on the error $\varepsilon(z;M)$, and in particular about the range for which we expect $\varepsilon(z;M)$ to be small, are provided under Section D of this chapter.

B. Examples

This section provides examples to test the accuracy of the numerical solution of the inverse scattering algorithm.

For certain special electron density profiles, the inverse scattering algorithm has been solved exactly by analytical means. Each of these special electron density profiles has parameters. To indicate certain important features of the numerical solution we create 3 general categories of electron density "levels" by appropriately choosing the parameters for each example. The categories are the Low-Level category, the Medium-Level category, and the High-Level category.

In the Low-Level category[1] the maximum electron density N_{max} is approximately 10^4 electrons/m^3.

In the Medium-Level category[2] the maximum electron density N_{max} is approximately 10^8 electrons/m^3.

In the High-Level category[3] the maximum electron density N_{max} is approximately 10^{16} electrons/m^3.

Examples 1,2,3,4 appear in a paper written by Sims[4]. Example 5 is easily obtained by solving the direct scattering problem for a constant electron density. Examples 1,4,5 have the same maximum electron density N_{max}. It occurs at $z = 0$. However in each of these examples the electron density behaves differently when z is large.

---

[1] These electron densities appear in interstellar space.

[2] These electron densities appear in the ionospheric D-layer.

[3] These electron densities appear in laboratory plasmas.

[4] See Reference 5.

In example 1, the electron density drops to zero for large z like $\frac{1}{z^2}$.

In example 4, the electron density drops to zero for large z like a decaying exponential.

In example 5, the electron density is constant. We do not test the numerical method for the Medium and High-Level categories of examples 2 and 3. They do not demonstrate any important principles.

The function H(z) appearing in the examples is defined by

$$H(z) = \begin{cases} 0, & z < 0 \\ 1, & z \geq 0 \end{cases}$$

Example 1

$$N(z) = \frac{1}{3.54 \times 10^{-14}} \quad \frac{8}{(D + 2z)^2} H(z)$$

$$R(ct) = -\frac{2}{D} e^{-ct/D} \sin(ct/D)\, H(ct)$$

Low-Level : $D = 10^5$ m

$N_{max} = N(o) \cong 2 \times 10^4$ el/m^3

Medium Level : $D = 10^3$ m

$N_{max} = N(o) \cong 2 \times 10^8$ el/m^3

High-Level : $D = 10$ cm

$N_{max} = N(o) \cong 2 \times 10^{16}$ el/m^3

Example 2

$$N(z) = \frac{1}{3.54 \times 10^{-14}} \frac{4(c_1 + 1)^2}{a(c_1 e^{dz} + e^{-dz})^2} H(z)$$

$$R(ct) = -\frac{2}{\sqrt{4a-b^2}} e^{-\frac{b}{2a}ct} \sin \frac{\sqrt{4a - b^2}}{2a} ct \quad H(ct)$$

where

$$c_1 = \frac{a - b^2}{a} - \frac{b}{a} \sqrt{b^2 - 2a}$$

$$d = \frac{\sqrt{b^2 - 2a}}{a}$$

Low-Level: $b = 1.5 \times 10^5$ m

$a = 10^{10}$ m^2

N_{max} $N(o) \cong 10^4$ el/m^3

Example 3

$$N(z) = \frac{1}{3.54 \times 10^{-14}} \frac{16}{b^2} \frac{(c_1 + 1)^2}{(c_1 e^{dz} + e^{-dz})^2} H(z)$$

$$R(ct) = \frac{4ct}{b^2} e^{-\frac{b}{2d}ct} \sin \frac{\sqrt{4a - b^2}}{2a} ct \quad H(ct)$$

where

$$c_1 = -(3 + 2\sqrt{2})$$

$$d = \frac{2\sqrt{2}}{b} m^{-1}$$

Low-Level : $b = 10^5$ m

$N_{max} = N(o) \cong 4 \times 10^4$ el/m^3

Example 4

$$N(z) = \frac{1}{3.54 \times 10^{-14}} \frac{8(c_1 + 1)^2}{b^2(c_1 e^{dz} + e^{-dz})^2} H(z)$$

$$R(ct) = -\frac{4}{b} e^{-\frac{3}{2b} ct} \sinh \frac{ct}{2b} H(ct)$$

where

$$c_1 = -\frac{7 + 3\sqrt{5}}{2}$$

$$d = \frac{\sqrt{5}}{b} m^{-1}$$

Low-Level : $b = 10^5$ m

$N_{max} = N(o) \cong 2 \times 10^4$ el/m^3

Medium-Level : $b = 10^3$ m

$N_{max} = N(o) \cong 2 \times 10^8$ el/m^3

High-Level : $b = 10^{-1}$ m

$N_{max} = N(o) \cong 2 \times 10^{16}$ el/m^3

Example 5

$$N(z) = \frac{1}{3.54 \times 10^{-14}} k_1^2 H(z)$$

$$R(ct) = -\frac{2}{ct} J_2(k_1 ct) H(ct)$$

Low-Level : $k_1 = \frac{2\sqrt{2}}{10^5}\ m^{-1}$

$N_{max} = N(z) \cong 2 \times 10^4\ el/m^3$

Medium-Level : $k_1 = \frac{2\sqrt{2}}{10^3}\ m^{-1}$

$N_{max} = N(z) \cong 2 \times 10^8\ el/m^3$

High-Level : $k_1 = 2\sqrt{2} \times 10\ m^{-1}$

$N_{max} = N(z) \cong 2 \times 10^{16}\ el/m^3$

The examples given in this section have a common characteristic. For $z \geq 0$ their electron densities are either monotonically decreasing or constant. We do not know of the existence of any other method except inverse scattering which can produce the electron density profile in a plasma region where the plasma density is decreasing with distance z.

The reflected waves examples 1,2,3,4,5 have been provided as inputs to the MAIN PROGRAM described in Appendix E. The resulting approximate electron densities profiles are plotted in the graphs appearing in Chapter 5 of the thesis. Each graph is labeled XXX The first X indicates the example displayed. The second X is the letter a orb. The letter a stands for results obtained with the parameter M = 20. The letter b stands for results with the parameter M = 10. The last X is a capital letter. It is L, M or H. It indicates the different plasma density category. For each example

in each category and for the same value of M we show two graphs. One has as its abscissa the percent error $|\varepsilon(z)|$

$$|\varepsilon(z)| = \left| \frac{N(z) - \tilde{N}(z)}{N(z)} \right| \times 100$$

between the exact value of the electron density $N(z)$, and the approximate value $\tilde{N}(z)$ obtained with the numerical solution of the inverse scattering algorithm. The coordinate is the distance z inside the plasma. The other graph displays the exact and approximate electron densities. Again the coordinate is the distance z inside the plasma.

C. Square Pulse

In this section we concern ourselves with the possibility of replacing the reflected wave $R(ct)$ appearing in the inverse scattering algorithm. We consider a replacement of $R(ct)$ by $B(ct)$. $B(ct)$ is the reflected wave due to an incident thin square pulse.

We observe that probing the plasma with a δ-function pulse is of theoretical importance. However, it presents experimental difficulties. We can never expect to manufacture the high frequency part of the δ-function spectrum. Can we use as a probing wave another wave that approximates in some "sense" a δ-function?

The inverse scattering algorithm is given by

$$R(z+ct) + C_1(z,ct) + \int_{-ct}^{z} C_1(z,z')R(z'+ct)dz' = 0,$$

$$z \geq 0 \ , \quad -z \leq ct \leq z \qquad \text{MAIN INTEGRAL EQUATION} \qquad (1)$$

$$\frac{d}{dz} C_1(z,z) = \frac{1}{2} k_p^2(z) \qquad \text{SIGNATURE RELATION} \qquad (2)$$

$$k_p^2(z) = 3.54 \times 10^{-14} N(z) \qquad k_p^2\text{-N RELATION} \qquad (3)$$

The reflected wave appearing in (1) is the transform of the reflection coefficient $r(k)$

$$R(ct) = \frac{1}{2\pi} \int_{-\infty}^{+\infty} r(k)\ e^{-ikct}\ dk \qquad (4)$$

$$r(k) = \int_{-\infty}^{+\infty} R(\xi)\ e^{ik\xi}\ d\xi \qquad (5)$$

In Appendix D we show that

$$r(k) = 0(\frac{1}{k^2}) \quad \text{as} \quad k \to \infty \tag{6}$$

We can also show that

$$t(k) = 1 + 0(\frac{1}{k}) \quad \text{as} \quad k \to \infty \tag{7}$$

A typical graph of the reflection coefficient appears in Figure 1.

For $|k| > k_{max}$ the reflection coefficient is very close to zero.

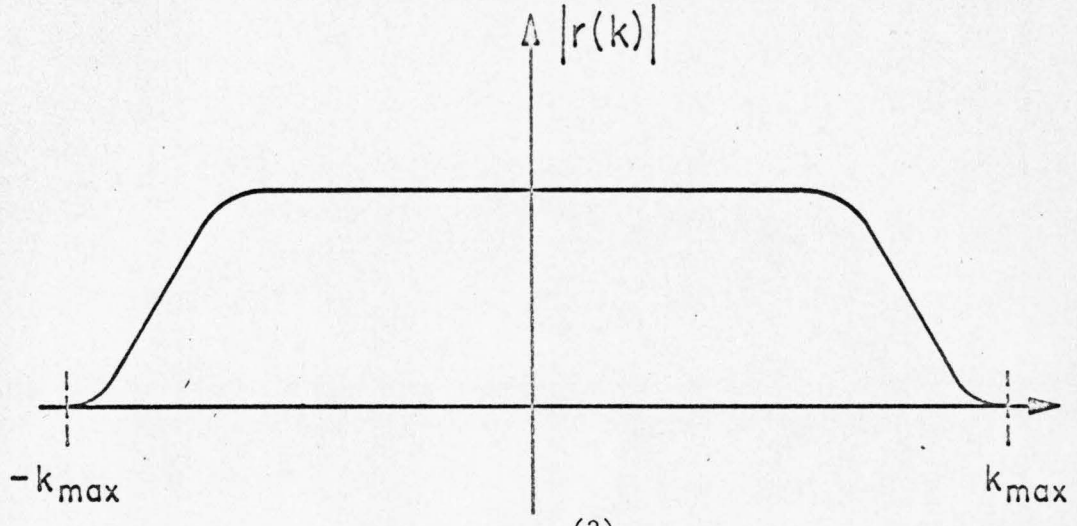

Figure 1

It seems reasonable to believe that the high frequency part of the spectrum of $r(k)$ is negligible for inverse scattering

---

[1] Equations (7) and (8) show that the plasma behaves like a high pass filter. The high frequencies go through; the low frequencies are reflected.

[2] The plot of $|r(k)|$ is symmetric around $k = 0$. This happens because $r(k)$ is the Fourier transform of a real function and thus

$$r(-k) = r^*(k)$$

calculations. After all, it is almost nonexistent because the high frequencies pass through the plasma. Thus the high frequencies of the reflection coefficient do not contain any information about the plasma except, of course, the information that they do not appear in the reflection coefficient.

The low frequencies of the incident δ-function probing wave go into the plasma and get reflected by the plasma. During this reflection the plasma leaves its imprint on the low frequencies. The inverse scattering algorithm is the means by which we unscramble the information about the plasma from these low frequencies of the reflected wave.

The direct scattering problem for the incident δ-function has been formulated in Chapter 2, Section A. We found that the Fourier transform of the electric field in the plasma obeys equations (8), (9), (10), (11)

$$\frac{d^2\hat{E}}{dz^2} + [k^2 - k_p^2(z)]\,\hat{E}(z,k) = 0 , \qquad z > 0 \tag{8}$$

$$\hat{E}(z,k) \ , \ \frac{\partial \hat{E}}{\partial z}(z,k) \quad \text{continuous across} \quad z = 0 \tag{9}$$

$$\hat{E}(z,k) = e^{ikz} + r(k)e^{-ikz} , \qquad z < 0 \tag{10}$$

$$\hat{E}(z,k) \sim t(k)e^{ikz} \qquad \text{as} \quad z \to \infty \tag{11}$$

Equation (8) shows that if k is greater than the maximum value $(k_p)_{max}$ of the plasma wave number, then $\hat{E}(z,k)$ behaves like a sinusoidal throughout the region $z > 0$. However, if k is less than $(k_p)_{max}$, then $\hat{E}(z,k)$ behaves like a damped exponential in some

parts of the region $z > 0$. This means that for $k > (k_p)_{max}$ there is much transmission through the plasma, but little reflection. For $k < (k_p)_{max}$ there is little transmission but much reflection from the plasma. We conclude that k_{max} of Figure 1 is the maximum value of the plasma wave number

$$k_{max} = (k_p)_{max} \tag{12}$$

Suppose that we have a plasma about which we have limited information, namely that its plasma density never becomes bigger than a certain number, say N. Then its wave number has an upper bound K , $K = \sqrt{3.5 \times 10^{-14} N}$. We show that this information is enough to describe the properties of probing incident waves that can be used for the inverse scattering algorithm. Our object is to use this limited information to describe properties of other incident waves, say A(z-ct), such that where we plug their reflected wave, say B(z+ct), into the main integral equation, we still get the electron density by solving the inverse scattering algorithm.

Suppose that a wave A(z-ct) is normally incident on a plasma whose maximum wave number is K . A reflected wave B(z+ct) results. The incident wave is given by (13)

$$A(z+ct) = \frac{1}{2\pi} \int_{-\infty}^{+\infty} a(k)\, e^{ik(z-ct)}\, dk \tag{13}$$

The reflected wave is given by (14)

$$B(z+ct) = \frac{1}{2} \int_{-\infty}^{+\infty} a(k)\, r(k) e^{-ik(z+ct)}\, dk \tag{14}$$

The inverse scattering altorithm unscrambles the information about the profile of the electron density from $r(k)$, $-K < k < K$. For $|k| > K$ there is no information of value; $r(k)$ is essentially zero for $|k| > K$. To make $B(z+ct)$ "look like" $R(z+ct)$ for the inverse scattering altorithm we need to preserve the plasma imprint for the low frequencies. Thus we need

$$a(k) = 1 \quad \text{for} \quad |k| < K \tag{15}$$

For the high frequencies we need to preserve the idea that there are no sizable reflections. In particular we need to retain the idea that for $|k| > K$ $r(k)$ goes to zero. Thus we need

$$a(k) \leq 1 \quad \text{for} \quad |k| > K \tag{16}$$

Equations (15) and (16) describe properties of the spectrum of an incident wave $A(z-ct)$. These properties must be satisfied if we want to replace $R(z+ct)$ by $B(z+ct)$ in the inverse scattering algorithm.

From equation (13) we obtain

$$a(k) = \int_{-\infty}^{+\infty} A(\xi) e^{-ik\xi}\, d\xi \tag{17}$$

For an $A(\xi)$ that is not a δ-function, but has some spread, say

$$\begin{aligned} &A(\xi) \neq 0 \quad , \quad -d < \xi < 0 \\ &A(\xi) = 0 \quad \text{for} \quad \xi > 0, \quad \xi < -d \end{aligned} \tag{18}$$

equations (15) and (16) show that equations (19) and (20) must be

satisfied

$$Kd \ll 2\pi \tag{19}$$

$$\int_{-d}^{0} A(\xi)\, d\xi = 1 \tag{20}$$

Equation (19) for $d = ct$ and $K = \frac{2\pi}{c} F$, $K = \sqrt{3.54 \times 10^{-14} N}$ gives equation (21)

$$T \ll \frac{1}{9\sqrt{N}} \tag{21}$$

where

T = time duration of the incident wave

N = maximum of the plasma electron density

Equation (20) shows that the incident wave must behave like a δ-function in the integral sense.[3]

We test equations (20) and (21) with a square pulse incident wave. For the electron density profile we take the profile of example 1 described in Section B.

For a square pulse incident wave $A(z-ct)$, at $t = 0$ we have

$$A(z) = \begin{cases} 0, & z > 0 \\ \frac{1}{2L}, & -2L < z < 0 \end{cases} \tag{22}$$

---

[3] Equation (20) is important. The main integral equation shows that if one doubles $R(z+ct)$, $C_1(z,ct)$ does not double. The relation between the reflected wave $R(z+ct)$ and the electron density $N(z)$ is a nonlinear one.

Its Fourier spectrum $a(k)$ is

$$a(k) = \int_{-\infty}^{+\infty} A(z)e^{-ikz}\, dz = e^{ikL}\,\frac{\sin kL}{kL}$$

At $z = 0$ the reflected wave $B(ct)$ becomes

$$B(ct) = \int_{-\infty}^{+\infty} A(y)\; R(y+ct)\; dy \tag{24}$$

For example 1, $R(ct)$ and $k_p^2(z)$ are given by

$$R(ct) = \begin{cases} -\frac{2}{D}\, e^{-ct/D}\, \sin(\frac{ct}{D}) & , \quad ct \geq 0 \\ 0 & , \quad ct < 0 \end{cases} \tag{25}$$

$$k_p^2(z) = \begin{cases} \frac{2}{(z+\frac{D}{2})^2} & , \quad z \geq 0 \\ 0 & , \quad z < 0 \end{cases} \tag{26}$$

The maximum value K of the plasma wave number occurs at $z = 0$ and is given by (27)

$$K \simeq 2.8/D \tag{27}$$

Equations (22),(25) when substituted into (24) give

$$B(ct) = \begin{cases} 0 & , \; ct \leq 0 \\ \frac{1}{2L}\left\{e^{-ct/D}(\sin\frac{ct}{D} + \cos\frac{ct}{D}) - 1\right\} & , \; 0 \leq ct \leq 2L \\ \frac{1}{2L}\left\{e^{-ct/D}(\sin\frac{ct}{D} + \cos\frac{ct}{D}) - e^{-\frac{ct-2L}{D}}\left[\sin(\frac{ct-2L}{D}) + \cos(\frac{ct-2L}{D})\right]\right\} & , \; ct \geq 2L \end{cases} \tag{28}$$

For the square pulse the spread d is given by

$$d = 2L \tag{29}$$

Using equations (27) and (29) on equation (19) we obtain

$$\frac{2.8}{D} \cdot 2L << 2\pi$$

or

$$\frac{L}{D} << 1 \tag{30}$$

Graph 1 of Chapter 5 gives the results that we obtained when we used B(ct) as given by equation (28) in the place of R(ct) appearing in the main integral equation of the inverse scattering altorithm. In Graph 1 the abcissa is the percent error $|\varepsilon(z)|$. $\varepsilon(z)$ is given by (31)

$$\varepsilon(z) = \frac{N(z) - \tilde{N}(z)}{N(z)} \times 100 \tag{31}$$

N(z) is the electron density for example 1,

$$N(z) = \frac{1}{3.54 \times 10^{-14}} \frac{2}{(z+\frac{D}{2})^2} , \quad z \geq 0$$

$\tilde{N}(z)$ is the approximate electron density obtained by solving numerically the inverse scattering algorithm with reflected wave B(ct).

Example 1 is in the low level category and thus the parameter D has the value 10^5m

$$D = 100 \text{ km} \tag{32}$$

The coordinate is the distance z inside the plasma. The parameter ℓ

needed for the numerical method has been taken to be 2 km. The value of the parameter M is 10; that is, we use a standard matrix size of 21 for all calculations. This means that to find the electron density at any point z inside the plasma we divide the distance record of B(ct) for ct = 0 to ct = 2z into 20 equal intervals. For example, for z = 100 km we sample B(ct) every Δct = 10 km. For z = 200 km we sample B(ct) every 20 km. The curves labeled L/D show the percent error for different values of L/D . The curve with L/D = 1D shows that the error is big even for z's in the range 50 to 150 km. However, for this range of z the error for L/D = 0.1, 0.01, 0.001 is much smaller, in fact, it is close to zero. The only reason for this is equation (30). For L/D = 1.0 equation (30) is not satisfied and thus we expect that we will not get good answers for the electron density. We cannot plot the results for L/D = 10. The percent error for L/D = 1D is extremely big (more than 200%). The curves for L/D = 0.1, 0.01, 0.001 show that the percent error is less than 10%. For the case of L/D = 0.001 we see from Graph 1 and Graph 2 (Graph 2 shows results for $z < 50$ km) that the error is less than 1% in the region $5 \text{ km} < z < 150 \text{ km}$. Such accuracy is quite remarkable.

The curve marked "with δ-function" has been included for comparison. The curve shows that the percent error is almost zero for $z < 250$ km. However, in the region $200 < z < 250$ km the L/D curves exhibit errors which are quite high. In the region $250 < z < 300$ km all percent errors displayed by the L/D curves are more than 50%.

If we define the range of the numerical solution of the inverse scattering algorithm the distance inside the plasma for which we get

errors less than 10% for a given M,ℓ Graph 1 shows that for high ratios L/D the range is smaller than for low ratios L/D. This is not unexpected. In fact since D is constant the smaller the ratio L/D the smaller L. And the smaller L the more $A(z)$, see equation (22), looks like a δ-function. In short, we expect that for $L/D \to 0$ the L/D error curves will fall on the δ-function curve.

Graph 2 shows that for $z < 5$ km the percent errors for $L/D = 0.1, 0.001$ become quite high. This is not surprising. In fact at $z = 0$ both errors should be 100%. To see this we go to equation (1) and we substitute $B(z+ct)$ for $R(z+ct)$. We obtain

$$B(z+ct) + C_1(z,ct) + \int_{-ct}^{z} C_1(z,z')B(z'+ct)dz' = 0$$

For $ct = z$ we obtain

$$B(2z) + C_1(z,z) + \int_{-z}^{z} C_1(z,z')B(z'+z)\ dz' = 0$$

Taking the derivative with respect to z we get

$$2B(2z) + \frac{d}{dz} C_1(z,z) + C_1(z,z)B(2z) - C_1(z,-z)B(0)$$

$$+ \int_{-z}^{z} \frac{\partial}{\partial z} C_1(z,z')B(z'+z)dz' + \int_{-z}^{z} C_1(z,z') \frac{\partial B}{\partial z}(z'+z)dz' = 0 \qquad (33)$$

But from (28) we see that

$$B(0) = 0 \qquad (34)$$

From Chapter 2, Section B we find that

$$C_1(0,0) = 0 \qquad (35)$$

Taking the limit of equation (33) as $z \to 0$, we find

$$2\dot{B}(0) + \frac{d}{dz} C_1(z,z)]_{z=0} = 0$$

Using the signature equation the above equation becomes

$$k_p^2(0) = -4\dot{B}(0) \tag{36}$$

Using equation (28) we find that

$$\dot{B}(0) = 0$$

Thus equation (36) yields $k_p^2(0) = 0$ and the k_p^2-N relation shows

$$N(0) = 0 \tag{37}$$

The inverse scattering algorithm for $B(ct)$ shows that the electron density at $z = 0$ must be 0. However, from equation (26) we see that

$$N(0) = \frac{1}{3.54 \times 10^{-14}} \frac{8}{D^2} , \qquad D = 100 \text{ km}$$

The same calculations for $R(ct)$ instead of $B(ct)$ in the inverse scattering algorithm show that indeed equation (36) is satisfied. That is, $\dot{R}(0)$ is such that

$$k_p^2(0) = -4\dot{R}(0) \tag{38}$$

From equation (25) we get

$$\dot{R}(0) = -\frac{2}{D^2} \tag{39}$$

Equation (26) shows that

$$k_p^2(0) = \frac{8}{D^2} \tag{40}$$

Equations (39),(40) when substituted into (38) produce an identity.

This discrepancy is explained when one considers the difference between a δ-function probing wave and a square pulse. We have reason to believe that the high frequency part of the reflection coefficient $r(k)$ carries the information about jump discontinuities in the plasma density. This shows that the high frequency content of the incident δ-function is important in determining these jump discontinuities. The square pulse incident wave has a spectrum that falls to zero for high frequencies. Thus, the square pulse reflection coefficient has a high frequency spectrum that is much smaller than the high frequency spectrum of $r(k)$. Hence, the inverse scattering algorithm sees not enough high frequencies in $B(ct)$ and concludes that there are no jump discontinuities. We need to point out, however, that this is not a big error of the inverse scattering algorithm. As Graph 2 shows for $z > 10$ km the approximate electron density $\tilde{N}(z)$ comes close to the actual electron density $N(z)$. In effect then, by using a square pulse we smooth out the jump discontinuities.

D. Physical Explanations

In this section we discuss the range of accuracy for the numerical solution of the inverse scattering algorithm. We provide a physical mechanism explaining the inverse scattering algorithm. We discuss graphs obtained by the numerical method for examples 1, 2, 3, 4, 5. We suggest possible ways for improving the numerical solution of the inverse scattering algorithm.

It is of interest to see how information about the plasma density profile gets recorded into the reflection coefficient.

An incident plane wave $e^{ik_1 z}$ falls on the plasma. The electric field inside the plasma obeys equation (1)

$$\frac{d^2\hat{E}}{dz^2} + [k_1^2 - k_p^2(z)]\,\hat{E}(z,k_1) = 0 \qquad (1)$$

Suppose that $k_p^2(z)$ has the profile shown in Figure 1.

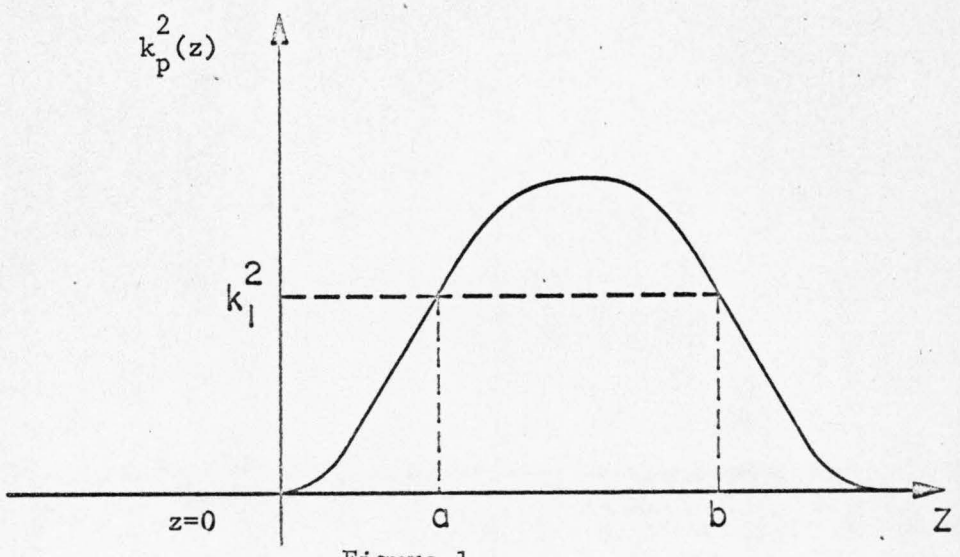

Figure 1

At points z = a and z = b the plasma wave number $k_p(z)$ is equal to k_1. Equation (1) shows that for $0 \leq z \leq a$, $z \geq b$ the electric

field behaves like a sinusoidal. For $a \leq z \leq b$ the field behaves like an exponential. The incident field $e^{ik_1 z}$ creates a sinusoidal plasma field which propagates in the +z direction. As soon as this field reaches the point $z = a$ a reflection results. At $z > a$ the field must change to a damped exponential. This drastic change creates a reflection. The field transmitted reaches the point $z = b$ but it loses strength since it behaves like a damped exponential in region $a \leq z \leq b$. At $z = b$ the field again undergoes a drastic change. Thus another reflected field appears. This reflected field returns to $z = a$; again it loses strength. At $z = a$ part of it gets transmitted. The transmitted part arrives at $z = 0$. This discussion points out that the reflected field at $z = 0$ has two parts. One part comes from a direct reflection at $z = a$ and the other from a reflection at $z = b$. However, this second part has a much smaller amplitude resulting from the attenuation of the field in the region $a \leq z \leq b$.

Suppose that a δ-function $\delta(z-ct)$ is incident on the profile $k_p^2(z)$ of Figure 1. The reflectd wave $R(ct)$ is given by (2)

$$R(ct) = \frac{1}{2} \int_{-\infty}^{+\infty} r(k)\, e^{-ikct}\, dk \qquad (2)$$

The δ-function propagates in the plasma and hits the electron concentrations of Figure 1 [1]. The electrons interact with the δ-function and this interaction produces fields. The fields created by electrons

---

[1] The electron density $N(z)$ is proportional to $k_p^2(z)$.

located at z_1 disturb other electrons located at z_2 . The fields generated by this interaction of electrons at z_1 and z_2 disturb other electrons at z_3 , etc. In short, the reflected field $R(ct)$ at any time $t = \tau$ contains information from all electrons in the region $z \leq c\tau/2$.

The inverse scattering algorithm

$$R(z_1+ct) + C_1(z_1,ct) + \int_{-ct}^{z_1} C_1(z_1,z')R(z'+ct)dz' = 0 \qquad (3)$$

MAIN INTEGRAL EQUATION

$$\frac{d}{dz} C_1(z_1,z_1) = \frac{1}{2} k_p^2(z_1) \qquad \text{SIGNATURE RELATION} \qquad (4)$$

$$k_p^2(z_1) = 3.54 \times 10^{-14} N(z_1) \qquad k_p^2\text{-N RELATION} \qquad (5)$$

obtains the electron density $N(z_1)$ using the values of the reflected wave in the time interval $0 \leq t \leq 2z_1/c$. Information about $N(z_1)$ appears "near" times $t = 2z_1/c$ [2]. The algorithm unscrambles this information about $N(z_1)$ by using the whole record of $R(ct)$ for $0 \leq t \leq 2z_1/c$. We expect that if the information about $N(z_1)$ is weakly recorded at times t "near" $2z_1/c$, then the numerical solution will have difficulty in obtaining $N(z_1)$.

Examples 1 and 4 discussed in Section B have the same maximum electron density. For both examples the maximum of $N(z)$ occurs at $z = 0$. However, away from $z = 0$ the electron densities behave differently. In example 1 $N(z)$ goes as $1/z^2$ for large z whereas in

---

[2] For a continuous electron density profile, information about the value of the electron density in a neighborhood of z_1 is just as good as information about the value of the electron density exactly at z_1 .

example 4 $N(z)$ behaves like a damped exponential for large z. In Chapter 5 we show a table of values of the reflection coefficient for each example. For example 1 the magnitude of $r(k)$ is given by

$$|r(k)| = \left[\frac{1}{\frac{k^2D^2}{2} + 1} \right]^{1/2} \tag{6}$$

For example 4, $r(k)$ is given by

$$|r(k)| = \left[\frac{1}{\frac{k^4D^4}{4} + \frac{5}{4} k^2D^2 + 1} \right]^{1/2} \tag{7}$$

The parameter D has the value $D = 10^5$ meters corresponding to the low level category. The wave number k is taken to be equal to the plasma wave number $k_p(z)$ of each example. This corresponds to the case of Figure 1 where $k_1^2 = k_p^2(b)$. The table has been constructed by varying the distance z inside the plasma. The table shows that at about $z = 400$ km, $|r(k)|$ for example 1 is 0.999. The magnitude of the reflection coefficient of example 4 is 0.999 at about 200 km. This shows that the information about the value of k_p (400 km) of example 1 is recorded in the reflected wave $R(ct)$ of example 1 at times t "near" $2\frac{400 \times 10^3}{c}$ with the same amplitude of the information about the value of k_p (200 km) of example 4 which is recorded in the reflected wave $R(ct)$ of example 4 at times "near" $2\frac{200 \times 10^3}{c}$. We expect then that the numerical method will show the same percent error for the electron density of example 1 at $z = 400$ km as for the electron density of example 4 at $z = 200$ km provided that we use the same M for both calculations. Graphs 1aL and 4aL verify our expectations.

Graph 1aL shows that the percent error at $z = 400$ km is about 10%. The same percent error is shown in Graph 4aL at $z = 200$ km.

Simple calculations for the field inside the region $a \leq z \leq b$ of Figure 1 show that the information about the value of $k_p(z)$ at $z = b$ is recorded in the reflection coefficient with strength given by

$$\text{strength of } |r(k_1)| \text{ due to reflection at } z = b \sim e^{-2\int_a^b \sqrt{k_p^2(b) - k_p^2(\xi)}\, d\xi} \tag{8}$$

The discussion for examples 1 and 4 shows that the smaller the quantity

$$e^{-2\int_a^b \sqrt{k_p^2(b) - k_p^2(\xi)}\, d\xi}$$

the bigger the percent error between the actual electron density at $z = b$ and the approximate one obtained by the numerical solution of the inverse scattering algorithm.[3].

Graphs 1bL and 1aL point out that by increasing M one is able to obtain the electron density farther inside the plasma. Graph 1bL shows that for $M = 10$ the percent error is negligible for $z < 300$ km. Graph 1aL shows that for $M = 20$ we can find the electron density up to a distance of 400 km inside the plasma. We expect that by taking M bigger than 20, say $M = 40$, we can find the electron density for distances bigger than 400 km inside the plasma of example 1.

---

[3] This points out that it is difficult to obtain the electron density near the bottom of a deep valley in the plasma electron density profile. Nevertheless, theoretically we can find the electron density at the bottom of a deep valley provided that we use the numerical method with M sufficiently large.

The graphs XXX for the electron densities of examples 1, 2, 3, 4, 5 show for a given value of M the percent error between the actual electron density and the approximate electron density obtained by the numerical solution. The graphs give the percent error for three categories: Low, Medium and High. The Low level category corresponds to electron densities which have a maximum density of about $10^4 el/m^3$. The Medium level corresponds to plasma densities which have a maximum density of about $10^8 el/m^3$. The High level corresponds to plasma densities which have a maximum density of about $10^{16} el/m^3$. All the graphs show that the percent error is almost zero up to a distance S inside the plasma. Then the error begins to climb very rapidly. The distance S is the range of accuracy of the numerical solution for a given M . All the graphs show that by increasing M we increase S The graphs also show that S changes value drastically from category to category. Graph 1aL gives a value of 400 km for S . Graph 1aM gives a value of 4 km for S . Graph 1aH gives a value of 40 cm for S . Similar drastic variations of S are exhibited by Graphs 4aL, 4aM, 4aH and 5aL, 5aM, 5aH. Graphs 1aL, 4aL, 5aL show that even within the same category and same M the value of S varies from example to example. It is clear that the range of accuracy depends on the electron density profile and the parameter M . Since the electron density profile is unknown, it is of no use to search for an exact formula for S(M) . However, with a little knowledge about N(z) an upper bound for S can be found. The upper bound is useful in a priori estimates of how far inside the plasma the numerical method can give the electron density profile.

The range of accuracy has an upper bound for a given M. Suppose that the plasma electron density has an upper bound N. Then the plasma wave number is smaller than K, $K = \sqrt{3.54 \times 10^{-14} N}$. In Section C we showed that the magnitude of the reflection coefficient drops to zero for $|k| > K$. The reflected wave is given by

$$R(ct) = \frac{1}{2} \int_{-\infty}^{+\infty} r(k)\, e^{-ikct}\, dk \tag{9}$$

Equation (9) shows that $R(ct)$ is composed of sinusoidals of wave number k where $0 \leq k \leq K$. The numerical solution to the inverse scattering algorithm uses uniformly samples values of $R(ct)$ instead of the time record of $R(ct)$. In Section C we showed that information about the plasma electron density profile is recorded in the spectrum of $r(k)$ for $-K \leq k \leq K$. We expect that if we sample well the reflected wave $R(ct)$ then all information about $N(z)$ will be preserved in the sampled values of $R(ct)$. We sample well $R(ct)$ if we sample adequately the sinusoidal with the maximum wave number K existing in $R(ct)$. A sampling of $\sin K\, ct$ five times in half a period seems adequate. We deduce we must sample $R(ct)$ every Δct, where Δct is given by

$$\Delta ct \leq \frac{\pi}{5K} \tag{10}$$

To obtain the electron density at z we divide the distance record of $R(ct)$ for $0 \leq ct \leq 2z$ into $2M$ equal subintervals of length Δct

$$\Delta ct = \frac{z}{M} \tag{11}$$

Equations (10),(11) show that the range of accuracy S(M) has the upper bound given by

$$S(M) \leq \frac{\pi M}{5K} \tag{12}$$

Using the k_p^2-N relation equations (10) and (12) become

$$\Delta t \leq \frac{1}{90\sqrt{N}} \tag{13}$$

(4)

$$S(M) \leq \frac{3.3 \times 10^6 \times M}{\sqrt{N}} \tag{14}$$

(4)

Equation (13) shows that if the plasma has a maximum electron density N , then we must sample the reflected wave at time intervals Δt given by (13). For a given M the range of accuracy S(M) cannot be greater than $\frac{3.3 \times 10^6 \times M}{\sqrt{N}}$. Equation (14) is easily verified for all our graphs.

The numerical method presented in this report can be improved to yield bigger ranges of accuracy. All the graphs show that S(M) increases with M . The parameter M is approximately equal to half the number of rows of the (2M+1) × (2M+1) square matrix $\mathcal{A}$ described in Section A . Our numerical method centers on the inversion of the matrix equation

---

[4] We note that equations (13) and (14) have been derived using intuitive arguments to avoid immense mathematical difficulties encountered when one tries to describe rigorously the percent error. However, equations (13),(14) give good "ball-park" numbers that are necessary for a priori estimates.

$$\mathcal{A}\chi = -R \tag{15}$$

described in Section A. We enlist the help of a computer to invert (15). For most computers practical reasons limit M to values up to 200 [5]. It is clear then that one cannot take M as big as one would wish. However, a good iterative solution of (15) can increase dramatically the permissible value of M especially since Section A shows that $\mathcal{A}$ has lots of zeros and symmetries. Also one can improve on the implementation of our numerical method by creating an efficient matrix inversion subroutine that takes advantage of the zeros and symmetries of $\mathcal{A}$. We use a standard IBM 360 subroutine designed to be efficient for inverting general matrices [6]. Also one can improve the range of accuracy by using higher order integration rules instead of the sinusoidal and trapezoidal rules used in Section A.

---

[5] Values of M bigger than 200 strain the storage capabilities of most computers. This happens because the computer places all the elements of matrix $\mathcal{A}$ in its storage. For M = 200, $\mathcal{A}$ has 160,000 elements.

[6] See Appendix E.

IV. ALTERNATIVE METHOD

This chapter presents an alternative method to the inverse scattering method for finding the electron density profile of a plane stratified plasma. The method is commonly known as the ionogram method.

A. Ionogram Method

This section describes briefly the ionogram method for obtaining the plasma density profile. The material in this section is drawn mainly from the excellent books of Budden and Davies[1]. We briefly sketch the method.

The W.K.B. solution to the direct scattering problem posed in Chapter II, Section A

$$\frac{d^2\hat{E}}{dz^2} + [k^2 - k_p^2(z)]\,\hat{E}(z,k) = 0 \tag{1}$$

$$\hat{E}(z,k),\ \frac{\partial \hat{E}}{\partial z}(z,k) \quad \text{continuous across } z = 0 \tag{2}$$

$$\hat{E}(z,k) = e^{ikz} + r(k)e^{-ikz} \qquad z \leq 0 \tag{3}$$

$$\hat{E}(z,k) \sim t(k)e^{ikz} \qquad \text{as} \quad z \to \infty \tag{4}$$

$$k_p^2(z) = 3.54 \times 10^{-14} N(z) \tag{5}$$

shows that if the electron density $N(z)$ is a monotonically increasing function of z, then for $k = k_1$ the reflection coefficient $r(k_1)$ is given by

---

[1] See References 28,29.

$$r(k_1) \sim -i\, e^{2i \int_0^{z_1} \sqrt{k_1^2 - k_p^2(\xi)}\, d\xi} \tag{6}$$

where

$$k_1^2 = k_p^2(z_1)$$

Equation (6) is derived if we assume that the incident wave $e^{ik_1 z}$ is a decaying exponential in the region $z > z_1$ and then we use the connection formulas[2] of the W.K.B. method.

For an incident wave $\hat{E}(0,k_1)e^{ik_1 z}$ the reflected wave $r(k_1)$ becomes

$$r(k_1) = -i\, e^{2i \int_0^{z_1} \sqrt{k_1^2 - k_p^2(\xi)}\, d\xi}\, \hat{E}(0,k_1) \tag{7}$$

If the incident wave in the time domain is a square pulse of duration T multiplied by a sinusoidal $\sin(k_1 ct)$ where

$$\frac{1}{F_1} \ll T \quad , \qquad F_1 = \frac{2\pi}{c} k_1 \tag{8}$$

then the incident wave $E(z,ct)$ has a Fourier transform $\hat{E}(z,k)$ which is peaked around $k = k_1$. The reflected wave in the time domain becomes

$$R(ct) \simeq \frac{1}{2\pi} \int_{-\infty}^{+\infty} \left\{ -i\, e^{2i \int_0^{z_1} \sqrt{k_1^2 - k_p^2(\xi)}\, d\xi}\, e^{-ikct}\, \hat{E}(0,k) \right\} dk \tag{9}$$

Using the principle of stationary phase in equation (9) we obtain

---

[2] See References 34,35.

$$\frac{ct}{2} = \int_0^{z(k_1)} \frac{1}{\sqrt{1 - \frac{k_p^2(\xi)}{k_1^2}}}\, d\xi \tag{10}$$

Calling $ct/2$ a virtual height $h'(k_1)$ we obtain Abel's integral equation

$$h'(k_1) = \int_0^{z(k_1)} \frac{1}{\sqrt{1 - \frac{k_p^2(\xi)}{k_1^2}}}\, d\xi \tag{11}$$

The quantity $\frac{h'(k_1)}{c}$ can be measured experimentally. It is half the time that it takes for the incident wave of predominant frequency $F = F_1$ to reach the point z_1 in the plasma where $k_1^2 = k_p^2(z_1)$, get reflected, and come back to $z = 0$. Experimentally one finds $h'(k_1)$ from the time it takes for the signal to reach the reflection point z_1 and come back to the station emitting the signal.

One finds $h'(k_1)$ for all k_1 up to k. Then he inverts equation (11) to obtain (12) [3]

$$z(k) = \frac{2}{\pi} \int_0^{\pi/2} h'(k \sin \phi)\, d\phi \tag{12}$$

Using $h'(k_1)$ for $0 \leq k_1 \leq k$, he obtains $z(k)$ from equation (12). The record of $h'(k_1)$ for the different k_1's is called the ionogram record.

Unfortunately the method has deficiencies [4]:

---

[3] See Reference 30

[4] See Reference 31

1. It fails in regions where there are valleys in the plasma density.

Suppose we had a linear $k_p^2(z)$ profile as shown in Figure 1.

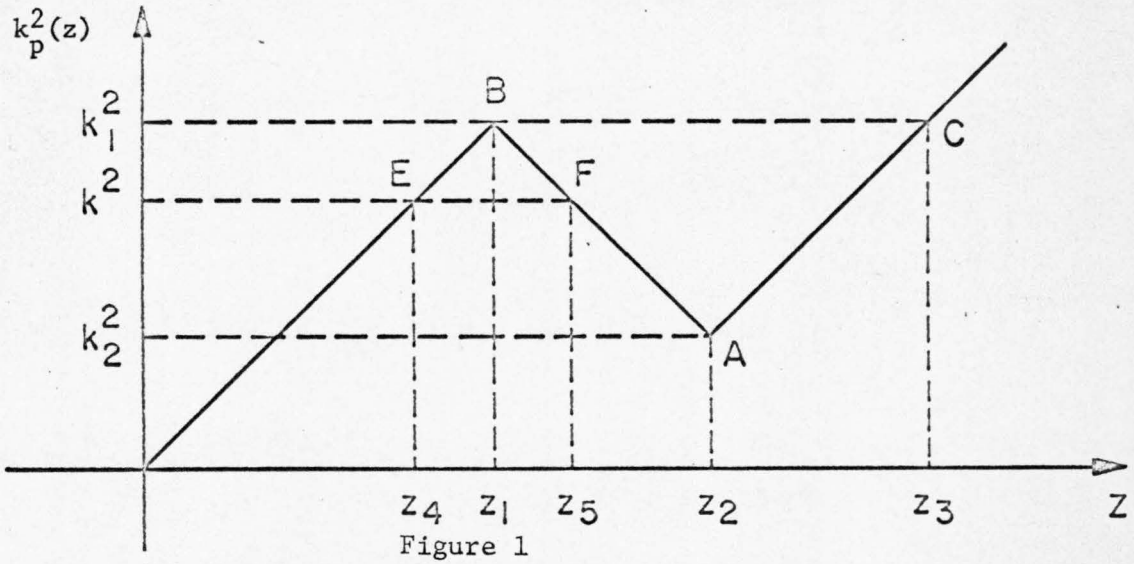

Figure 1

The region BAC is called a valley of the electron density N(z), $N(z) = \frac{1}{3.54 \times 10^{-14}} k_p^2(z)$. The valley region is "masked" by the region $0 \leq z \leq z_1$. In order that one finds the valley electron density at $z = z_5$, he has to consider penetrations of wave numbers k, $k_2^2 \leq k^2 \leq k_1^2$. In short, he has to include reflections from the point F in Figure 1. This requires that he sets up the full W.K.B. solutions in region $z_4 \leq z \leq z_5$. However, it is not clear whether such a treatment will yield an integral equation which can be inverted to find the distance z_5.

An approach that appears in the literature is to try to determine the valley electron density from measurements of the virtual height for wave numbers k greater than k_1. However, this is erroneous. In Appendix G we show that even if we assume that the point A (minimum of the valley) lies on the line $k_p^2 = k_2^2$ and we also assume

that the valley is composed of two straight lines that start at points B and C and meet at A, even then we show there is an infinite set of linear valleys that give the same virtual heights for $k > k_1$. This observation is in direct contradiction to suggestions in the literature. We quote:

> "It seems perhaps that the best method of dealing with the valley problem would be to assume some simple model for the ionosphere within that region, perhaps with two parameters specifying the height and the depth of the valley, then using values of h' for the higher region, fit the parameters of the valley, taking into account the retardation produced above the valley by the ionization already computed as existing below it."(5)

2. It fails near maxima of the electron density.

The reason for this failure of the ionogram method is directly traced to the W.K.B. approximation involved.

3. The method does not have a "built-in" error control. That is, if we get an answer for the electron density profile the method does not provide a mechanism by which we can check the answer.

4. The method fails when the electron density has steep gradients.

In regions where the electron density increases rapidly, the accuracy of the W.K.B. approximations decreases. Hence the

---

[5] See Reference 32, p. 1158

reliability of the virtual height record diminishes. We quote:

"Virtual height precision of +1.0 km is desirable everywhere..."[6]

---

[6] See Reference 33, p. 1159

B. Comparisons

The inverse scattering numerical method has several advantages over the ionogram method. The inverse scattering method shows that the electron density can be found on, in front, or behind maxima of the plasma frequency. Also the method does well in regions of sharp gradients of the plasma frequency. The inverse scattering method shows that the electron density can be found and then verified through an error control feature.

V. GRAPHS

This chapter contains all the graphs obtained by our numerical method.

Table 1 and Graphs 1,2 are explained in Chapter 2, Section D. Graphs labeled XXX are explained in Chapter 2, Sections B and D. In each page of Graphs XXX there is a plot of the exact electron density, the approximate electron density which is obtained by solving the inverse algorithm numerically, and the percent error between them. The coordinate is always z, the distance inside the plasma.

TABLE 1

Low-Level Category

Example 1

(1) $$|r(k)| = \left[\frac{1}{\frac{k^2D^2}{2} + 1}\right]^{1/2}$$

where

$$k^2 = \frac{2}{\left(z + \frac{D}{2}\right)^2}$$

$$D = 10^5 \text{ met}$$

(2) $$|r(k)| = \left[\frac{1}{\frac{k^4D^4}{4} + \frac{5}{4}k^2D^2 + 1}\right]^{1/2}$$

where

$$k^2 = \frac{8(c_1+1)^2}{D^2(c_1e^{dz}+e^{-dz})^2},$$

$$c_1 = -\frac{7+3\sqrt{5}}{2}$$

$$d = \frac{\sqrt{5}}{D}$$

$$D = 10^5 \text{ met}$$

z = 50 km	|r(k)| = 0.707	z = 50 km	|r(k)| = 0.724
z = 100 km	|r(k)| = 0.914	z = 100 km	|r(k)| = 0.960
z = 150 km	|r(k)| = 0.970	z = 150 km	|r(k)| = 0.996
z = 200 km	|r(k)| = 0.987	z = 200 km	|r(k)| = 0.999
z = 250 km	|r(k)| = 0.994	z = 250 km	|r(k)| = 1.000
z = 300 km	|r(k)| = 0.997		
z = 350 km	|r(k)| = 0.998		
z = 400 km	|r(k)| = 0.999		
z = 450 km	|r(k)| = 0.999		
z = 500 km	|r(k)| = 1.000		

GRAPH 1

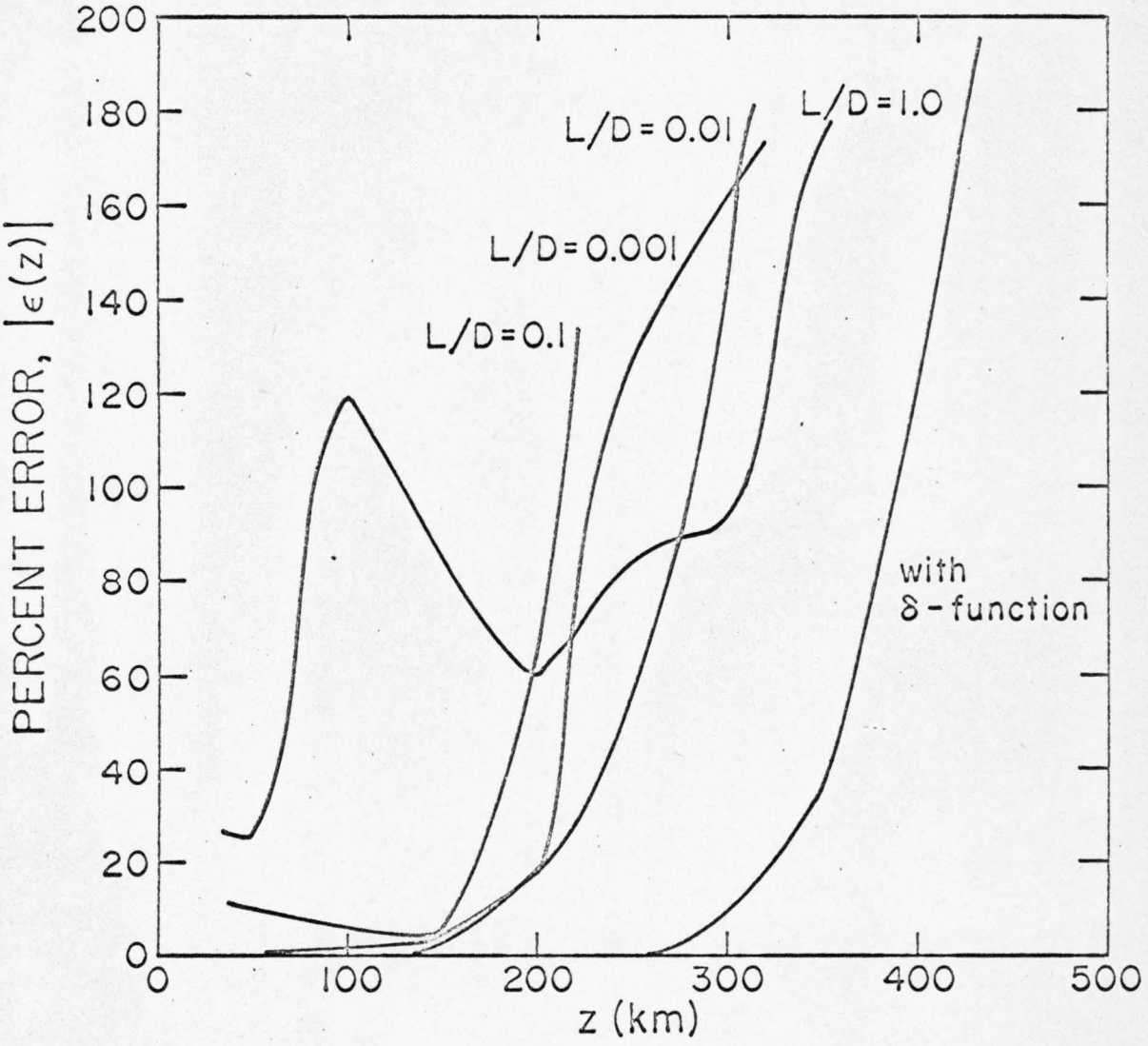

Example 1. Squarewave Incident Pulse, Low-Level Category

M = 10, ℓ = 2 km, D = 100 km.

GRAPH 2

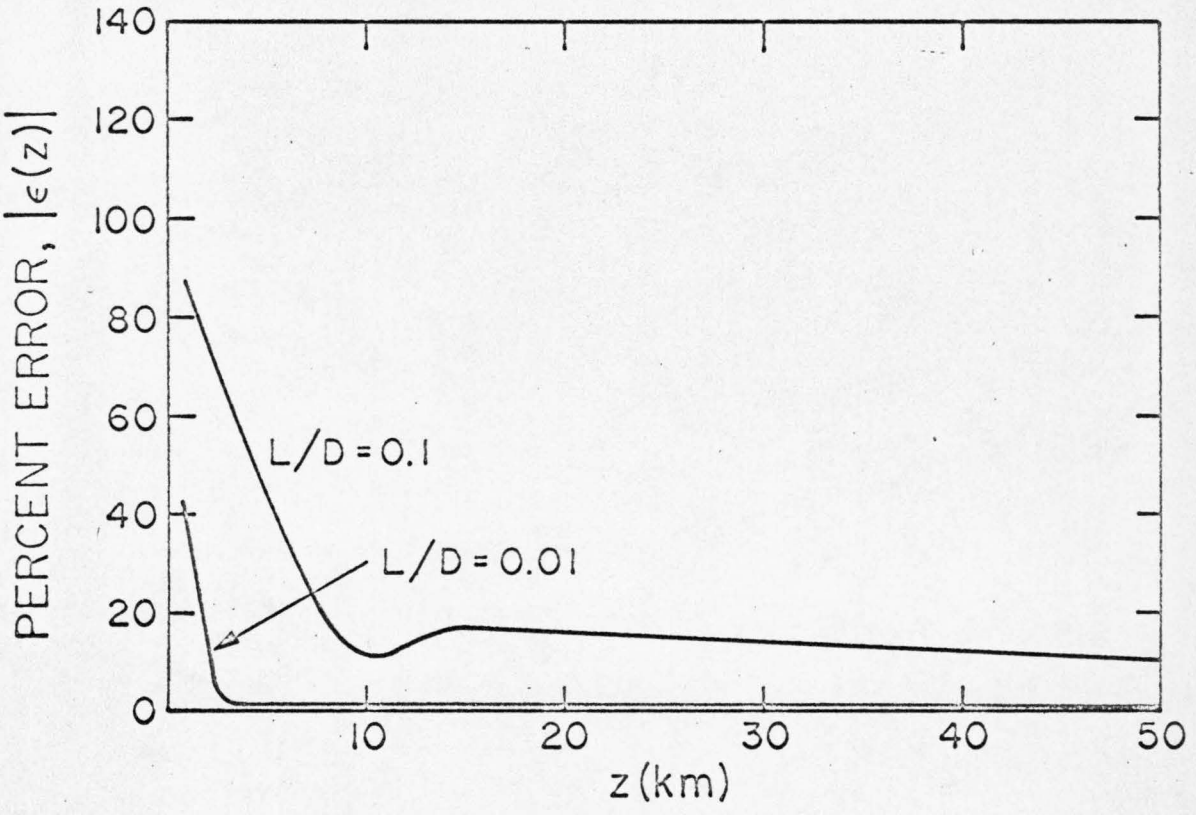

Example 1. Squarewave Incident Pulse, Low-Level Category.

M = 10, ℓ = 2 km, D = 100 km.

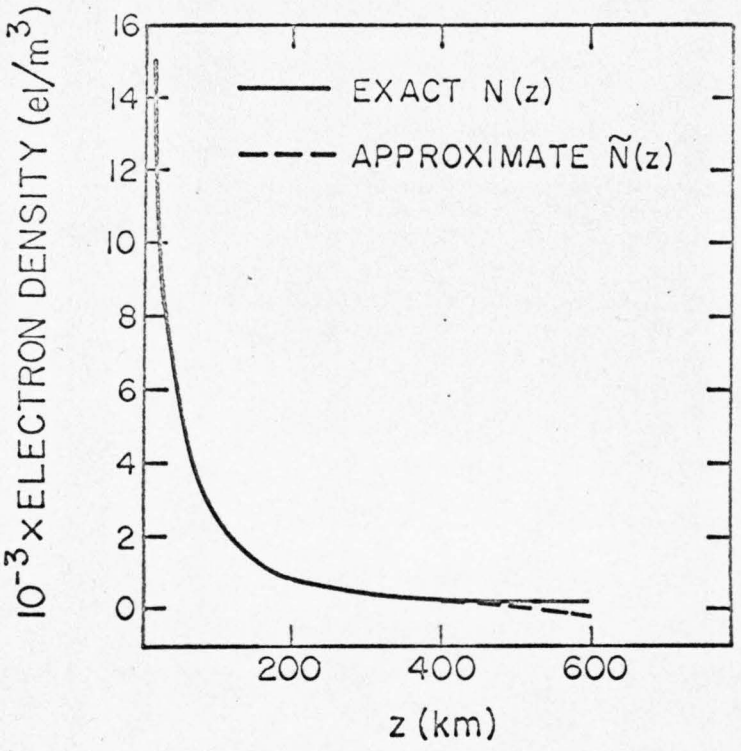

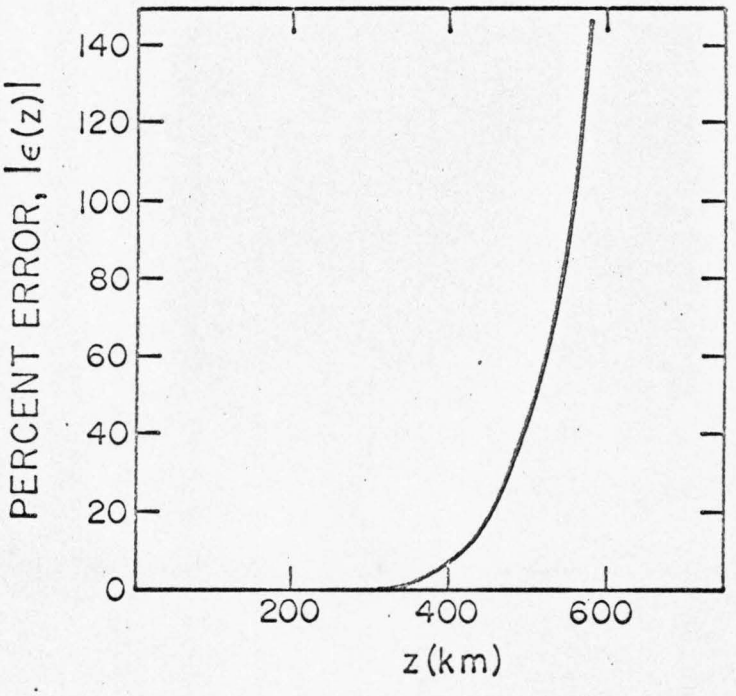

GRAPH 1aL

M = 20, ℓ = 2 km.

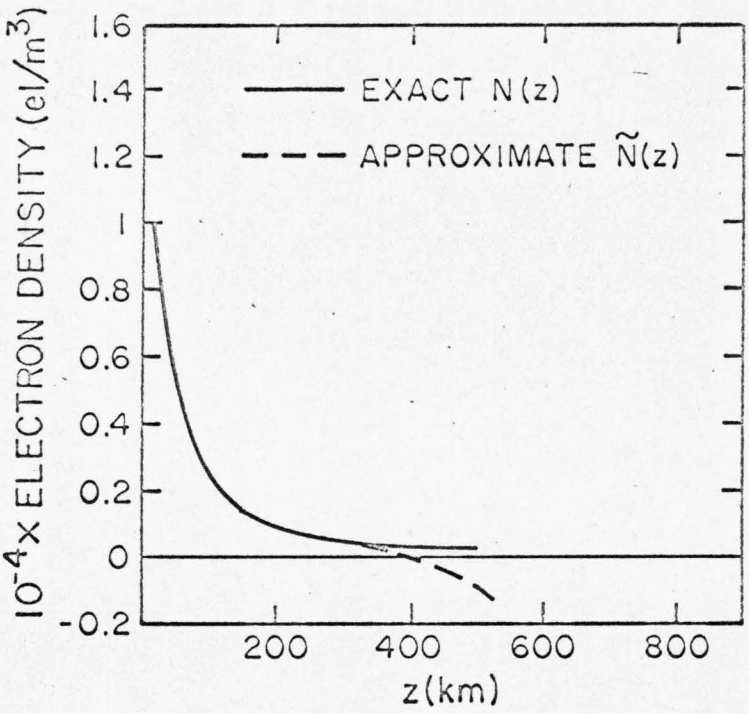

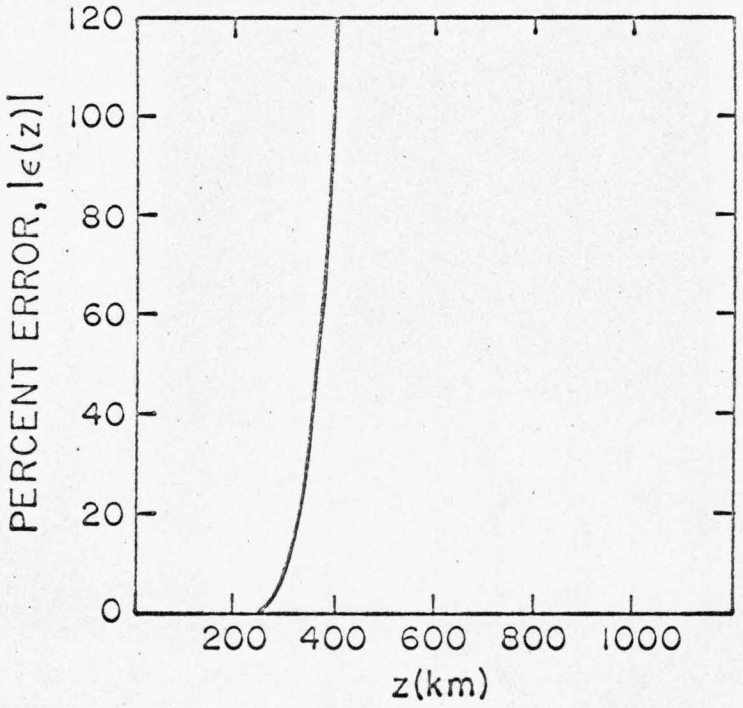

GRAPH 1bL

M = 10, ℓ = 2 km.

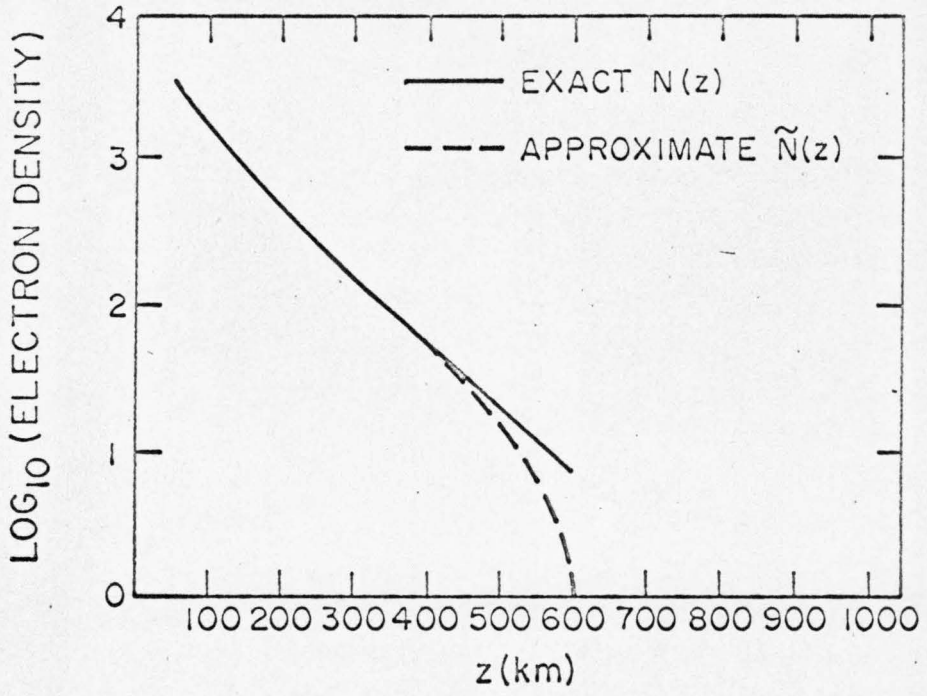

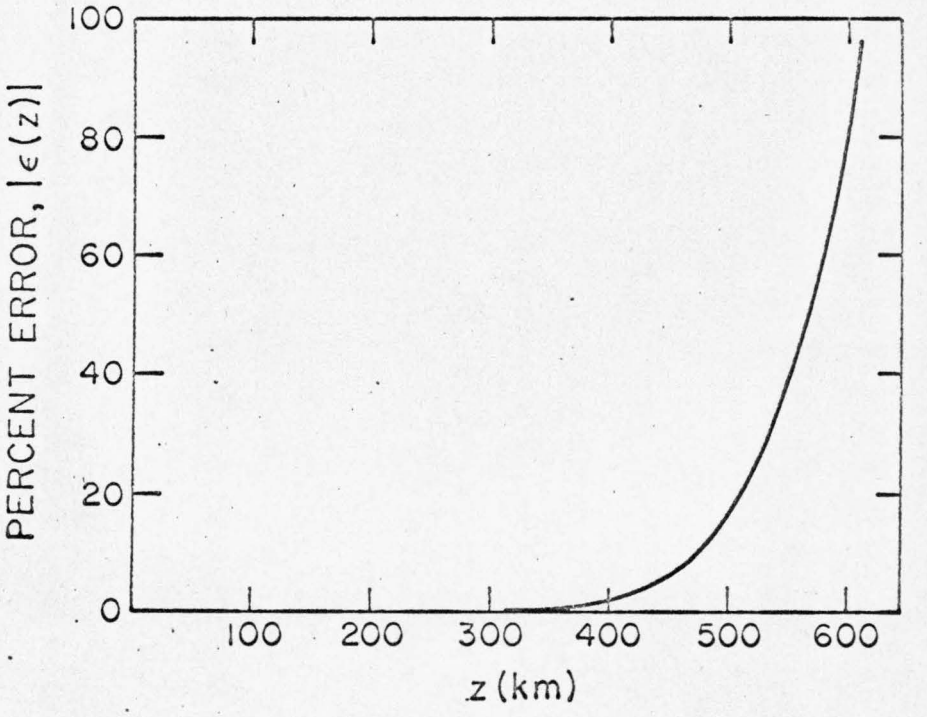

GRAPH 2aL

M = 20, ℓ = 2 km.

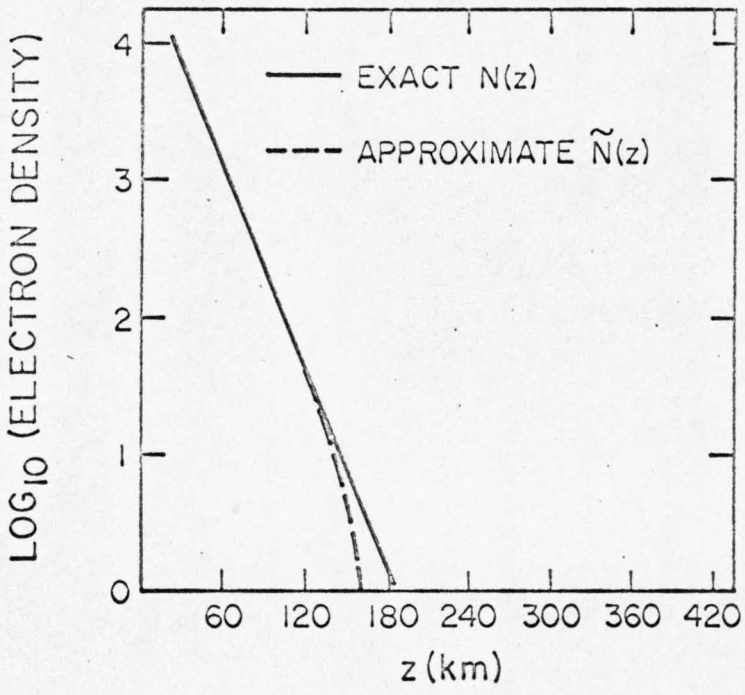

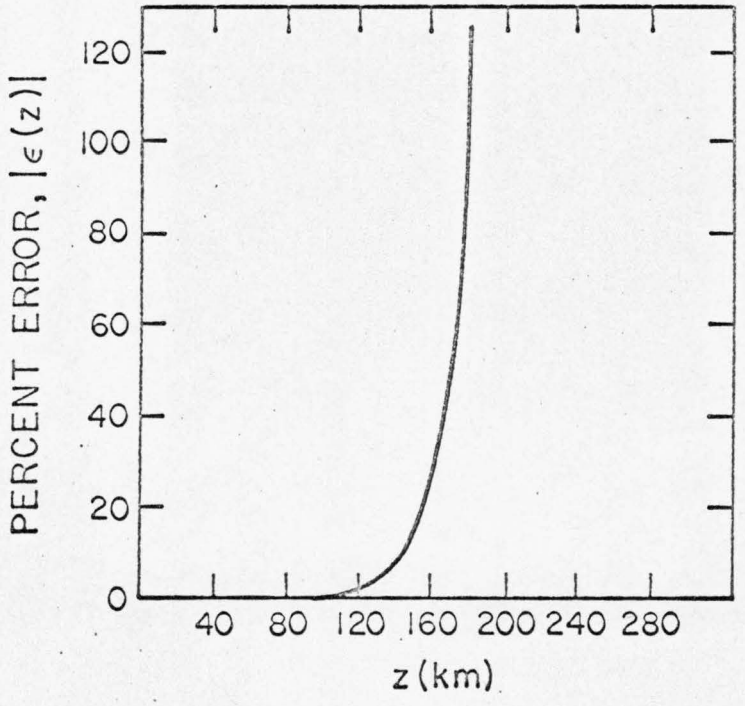

GRAPH 3aL

M = 20, ℓ = 2 km.

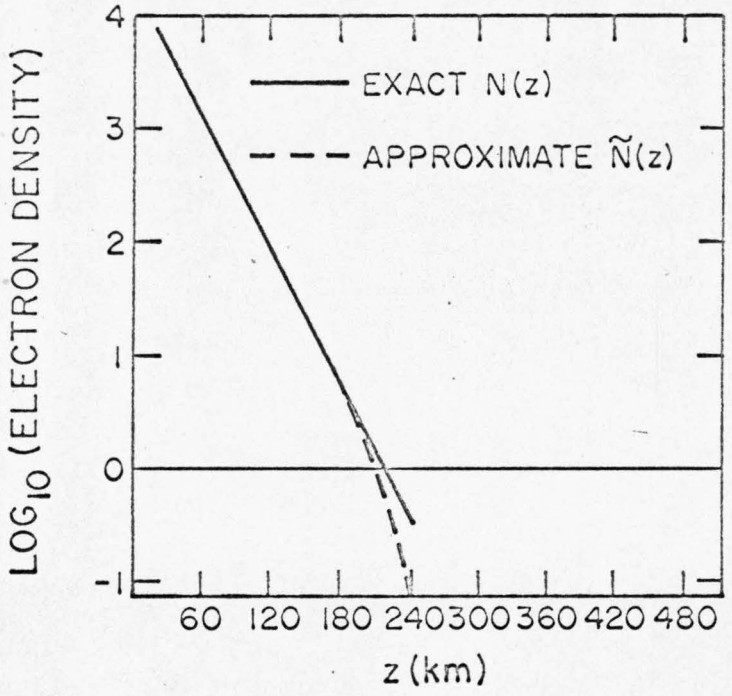

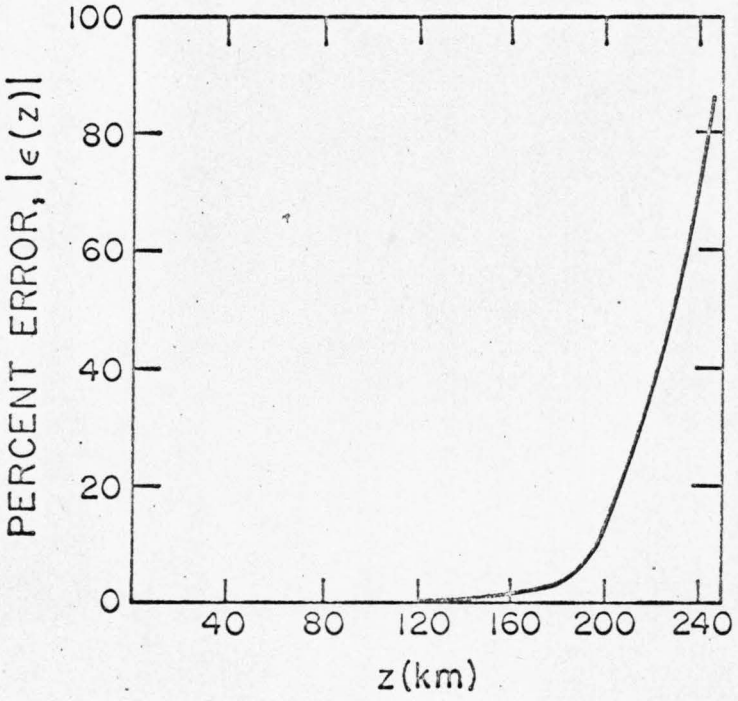

GRAPH 4bL

M = 10, ℓ = 2 km.

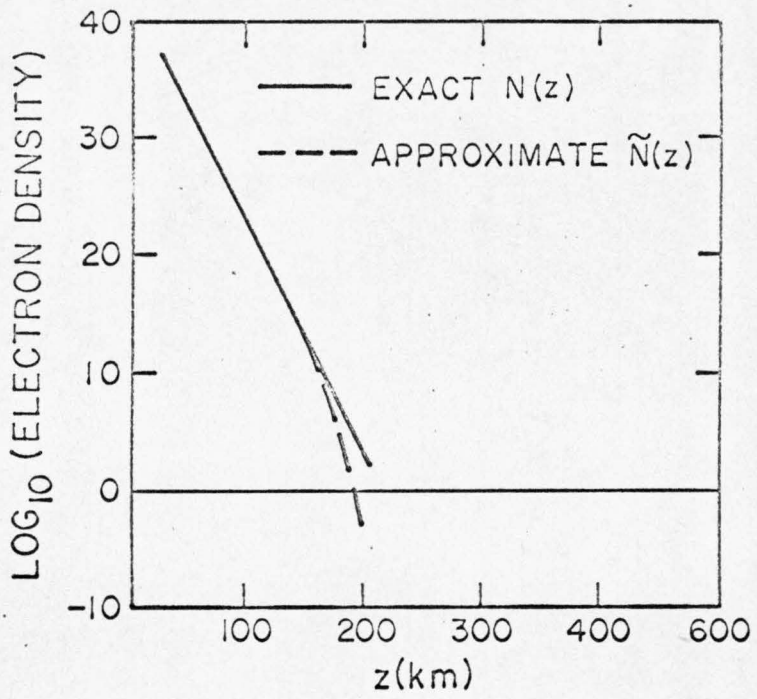

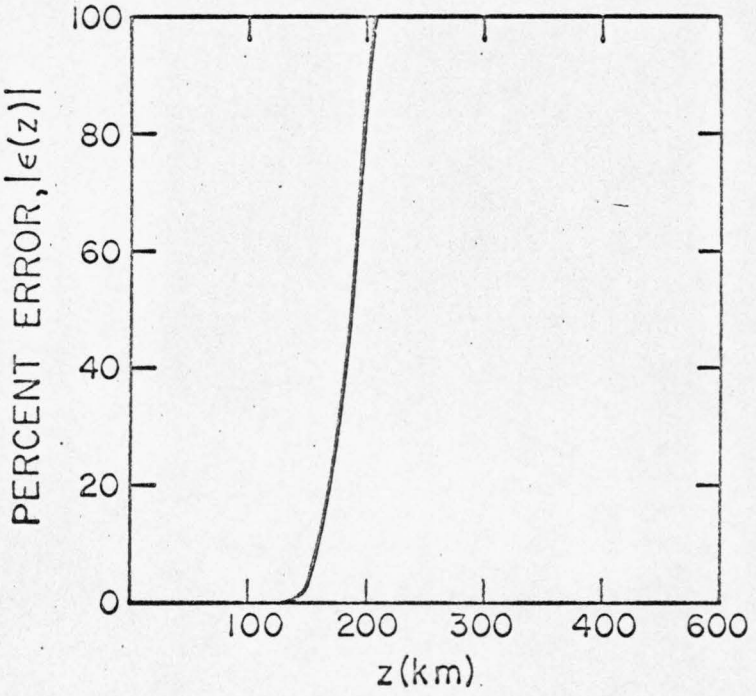

GRAPH 4bL

M = 10, ℓ = 2 km.

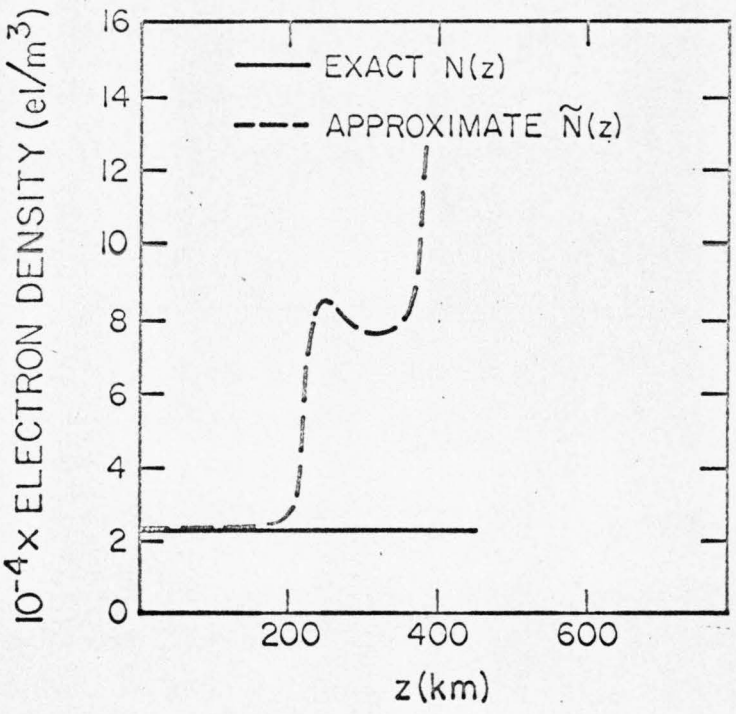

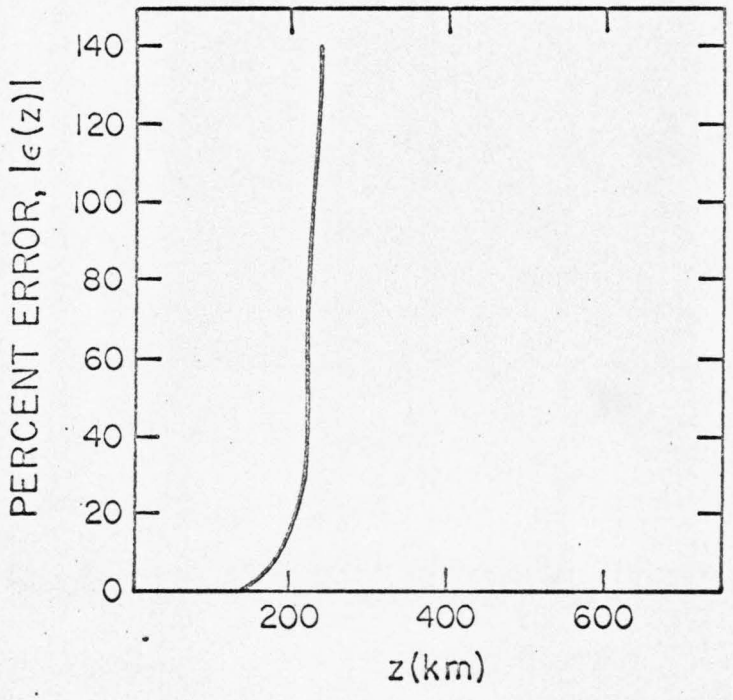

GRAPH 5aL

M = 20, ℓ = 2 km.

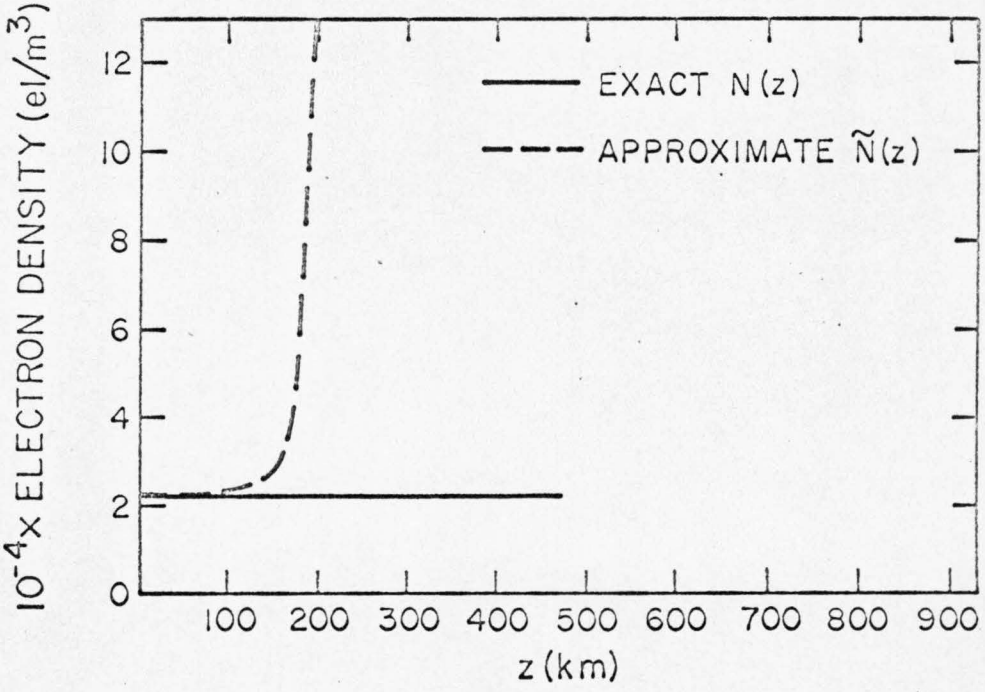

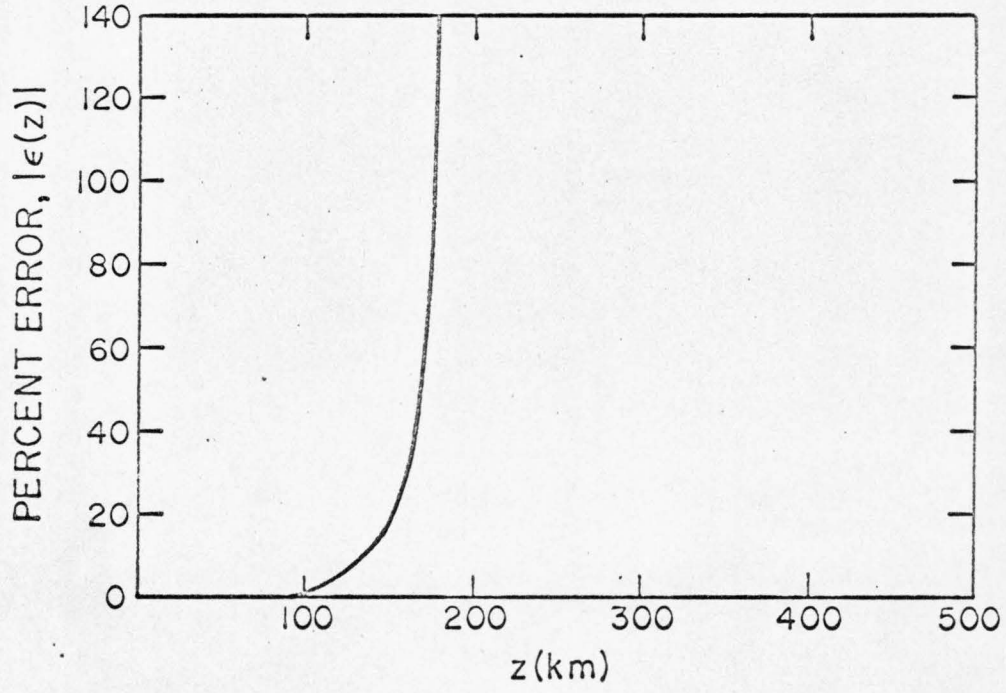

GRAPH 5bL

M = 10, ℓ = 2 km.

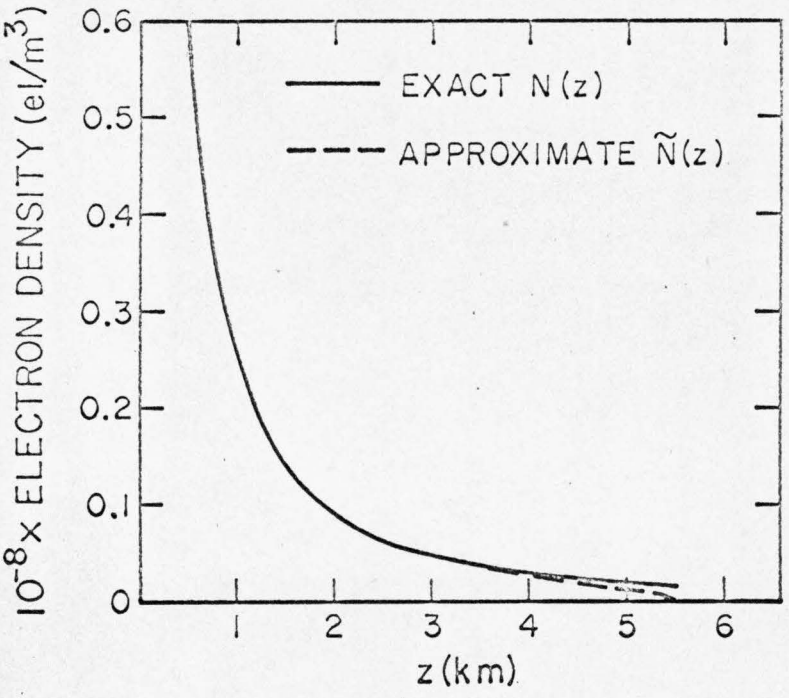

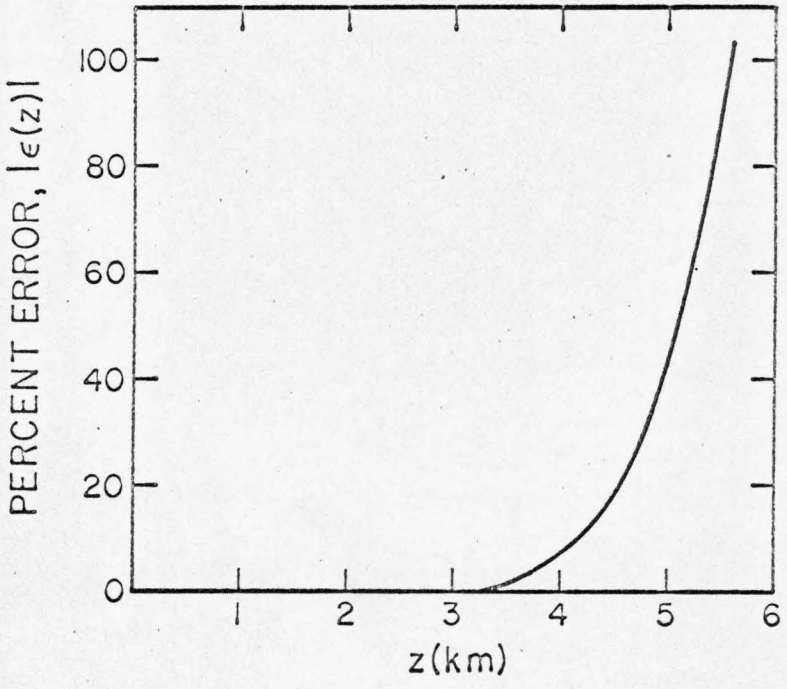

GRAPH 1aM

M = 20, ℓ = 50 m

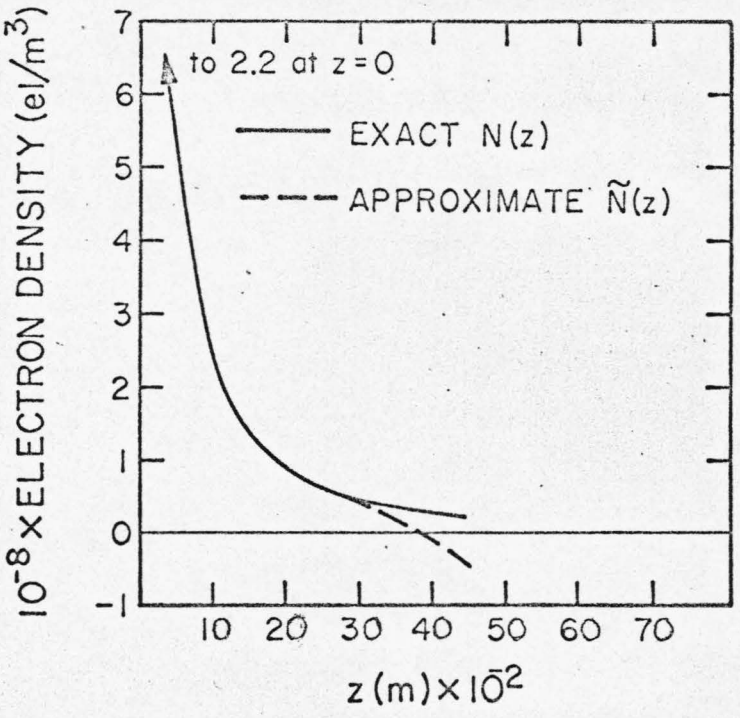

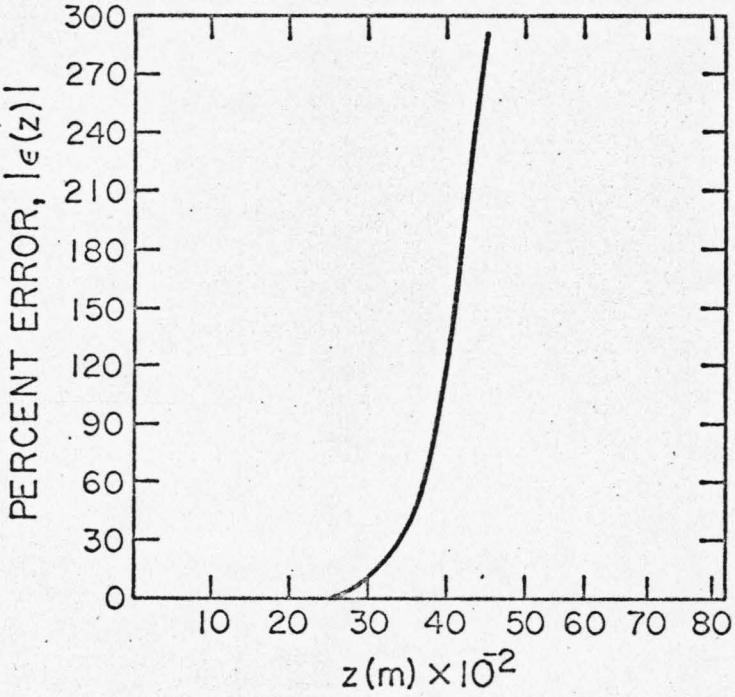

GRAPH 1bM

M ≒ 10, ℓ = 50 m

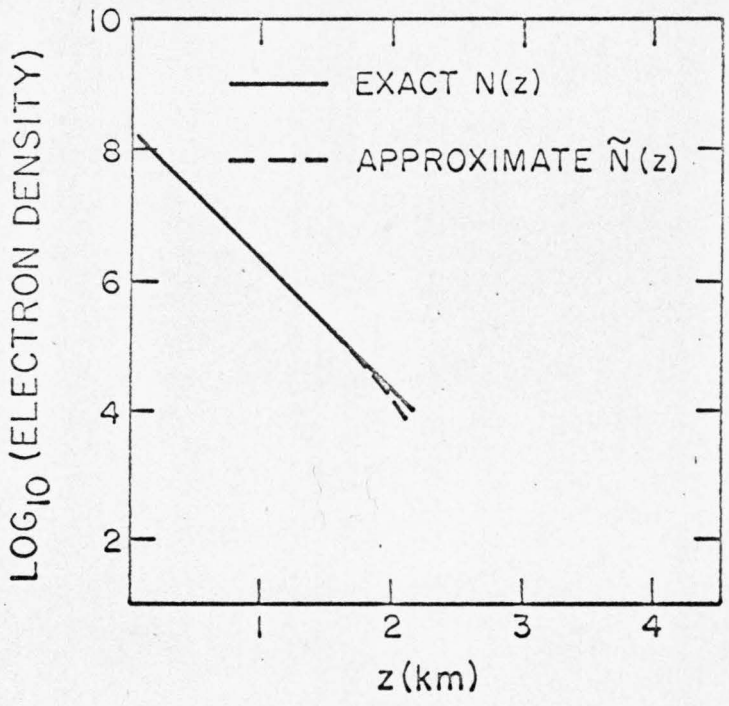

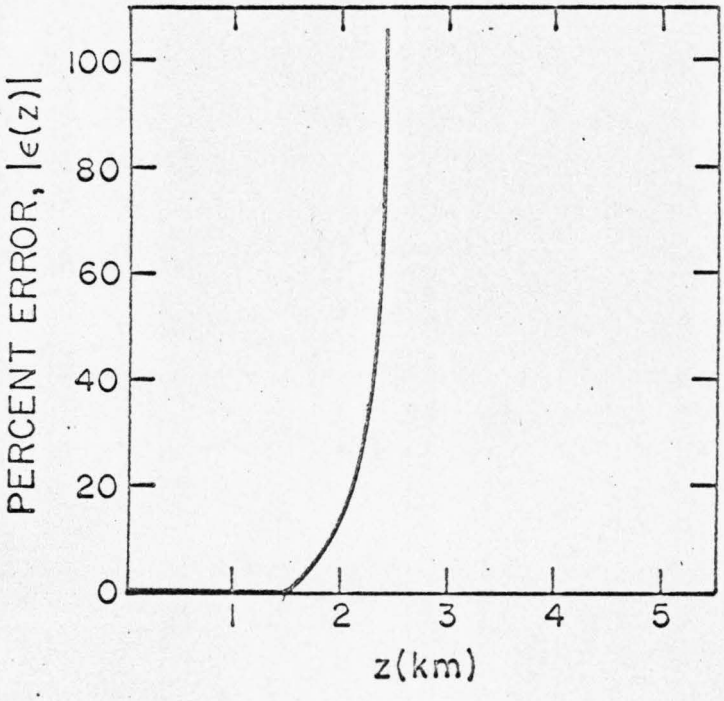

GRAPH 4aM

M = 20, ℓ = 50 m

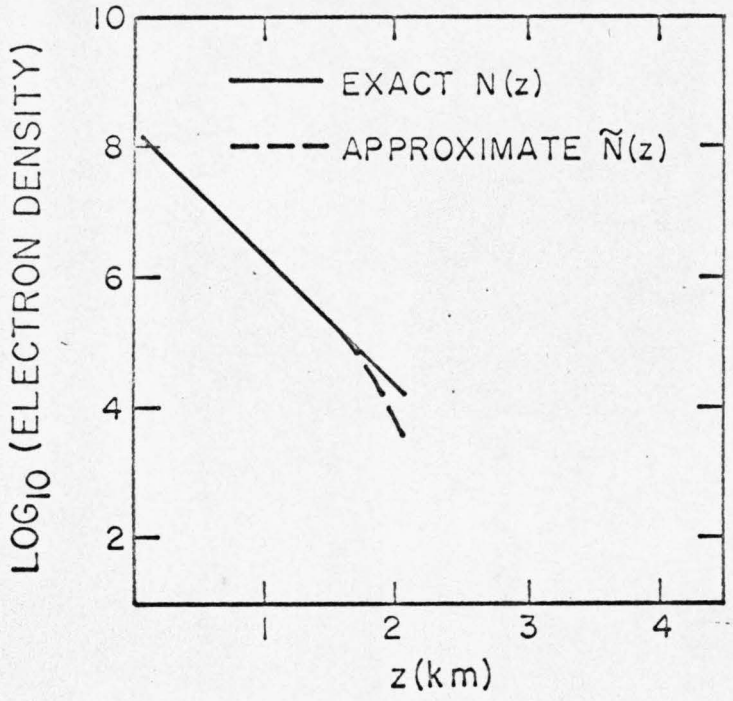

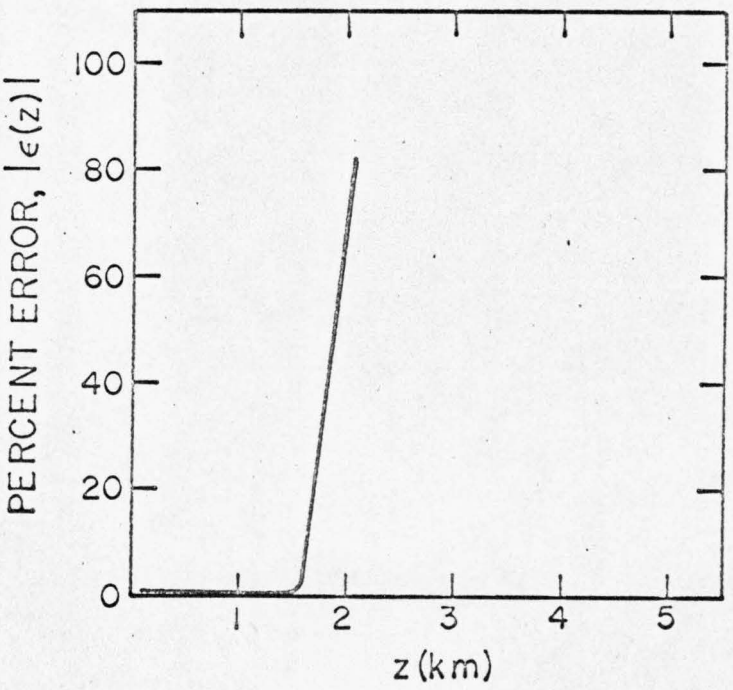

GRAPH 4bM

M = 10, ℓ = 50 m

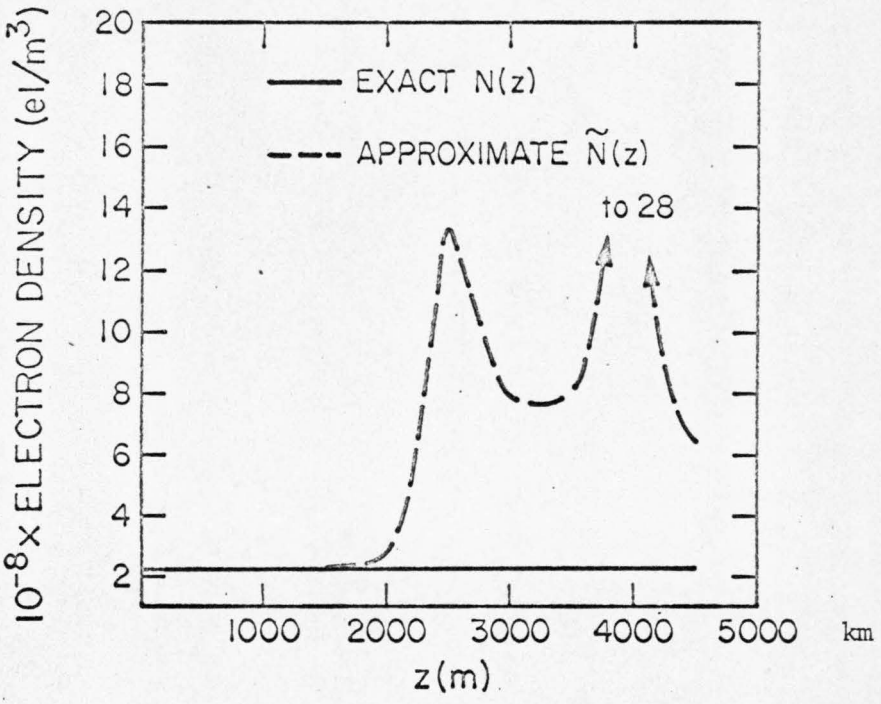

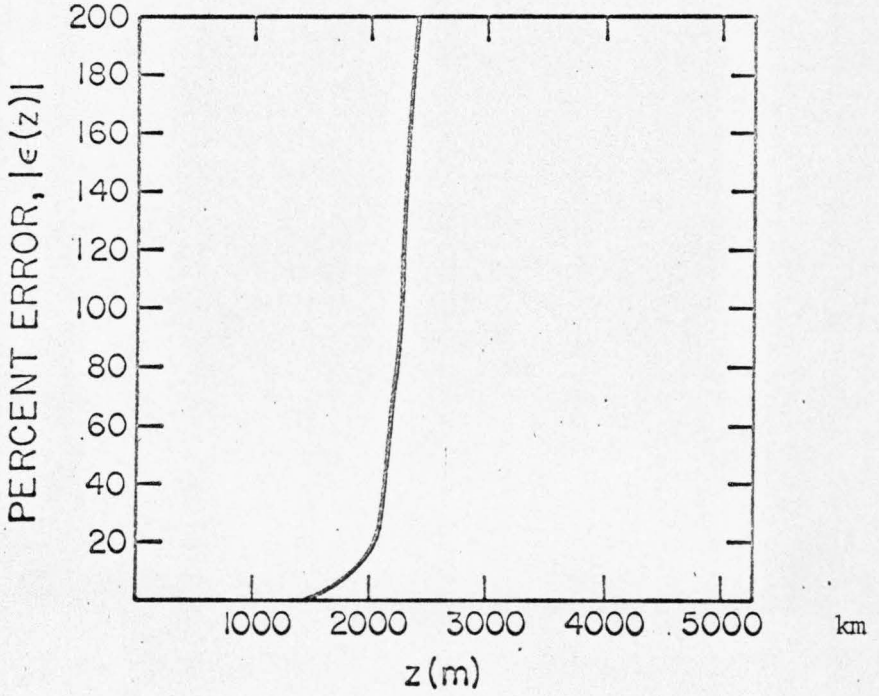

GRAPH 5aM

M = 20, ℓ = 50 m

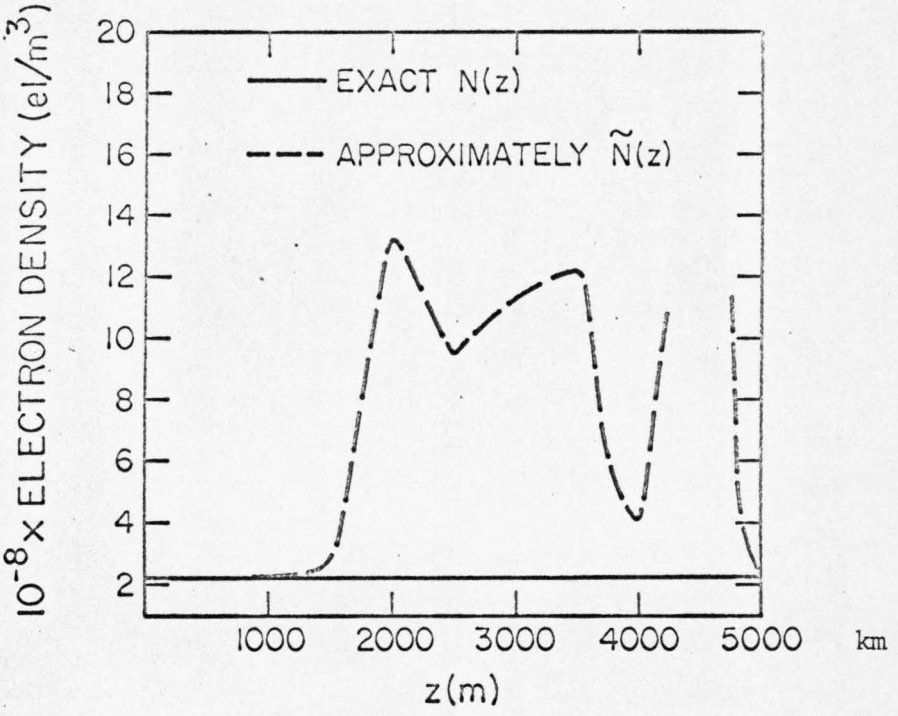

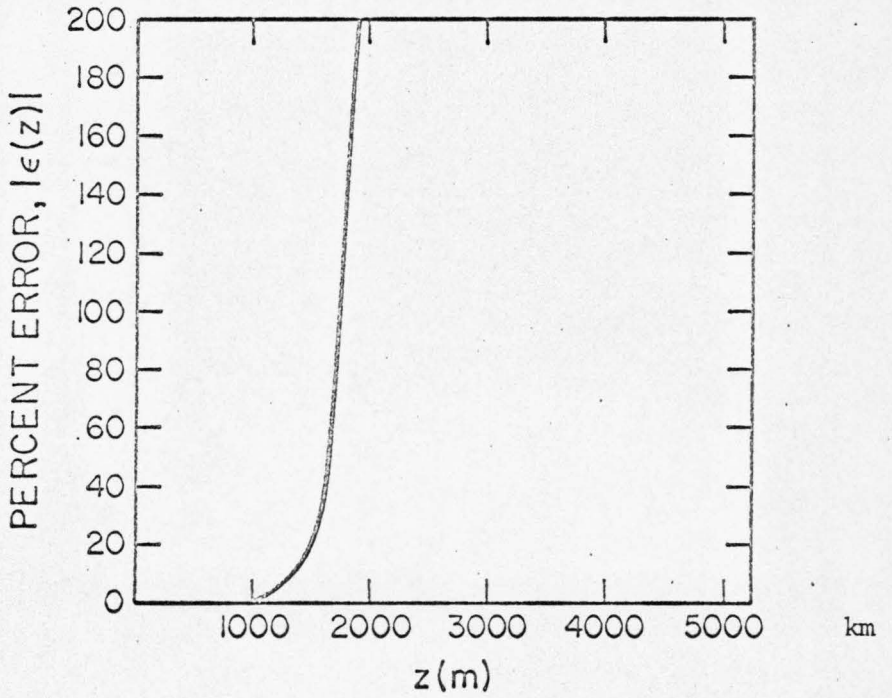

GRAPH 5bM

M = 10, ℓ = 50 m

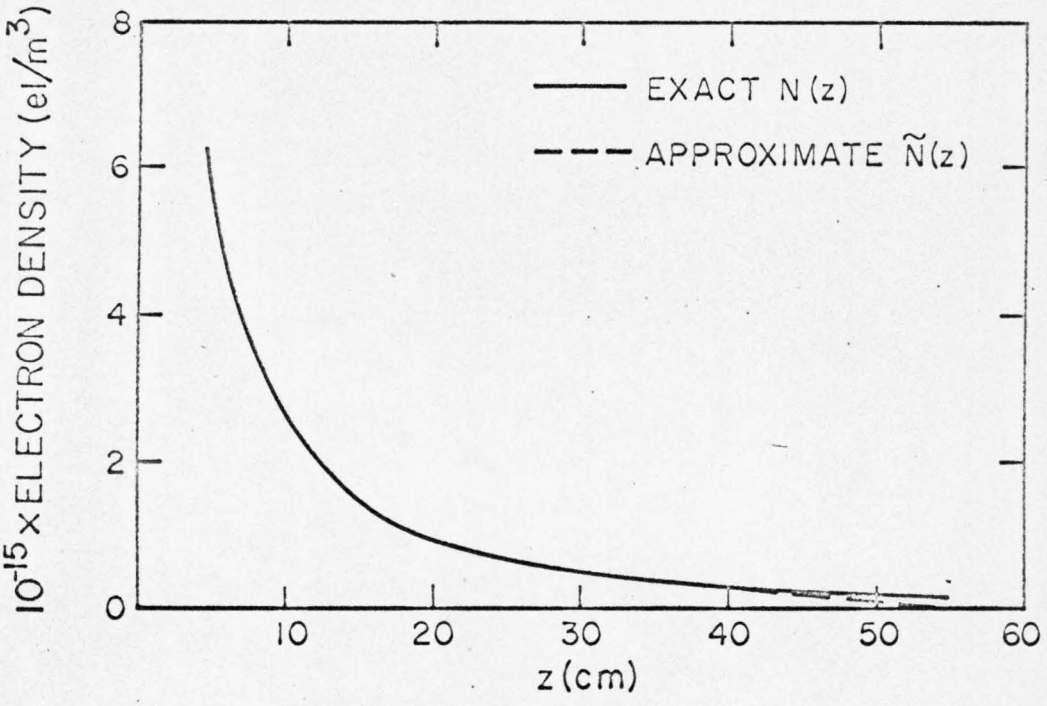

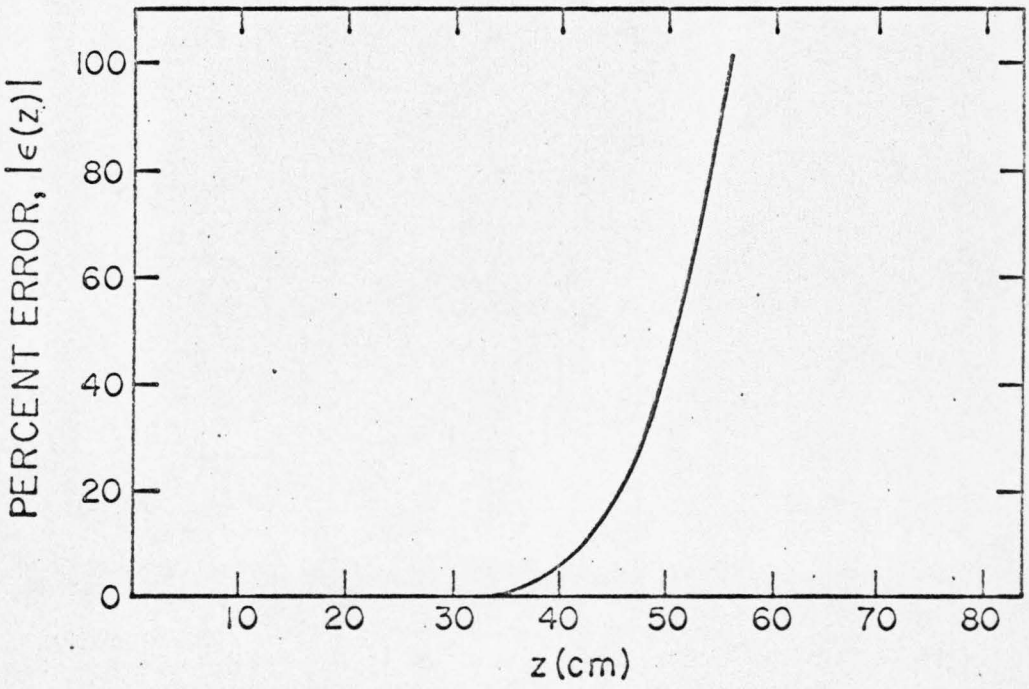

GRAPH 1aH

M = 20, ℓ = 5 mm

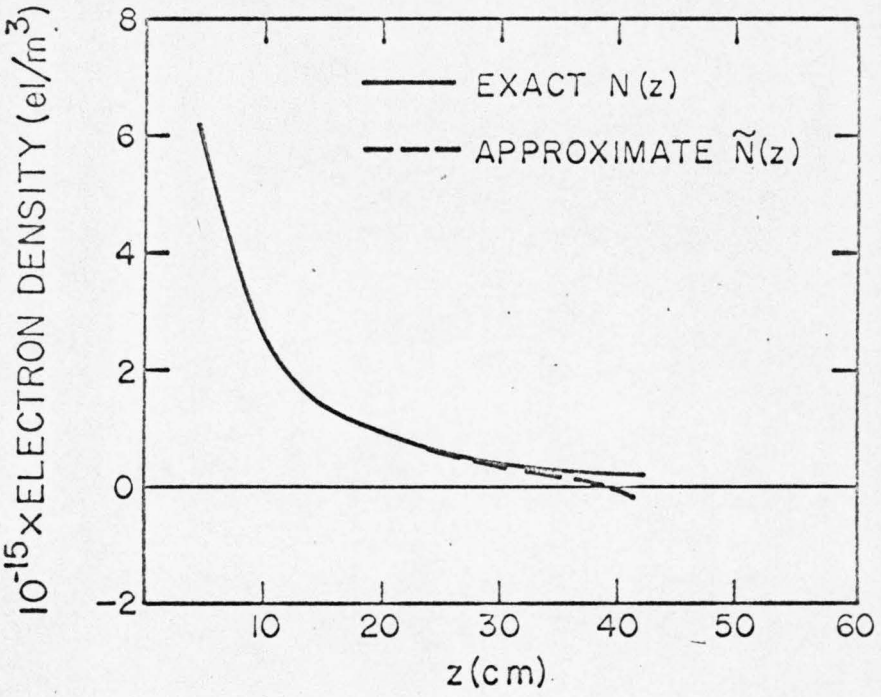

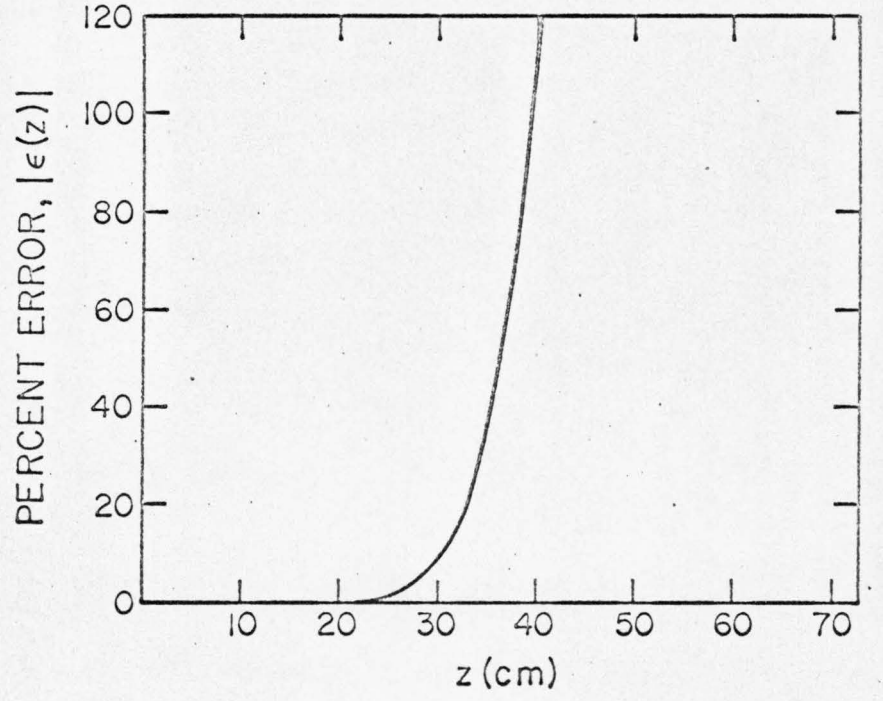

GRAPH 1bH

M = 10, ℓ = 5 mm

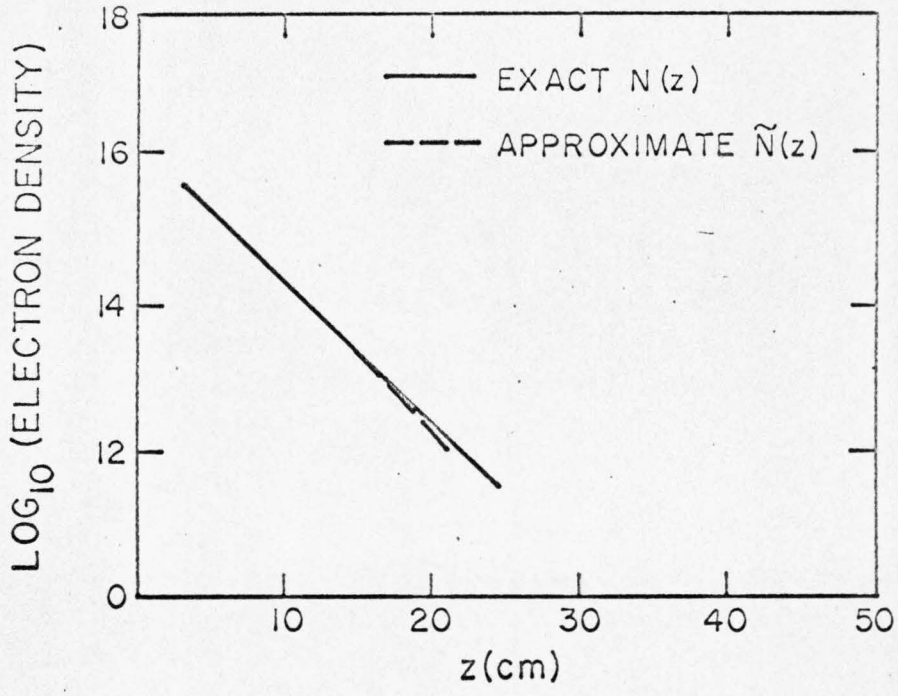

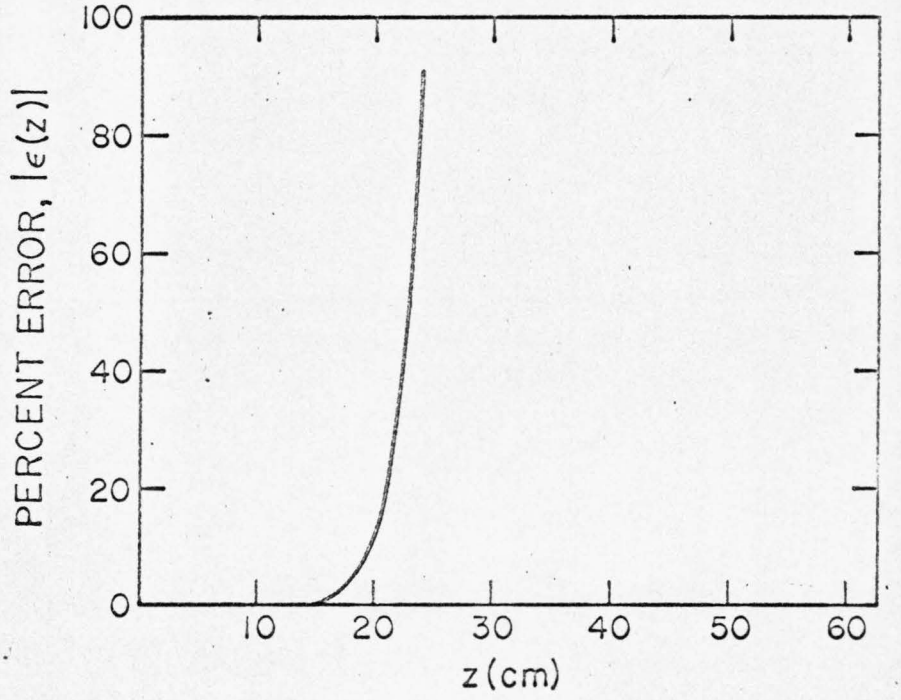

GRAPH 4aH

M = 20, ℓ = 5 mm

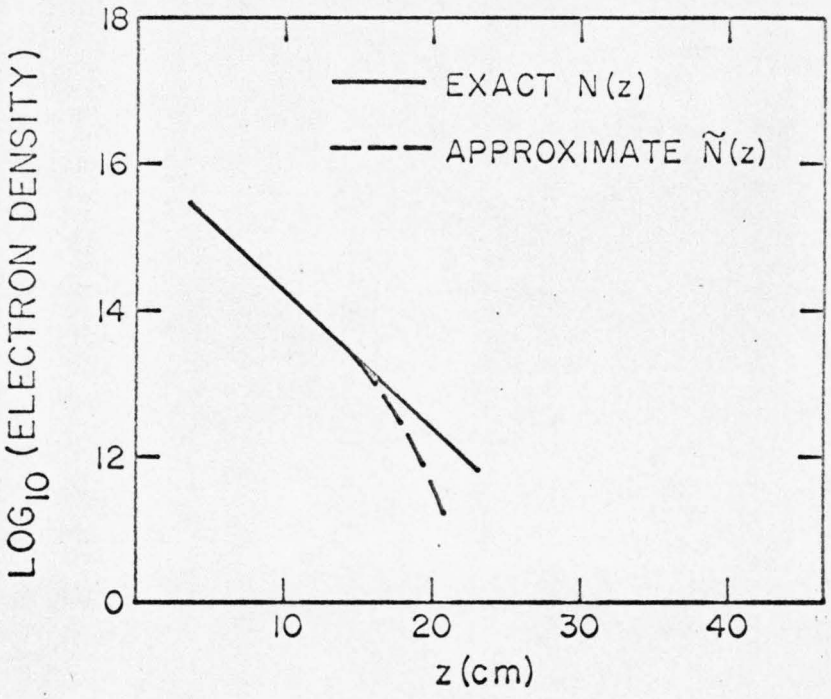

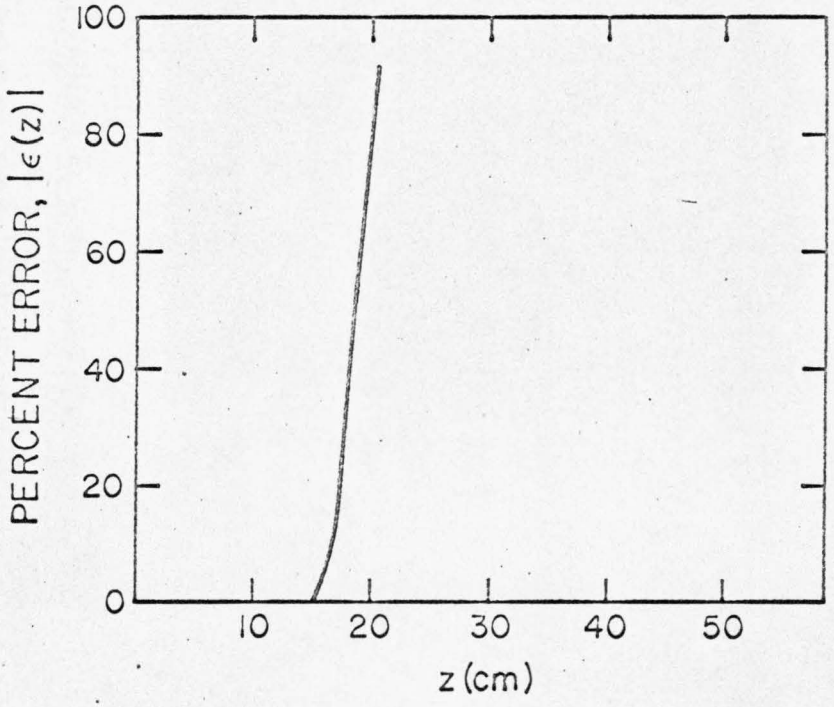

GRAPH 4bH

M = 10, ℓ = 5 mm

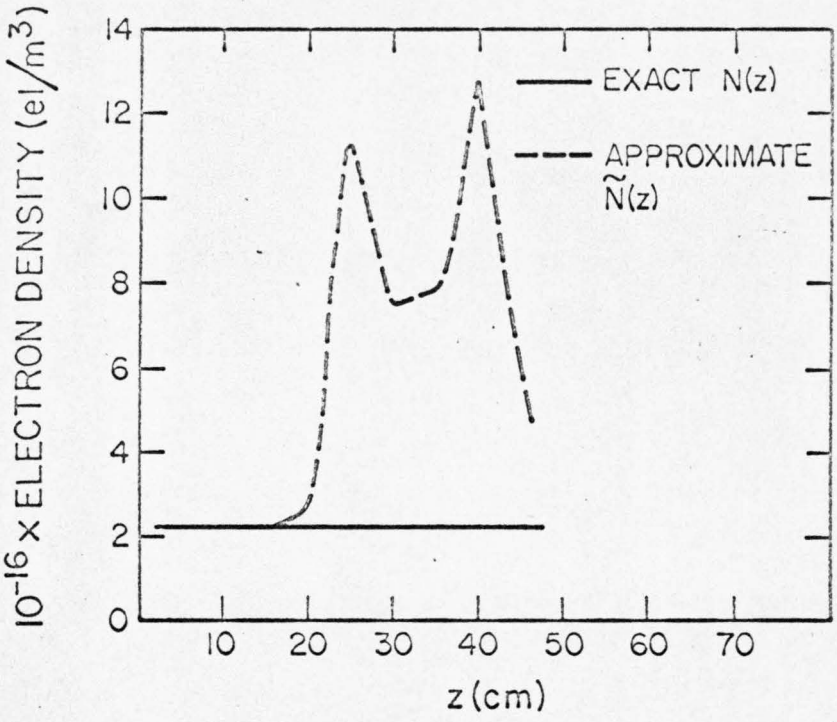

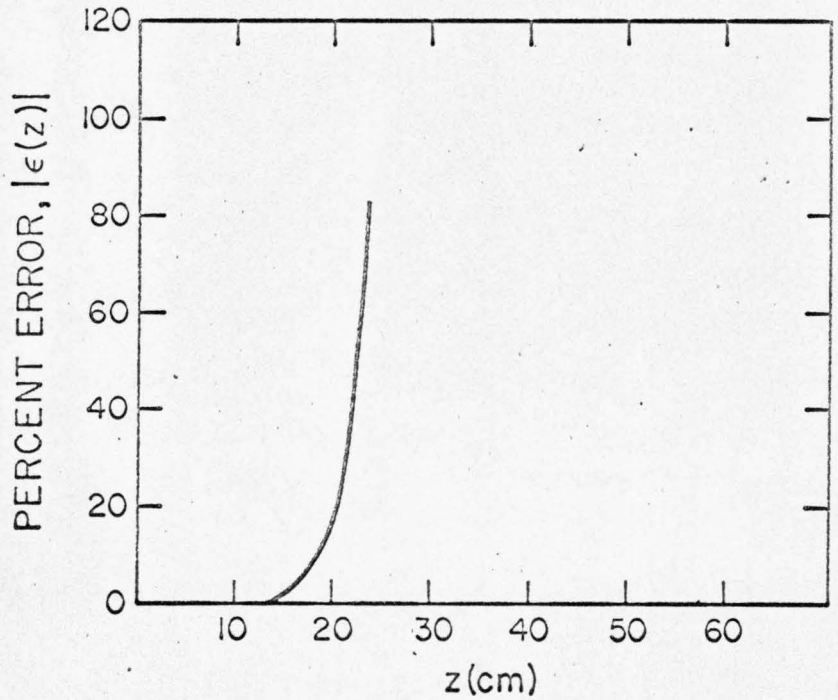

GRAPH 5aH

M = 20, ℓ = 5 mm

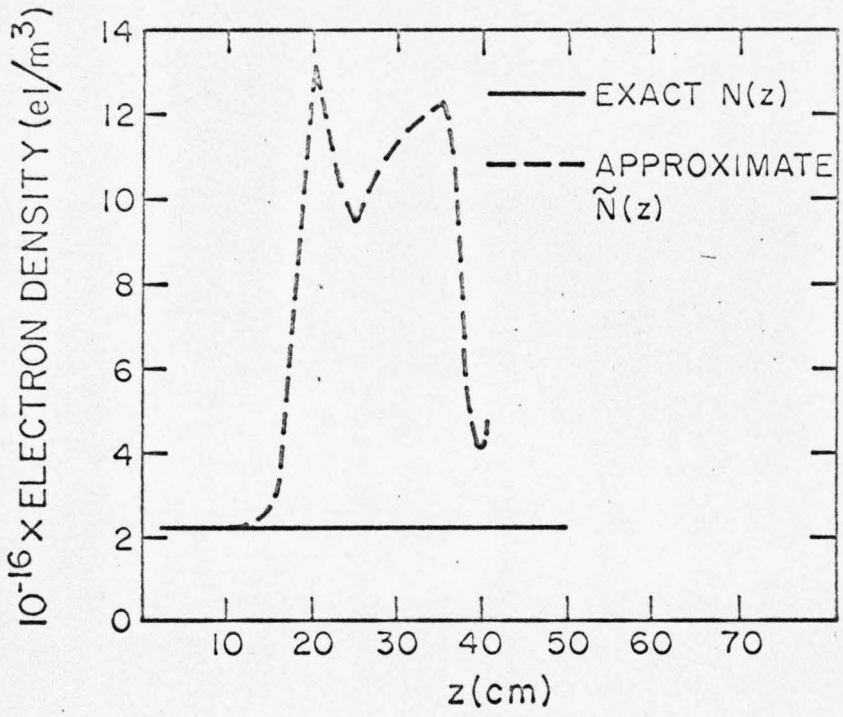

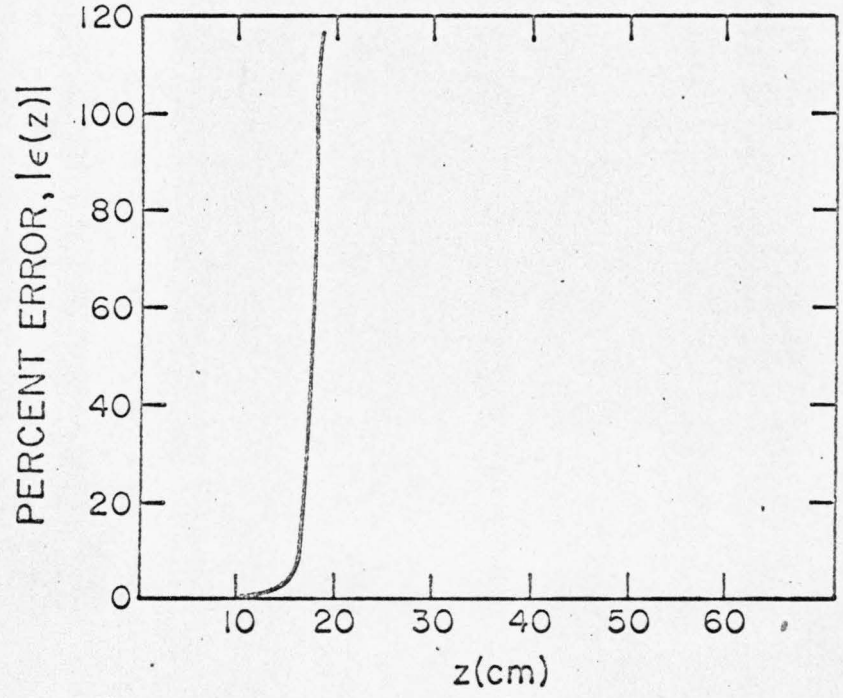

GRAPH 5bH

M = 10, ℓ = 5 mm

VI. CONCLUSIONS

In this report a numerical solution has been developed for the inverse scattering problem of inhomogeneous plane-stratified plasmas. The theory has been applied to the problem of determining the profile of a collisionless, unbiased plasma from a knowledge of the back-scattered wave of a normally incident pulse.

The back-scattered wave is monitored as a function of time and sampled with a uniform sampling rate. The sampled values are fed into a computer program that produces the electron density at each desired point inside the plasma.

It has been discovered that a square pulse can serve as the normally incident wave. A relation exists between the time duration of the pulse and the sampling time interval used on the backscattered wave. Both time intervals must be much less than $1/F$, where F is the maximum of the plasma frequency in the region included between the beginning of the plasma and the point inside the plasma where the electron density is desired.

The inverse scattering theory is an exact theory. In particular, it does not employ the "popular" W.K.B. approximation. A consequence of the exactness of the theory is the dependence of the error on the back scattered wave sampling rate. The faster we sample the back scattered wave, the smaller the difference between the actual and deduced electron densities.

Many of the troubles encountered in applying the currently employed ionogram method for plasma inverse scattering do not appear when one uses the inverse scattering method. In particular, we have

demonstrated that the inverse scattering method reproduces maxima and valleys of the plasma profile.

We hope that more research on the inverse scattering method will create a practical alternative to the ionogram method for ionospheric studies.

APPENDIX A

This appendix shows a claim made in Chapter 2, Section B, namely that the boundary value problem

$$\frac{\partial^2 C_1}{\partial z^2} - \frac{1}{c^2}\frac{\partial^2 C_1}{\partial t^2} - k_p^2(z)\, C_1(z,t) = k_p^2(z)\, \delta(z-ct), \quad z > 0 \tag{1}$$

$$C_1(0,ct) = \frac{\partial C_1}{\partial z}(0,ct) = 0 \tag{2}$$

is equivalent to

$$\frac{\partial^2 C_1}{\partial z^2} - \frac{1}{c^2}\frac{\partial^2 C_1}{\partial z^2} - k_p^2(z)\, C_1(z,ct) = 0 \quad , \qquad -z < ct < z \tag{3}$$

$$\frac{d}{dz} C_1(z,z) = \frac{1}{2} k_p^2(z) \tag{4}$$

$$C_1(z,-z) = 0 \tag{5}$$

$$C_1(z,ct) = 0 \quad , \qquad ct > z \tag{6}$$

$$C_1(z,ct) = 0 \quad , \qquad ct < -z \tag{7}$$

Proof of Claim

Equation (1) shows that

$$\frac{\partial^2 C_1}{\partial z^2} - \frac{1}{c^2}\frac{\partial^2 C_1}{\partial t^2} - k_p^2(z)\, C_1(z,ct) = 0 \quad , \qquad ct \neq z,\ z > 0 \tag{8}$$

and thus equation (3) is established.

The theory of characteristics for hyperbolic partial differential equations (equation (8) in a hyperbolic p.d.e.) shows that Cauchy

type boundary conditions on a line determine the solution in a region bounded by the line and the characteristic curves passing from the end points of the line. The characteristic curves of (8) are lines parallel to the lines $ct = z$, $ct = -z$. The Cauchy boundary conditions (2) and equation (8) show that in region (I) of Figure 1 $C_1(z,ct)$ must be zero. This proves equation (6). The Cauchy boundary conditions (2) and equation (8) show that in region (II) of Figure 1, $C_1(z,ct)$ must be zero. This proves equations (5) and (7).

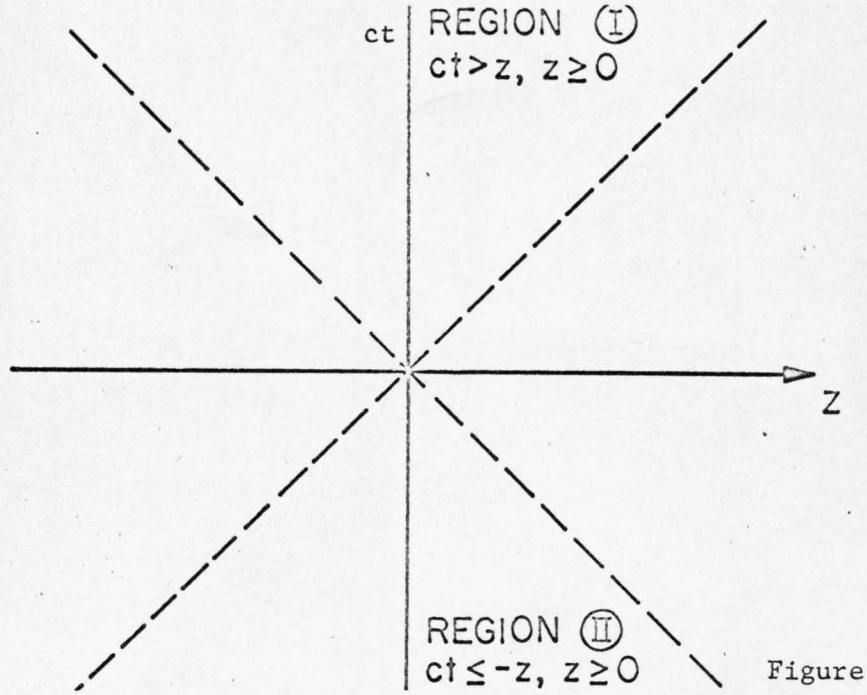

Figure 1

The δ-function on the right hand side of equation (2) shows that $C_1(z,ct)$ has discontinuous derivatives across the line $z = ct$. To find the nature of the discontinuity we introduce the characteristic coordinates

$$\xi = z + ct$$

$$\eta = z - ct$$

In this new coordinate system equation (1) becomes

$$4 \frac{\partial^2}{\partial \xi \, \partial \eta} Q(\xi,\eta) - k_p^2(\tfrac{\xi+\eta}{2}) \, Q(\xi,\eta) = k_p^2(\tfrac{\xi+\eta}{2}) \, \delta(\eta) \qquad (9)$$

where $C_1(z,ct)$ is in the new coordinate system

$$Q(\xi,\eta) = C_1(z,ct) \qquad (10)$$

Integrating equation (9) around a small region including $\eta = 0$ we find

$$4 \frac{\partial}{\partial \xi} Q(\xi,0) = k_p^2(\tfrac{\xi}{2}) \qquad (11)$$

Equations (10) and (11) prove equation (4).

APPENDIX B

This appendix shows a claim made in Chapter 2, Section B, namely that

$$R(z+ct) + C_1(z,ct) + \int_{-\infty}^{z} C_1(z,z')\, R(z'+ct)\,dz' = 0, \quad z \geq 0, \quad ct < z \qquad (1)$$

is satisfied even for $ct = z$.

Mathematically speaking it is intuitively clear that (1) must hold even for $ct = z$, since the functions $R(z+ct)$, $C_1(z,ct)$ are continuous.

We prove the claim using the description of the direct scattering problem given in Chapter 2, Section A. We can show that the solution $\hat{E}(z,k)$ of

$$\frac{d^2\hat{E}}{dz^2} + [k^2 - k_p^2(z)]\,\hat{E}(z,k) = 0 \qquad (2)$$

$$\hat{E}(z,k),\ \frac{\partial \hat{E}}{\partial z}(z,k) \quad \text{continuous across} \quad z = 0 \qquad (3)$$

$$\hat{E}(z,k) = e^{ikz} + r(k)e^{-ikz}, \quad z \leq 0 \qquad (4)$$

$$\hat{E}(z,k) \sim t(k)e^{ikz}, \quad z \to \infty \qquad (5)$$

obeys the integral equation[1]

---

[1] Equation (6) is easily obtained with the use of Green's function for the problem (2),(3),(4),(5).

$$f(z,k) = e^{ikz} + \int_z^\infty \frac{\sin k(y-z)}{k} k_p^2(y)\ f(y,k)\ dy \qquad (6)$$

with $t(k)$ given by

$$\frac{1}{t(k)} = 1 - \frac{1}{2ik} \int_0^\infty e^{-iky}\ k_p^2(y)\ f(y,k)\ dy \qquad (7)$$

where $f(y,k)$ is defined to be

$$f(y,k) = \frac{\hat{E}(y,k)}{t(k)} \qquad (8)$$

We write

$$f(z,k) = e^{ikz} - \frac{e^{ikz}}{2ik} \int_z^\infty k_p^2(y)\ dy + f_1(z,k) \qquad (9)$$

$$t(k) = 1 + \frac{1}{2ik} \int_0^\infty k_p^2(y)\ dy + t_1(k) \qquad (10)$$

Using (9) and (10) we write

$$\hat{E}(z,k) = e^{ikz} + \frac{e^{ikz}}{2ik} \int_0^z k_p^2(y)\ dy + \hat{E}_1(z,k) \qquad (11)$$

Taking Fourier transform of (11) with $ct = z$, we obtain

$$E(z,z) = \delta(0) - \frac{1}{4} \int_0^z k_p^2(y)\ dy + E_1(z,z) \qquad (12)$$

where

$$E_1(z,z) = \frac{1}{2\pi} \int_{-\infty}^{+\infty} \hat{E}_1(z,k)\ e^{-ikz}\ dk$$

Using (8), (9), (10), (11) we can show that

$$\hat{E}_1(z,k) = e^{ikz}\, 0(\tfrac{1}{k^2}) \quad \text{for} \quad |k| \to \infty\ ,\ k = 6 + i\tau\ ,\ \tau \geq 0$$

Thus $E_1(z,z) = 0$. Finally we obtain

$$E(z,z) = \delta(0) - \frac{1}{4}\int_0^z k_p^2(y)\, dy \tag{13}$$

In Chapter 2, Section B we found that the electric field $\hat{E}(z,k)$ is given by

$$\hat{E}(z,k) = e^{ikz} + r(k)\, e^{-ikz} + \hat{C}_1(z,k) + r(k)\, \hat{C}_1(z,-k),\ z \geq 0 \tag{14}$$

Taking the Fourier transform of (14)

$$E(z,ct) = \delta(z-ct) + R(z+ct) + \int_{-\infty}^{z} C_1(z,z')\, \delta(z'-ct)\, dz'$$

$$+ \int_{-\infty}^{z} C_1(z,z')\, R(z'+ct)dz'\ ,\quad z \geq 0 \tag{15}$$

where

$$E(z,ct) = \frac{1}{2\pi}\int_{-\infty}^{+\infty} E(z,k)\, e^{-ikct}\, dk$$

$$\delta(z-ct) = \frac{1}{2\pi}\int_{-\infty}^{+\infty} e^{ik(z-ct)}\, dk$$

$$R(z+ct) = \frac{1}{2\pi}\int_{-\infty}^{+\infty} r(k)\, e^{-ik(z+ct)}\, dk$$

$$C_1(z,ct) = \frac{1}{2\pi}\int_{-\infty}^{+\infty} C_1(z,k) e^{-ikct}\, dk$$

We let $ct = z$ in equation (15). We obtain

$$E(z,z) = \delta(0) + R(2z) + \frac{1}{2} C_1(z,z) + \int_{-\infty}^{z} C_1(z,z') R(z'+z)dz' \qquad z \geq 0 \qquad (16)$$

From the signature equation

$$\frac{d}{dz} C_1(z,z) = \frac{1}{2} k_p^2(z) \qquad (17)$$

we obtain

$$C_1(z,z) = \frac{1}{2} \int_{0}^{z} k_p^2(y)\, dy \qquad (18)$$

Equating equations (13) and (16) and using (18) we obtain

$$R(2z) + C_1(z,z) + \int_{-\infty}^{z} C_1(z,z') R(z'+z)dz' = 0, \quad z \geq 0, \qquad (19)$$
$$z = ct$$

Equation (19) proves the claim.

APPENDIX C

This appendix shows a claim made in Chapter 2, Section B, namely that if the integral equation

$$R(z+ct) + f(z,ct) + \int_{-\infty}^{z} f(z,z')\, R(z'+ct)dz' = 0,\ z > 0,\ ct \leq z$$

has a solution $f(z,ct)$, then the solution is unique.

Statement

If the integral equation

$$R(z+ct) + f(z,ct) + \int_{-\infty}^{z} f(z,z')\, R(z'+ct)\, dz' = 0,\ z \geq 0,\ ct \leq z \tag{1}$$

has a solution $f(z,ct)$, then the solution is unique.

Proof:

The proof of this statement has been given by I. Kay.[1] We just sketch his proof.

Suppose (1) is solved by two different solutions $f_1(z,ct)$ and $f_2(z,ct)$. Their difference $W(z,ct)$ solves

$$W(z,ct) + \int_{-\infty}^{z} W(z,z')\, R(z'+ct)\, dz' = 0\ ,\quad z \geq 0,\ ct \leq z \tag{2}$$

The statement is proved if it is shown that $W(z,ct)$ is necessarily equal to zero.

I. Kay uses equations (3), (4)

$$r^*(k) = r(-k) \tag{3}$$

(a consequence of the fact that the reflected wave is a real function)

---

[1] See Reference 1

$$|r(k)|^2 + |t(k)|^2 = 1 \quad \text{(energy conservation)} \tag{4}$$

where $r(k)$, $t(k)$ are the reflection and transmission coefficients

to establish the identity

$$\delta(z'-ct) + R(z'+ct) = \frac{1}{2\pi}\int_0^\infty |t(k)|^2 e^{ik(z'-ct)}\, dk$$

$$+ \frac{1}{2\pi}\int_{-\infty}^0 [e^{ikz'} + r(k)e^{-ikz'}]\,\{[e^{ikct} + r(k)e^{-ikct}]\}^*\, dk \tag{5}$$

He writes (2) in the form

$$\int_{-\infty}^z W(z,z')[\delta(z'-ct) + R(z'+ct)]dz' = 0\ ,\ z \geq 0,\ ct \leq z \tag{6}$$

Using (5) on equation (6) he is able to show

$$\int_{-\infty}^z W(z,z')e^{-kz'}\, dz' = 0$$

It follows that

$$W(z,ct) = 0$$

---

*complex conjugate

APPENDIX D

This appendix shows that for plasma wave numbers $k_p(z)$ which have the properties

$$k_p^2(z) \text{ is a piecewise continuous, bounded function of } z \tag{1}$$

$$k_p^2(z) \to 0 \text{ "fast enough" as } z \tag{2}$$

$$k_p^2(z) = 0 \quad \text{for} \quad z < 0 \tag{3}$$

the reflected wave $R(ct)$

$$R(ct) = \frac{1}{2} \int_{-\infty}^{+\infty} r(k)\, e^{-ikct}\, dk \tag{4}$$

where $r(k)$ is the reflection coefficient of the plasma, is a continuous function of ct

$$R(ct) \text{ continuous function of } ct \tag{5}$$

bounded function of ct

$$R(ct) \text{ bounded function of } ct \tag{6}$$

and equal to zero for $ct \leq 0$

$$R(ct) = 0 \quad \text{for} \quad ct \leq 0 \tag{7}$$

Proof:

To prove the properties (5), (6), (7) of the reflected wave, we need to show that the reflection coefficient $r(k)$ obeys equations (8), (9), (10)

$$r(k) \text{ has no poles in the upper half of the complex k-plane} \tag{8}$$

$$r(k) = 0(\frac{1}{k^2}) \quad \text{as} \quad |k| \to \infty \ , \ k \text{ real} \tag{9}$$

$$r(k) \quad \text{is a regular function of} \quad k \ , \ k \text{ real} \tag{10}$$

Properties (9) and (10) show that

$$\int_{-\infty}^{+\infty} |r(k)|dk \qquad \text{exists} \tag{11}$$

Schwartz on page 180 of Reference 23 shows that (11),(10) imply equation (5) and (6).

Taking the Fourier transform in the upper half complex k-plane and using equations (8),(9) and Cauchy's theorem we easily show equation (7).

Under the conditions that $k_p^2(z)$ satisfies

$$\int_0^{\infty} k_p^2(y)\, dy \tag{12}$$

$$\int_0^{\infty} y\, k_p^2(y)\, dy \tag{13}$$

I. Kay[1] shows that equations (8),(10) are satisfied. Equations (12), (13) are satisfied by properties (1), (2), (3) of $k_p^2(z)$. Thus we only need to show equation (9).

The direct scattering problem posed in Chapter 2, Section A shows that $\hat{E}(z,k)$ satisfies

$$\frac{d^2\hat{E}}{dz^2} + [k^2 - k_p^2(z)]\, \hat{E}(z,k) = 0 \tag{14}$$

---

[1] See Reference 3, p. 374

$$\hat{E}(z,k),\ \frac{\partial \hat{E}}{\partial z}(z,k) \quad \text{continuous across} \quad z = 0 \tag{15}$$

$$\hat{E}(z,k) = e^{ikz} + r(k)e^{-ikz}\ , \qquad z \leq 0 \tag{16}$$

$$\hat{E}(z,k) \sim t(k)e^{ikz}\ , \qquad \text{as} \quad z \to \infty \tag{17}$$

Defining $f(z,k)$

$$f(z,k) = \frac{\hat{E}(z,k)}{t(k)} \tag{18}$$

and using Green's function techniques we obtain

$$f(z,k) = e^{ikz} + \int_z^\infty \frac{\sin[k(y-z)]}{k}\, k_p^2(y)\, f(y,k)\, dy \tag{19}$$

$$\frac{r(k)}{t(k)} = \frac{1}{2ik} \int_0^\infty e^{iky}\, k_p^2(y)\, f(y,k)\, dy \tag{20}$$

$$\frac{1}{t(k)} = 1 - \frac{1}{2ik} \int_0^\infty e^{-iky}\, k_p^2(y)\, f(y,k)\, dy \tag{21}$$

Stone[2] has shown that for any $k_p^2(z)$ satisfying (12),(13), $f(z,k)$ is given by

$$f(z,k) = e^{ikz}\left[1 + \frac{m(z,k)}{k}\right] \quad \text{for large enough} \quad k \tag{22}$$

The function $m(z,k)$ is a uniformly bounded function of z and of k. Using (22) we easily show that

$$\frac{1}{t(k)} = 1 + 0\left(\frac{1}{k}\right) \qquad \text{as} \quad k \to \infty \tag{23}$$

---

[2] See Reference 20

Equations (23) and (22) when substituted in equation (20) show that

$$r(k) = 0(\frac{1}{k^2}) \quad \text{as} \quad |k| \to \infty \ , \quad k \text{ real}$$

Thus, we proved equation (9). This completes the proof of equations (5), (6), (7) under assumptions (1), (2), (3).

APPENDIX E

In this appendix we present a computer program designed to carry out the numerical solution of the inverse scattering algorithm presented in Chapter 3, Sections Aa, Ab.

A computer program named MAIN PROGRAM implements the numerical solution of the inverse scattering algorithm described in Chapter 3, Sections Aa, Ab. The program has two main parts, a subroutine named INVER and a subroutine named ELECTRON DENSITY.

Subroutine INVER performs two jobs. INVER uses the supplied uniformly samples values of the distance record of the reflected wave R(ct) from ct = 0 to ct = 2z to create the (2M+1) × 1 vector R and the (2M+1) × (2M+1) matrix a.

$$R = (r_i)$$

$$r_i = R[(i-1)h] \quad \text{for} \quad i=1,2,3,\cdots,2M+1$$

$$h = z/M$$

$$a = (a_{ij})$$

a_{ij} as defined in Chapter 3, Section Aa

Then subroutine INVER solves the matrix equation

$$a\chi = -R \tag{1}$$

using a standard IBM 360 subroutine called MATIN[1]

---

[1] MATIN solves equation (1) $a\chi = -R$, through matrix inversion.

$$\chi = a^{-1}(-R)$$

MATIN is a general purpose subroutine. It inverts equation (1) for any square matrix a.

Subroutine INVER selects the top element of χ which is $C_1(z,z)$. The output of INVER is $C_1(z,z)$.

Subroutine ELECTRON DENSITY has as its inputs the characteristic fields $C_1(z+\ell,z+\ell)$, $C_1(z-\ell,z-\ell)$. ELECTRON DENSITY finds $N(z)$ from

$$N(z) = \frac{2}{3.54 \times 10^{-14}} \frac{C_1(z+\ell,z+\ell) - C_1(z-\ell,z-\ell)}{\ell}$$

The flow chart of MAIN PROGRAM is as follows

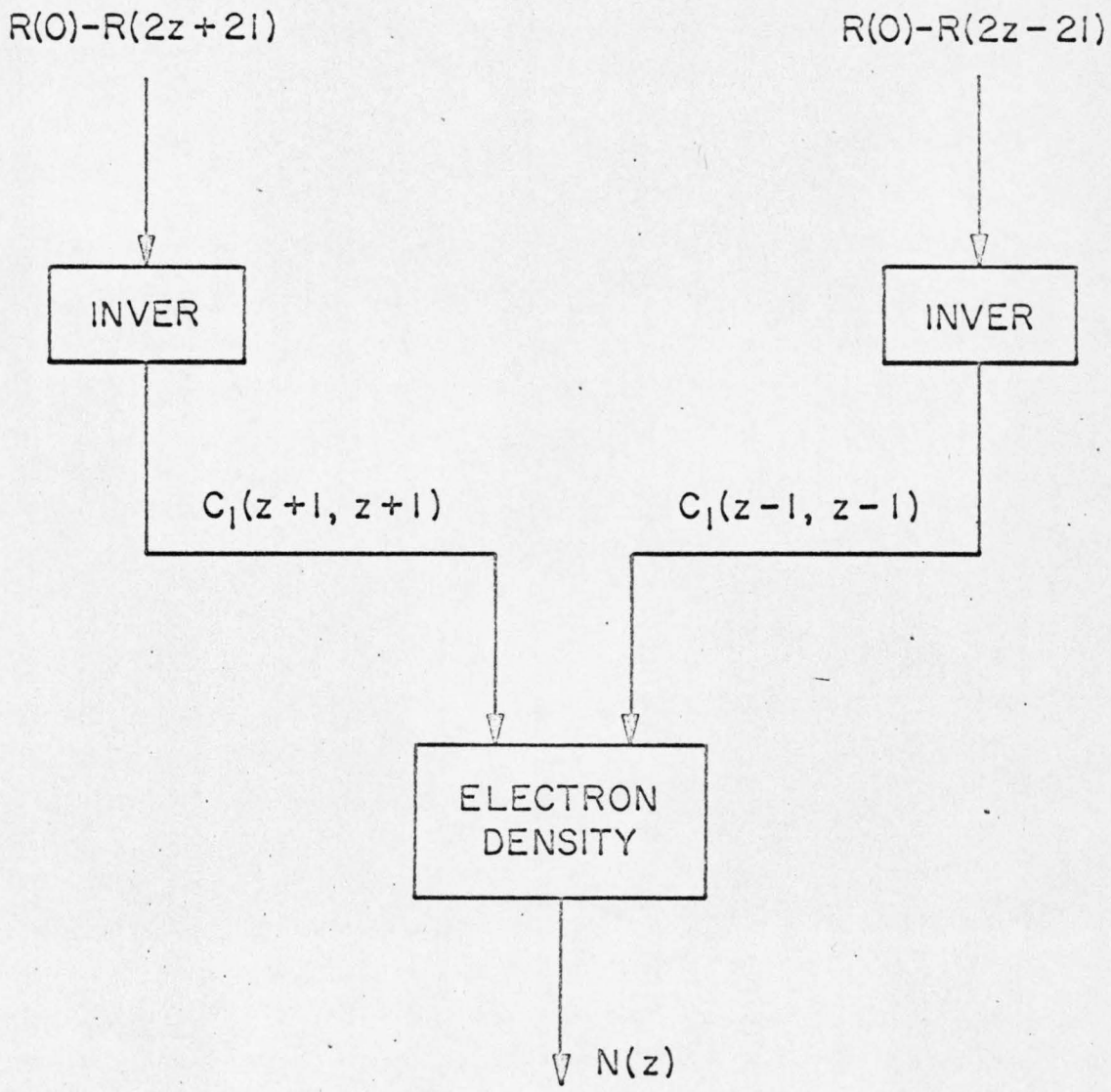

COMPUTER PROGRAM FLOW CHART

APPENDIX F

This appendix shows the following statement made in Chapter 3, Section Ac.

Error Statement

For small percent errors $\varepsilon(z;M)$, $\varepsilon(z;M)$ is to a good approximation inversely proportional to the fourth power of M.

To prove the statement we recall that we find the electron density $N(z)$ from a numerical solution of the inverse scattering algorithm.

We replaced the algorithm

$$R(z+ct) + C_1(z,ct) + \int_{-ct}^{z} C_1(z,z')\, R(z'+ct)\, dz' = 0 \tag{1}$$

$$\frac{d}{dz} C_1(z,z) = \frac{1}{2} k_p^2(z) \tag{2}$$

$$k_p^2(z) = 3.54 \times 10^{-14} N(z) \tag{3}$$

by

$$R(z+ct_i) + \tilde{C}_1(z,ct_i) + I(z;M) = 0 \tag{4}$$

$$\frac{d}{dz} \tilde{C}_1(z,z) = \frac{1}{2} \tilde{k}_p^2(z) \tag{5}$$

$$\tilde{k}_p^2(z) = 3.54 \times 10^{-14} \tilde{N}(z) \tag{6}$$

where $I(z;M)$ is an expansion of the integral

$$\int_{-ct_i}^{z} C_1(z,z')\, R(z'+ct_i)\, dz'$$

using a combination of Simson's and trapezoidal rules. For $ct_i = z$

equation (4) becomes

$$R(2z) + \tilde{C}_1(z,z) + I(z;M) = 0 \tag{7}$$

where $I(z;M)$ is the Simson rule approximation to the integral

$$\int_{-z}^{z} C_1(z,z')\, R(z'+z)\, dz'$$

$I(z;M)$ is given by

$$I(z;M) = \frac{h}{3}\left[\tilde{C}_1(z,z;M)\, R(2z) + 4\tilde{C}_1(z,z-h;M)\, R(2z-h)\right.$$
$$\left. + 2\tilde{C}_1(z,z-2h;M)\, R(2z-2h) + \cdots + \tilde{C}_1(z,-z)\, R(0)\right] \tag{8}$$

where $h = z/M$.

For small percent errors $\varepsilon(z;M)$

$$\varepsilon(z;M) = \frac{N(z) - \tilde{N}(z;M)}{N(z)} \times 100 \tag{9}$$

the approximate characteristic field values $\tilde{C}(z,ct_i)$ are close to the exact characteristic field values $C(z,ct_i)$. Equation (8) can be rewritten as

$$I(z;M) \sim \frac{h}{3}\left\{C_1(z,z;M)\, R(2z) + 4C_1(z,z-h;M)\, R(2z-h)\right.$$
$$\left. + 2C_1(z,z-2h;M)\, R(2z-2h) + \cdots + C_1(z,-z)\, R(0)\right\} \tag{10}$$

Subtracting equation (4) from equation (1) evaluated at $ct = z$, we find

$$C_1(z,z) - \tilde{C}_1(z,z;M) \sim \int_{-z}^{z} C_1(z,z')\, R(z'+z)dz' - I(z;M) \qquad (11)$$

where $I(z;M)$ is given by (10). The value of (11) is the error created when one approximates the integral in the right hand side of (11) by its Simson sum. The value of the right hand side of (11) is[1]

$$C_1(z,z) - \tilde{C}_1(z,z;M) \sim \frac{M}{90} h^5 \frac{\partial^4}{\partial z'^4} C_1(z,z')\, R(z'+z) \quad , \qquad (12)$$
$$|z'| \leq z$$

The characteristic field percent error $\mu(z;M)$ is defined by

$$\mu(z;M) = \frac{C_1(z,z) - \tilde{C}_1(z,z;M)}{C_1(z,z')} \times 100 \qquad (13)$$

Using (12) and (13) we get

$$\mu(z;M) = \frac{1}{0.9M^4} \frac{z^5}{C_1(z,z)} \frac{\partial^4}{\partial z'^4} \{C_1(z,z')\, R(z'+z)\} \quad , \quad |z'| \leq z \qquad (14)$$

In Chapter 3, Section Ac we show that simple differentiation of (13) gives

$$\varepsilon(z;M) = \mu(z;M) + \frac{C_1(z,z)}{\frac{d}{dz} C_1(z,z)} \frac{d}{dz} \mu(z;M) \qquad (15)$$

Equations (14) and (15) show that $\varepsilon(z;M)$ depends on $1/M^4$. This proves the statement.

---

[1] See Reference

APPENDIX G

This appendix discusses the non-uniqueness of valley profiles when deduced by the ionogram method.

Suppose the plasma frequency profile is as shown with solid lines in Figure 1. Another possible profile is the one with dotted lines. Both profiles are the same in regions $z \leq z_1$, $z \geq z_3$. They differ only in the valley region $z_1 < z < z_3$

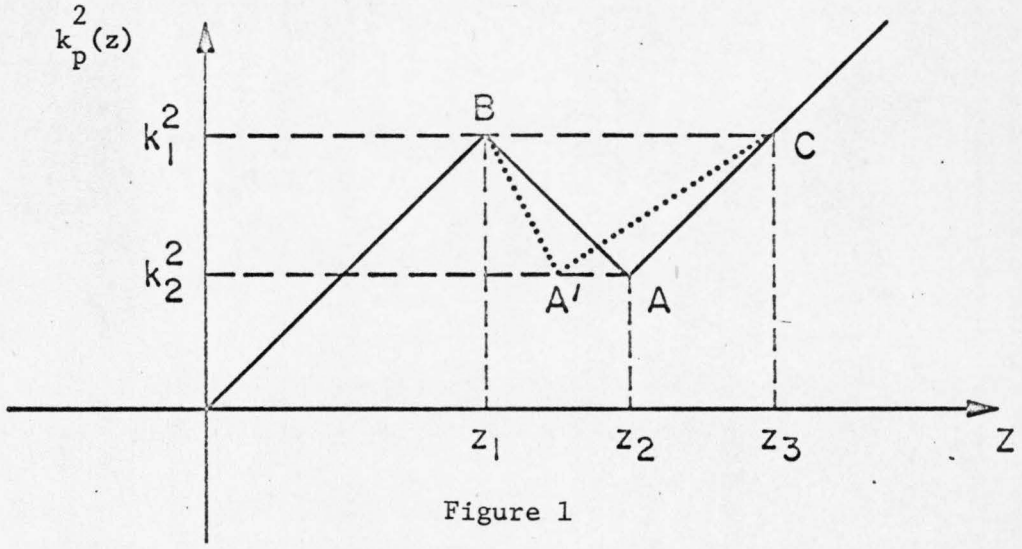

Figure 1

The phase acquired by the wave when it passes over the valley region BAC is

$$\phi = \int_{z_1}^{z_2} \sqrt{k^2 - k_p^2(\xi)}\, d\xi + \int_{z_2}^{z_3} \sqrt{k^2 - k_p^2(\xi)}\, d\xi$$

$$= \frac{2}{3p_1} \left[(k^2 - k_2^2)^{3/2} - (k^2 - k_1^2)^{3/2} \right]$$

$$+ \frac{2}{3p_2} \left[(k^2 - k_2^2)^{3/2} - (k^2 - k_1^2)^{3/2} \right]$$

where

$$p_1 = \frac{k_1^2 - k_2^2}{z_2 - z_1}$$

$$p_2 = \frac{k_1^2 - k_2^2}{z_3 - z_2}$$

Using the values for p_1, p_2 one gets

$$\phi = \frac{2}{3} \frac{z_3 - z_1}{k_1^2 - k_2^2} \left[(k^2 - k_2^2)^{3/2} - (k^2 - k_1^2)^{3/2} \right]$$

We see that the phase acquired in passing over the valley is independent of the position z_2 of point A . Clearly there is an infinite set of linear valleys that will give the same phase delay for $k > k_1$ and thus the same virtual height.

REFERENCES

Electromagnetic Inverse Scattering

1. Kay, Irvin, The Inverse Scattering Problem, Research Report No. EM-74, New York University Division of Electromagnetic Research (1955).

2. Kay, Irvin, On the Determination of the Free Electron Distribution of an Ionized Gas, Research Report No. EM-141, New York University Division of Electromagnetic Research (1959).

3. Kay, Irvin, The Inverse Scattering Problem when the Reflection Coefficient is a Rational Function, Communications on Pure and Applied Mathematics, Vol. XII, 371-393 (1960).

4. Kay, Irvin, The Three-Dimensional Inverse Scattering Problem, Research Report No. EM-174, New York University Division of Electromagnetic Research (1962).

5. Sims, A.R., Certain Aspects of the Inverse Scattering Problem, Society of Industrial and Applied Mathematics, Vol. 4, 183-205 (Dec. 1957).

6. Portinari, J.C., The One-Dimensional Inverse Scattering Problem, Ph.D. Thesis in Electrical Engineering, Massachusetts Institute of Technology (June 1966).

7. Sharpe, C.B., The Synthesis of Infinite Lines, Quarterly of Applied Mathematics, Vol. 21, No. 2, 105-120 (1963).

8. Sharpe, C.B., Some Properties of Infinite Lines, Quarterly of Applied Mathematics, Vol. 21, No. 4, 337-342 (1964).

9. Moses, H.E. and deRidder, C.M., Properties of Dielectrics from Reflection Coefficients in One Dimension, M.I.T. Lincoln Laboratory, Technical Report No. 322 (July 1963).

General Inverse Scattering

10. Lord Rayleigh, The Theory of Sound, Dover Publications, New York, Vol. I, 214-216 (1945).

11. Ambartsumyan, V.A., Uber eine Frage der Eigenwertheorie, Z. Phyzik, 53, 690-695 (1929).

12. Borg, G., Eine Umkerhrung der Sturm-Liouvillescheu Eigenwertaufgabe, Acta Mat 78-79, 1-96 (1946-47).

13. Levinson, N., Certain Explicit Relationships between Phase Shift and Scattering Potential, Phys. Rev., Vol. 89, No. 4, p. 755-757 (Feb. 1953).

14. Levitan, B.M. and Gasymov, M.G., Determination of a Differential Equation by Two of Its Spectra, Russian Math Surveys, 19, 2, 1-63 (1964).

15. Langer, R. E., An Inverse Problem in Differential Equations, American Math. Soc. Bull. 39, 814-829 (1933).

16. Gelfand, I.M. and Levitan, B.M., On the Determination of a Differential Equation from Its Spectral Function, American Math. Soc. Translations, Ser. 2, 1, 253 (1955)

17. Marchenko, V. A., Some Problems in the Theory of One-Dimensional Second-Order Differential Operators, Part I, Trudy Mosk. Nat. Obs. 1, 327-420 (1952) and: ibid 2, 3-82 (1953).

18. Agranovitch, Z.S. and Marchenko, V.A., The Inverse Problem of Scattering Theory, Gordon and Breach Co., New York (1963).

19. Levinson, N., On the Uniqueness of the Potential in a Schrodinger Equation for a Given Asymptotic Phase, Det. Kgl. Danske Violenskabernes Sclskab Mat.Fys, Bind XXV, Nr. 9 (1949).

20. Stone, M.H., Certain Integrals Analogous to Fourier Integrals, Math. Zeit 28, 654-676 (1928).

21. Faddeyev, L. D., The Inverse Problem in the Quantum Theory of Scattering, Research Report No. EM-165, NYU Div. of EM Research (1960).

22. Regge, T. and de Alfar, V. Potential Scattering, Interscience (1965).

Mathematical Texts

23. Schwartz, L., Mathematics for the Physical Sciences, Addison-Wesley (1966).

24. Mikhlin, S. G., Linear Equations of Mathematical Physics, Holt Rinehart and Winston, New York (1967).

25. Tricomi, F. G., Integral Equations, Interscience, New York (1967)

26. Hildebrand, F. B., Introduction to Numerical Analysis, McGraw-Hill Book Co., New York (1956).

Electromagnetism, Ionospheric Studies

27. Papas, C. H., Theory of Electromagnetic Wave Propagation, McGraw-Hill Book Co., New York (1965).

28. Budden, K. G., Radio Waves in the Ionosphere, Cambridge U. Press, (1966).

29. Davies, K. Ionospheric Radio Waves, Blaisdell Publishing Co., Waltham, Mass. (1969).

30. Manning, L. A., The Determination of Ionospheric Electron Distribution, Proc. IRE, 1203-1207 (Nov. 1947)

31. Manning, L. A., The Reliability of Ionospheric Height Determinations, Proc. IRE 599-603 (June 1949).

32. Howe, H.H. and McKinnis, D.E., Ionospheric Electron-Density Profiles with Continuous Gradients and Underlying Ionization Corrections II. Formulation for a Digital Computer, Radio Science 2, (New Series), 1135-1158 (1967).

33. Wright, J. W., Ionospheric Electron-Density Profiles with Continuous Gradients and Underlying Ionization Corrections III. Practical Procedures and Some Instructive Examples, Radio Science 2 (New series) 1159-1168 (1967).

WKB Method

34. Merzbacher, E. Quantum Mechanics, John Wiley and Sons, New York (1961), pp. 112-134.

35. Bohm, D. Quantum Theory, Prentice Hall, Englewood Cliffs, New Jersey (1951), p. 264-280.